

cc/Bali ✓

Donated by Dr. A. Goswami  
Scientist-E Physical Chemistry  
Division N.C.I. PUNE-411 008.

**COMPUTERISED**

# STUDIES OF SURFACE STRUCTURES

BY

# ELECTRON DIFFRACTION

COMPUTERISED

**S. B. Badachhape**

M.Sc.

STUDIES OF SURFACE STRUCTURES

BY

ELECTRON DIFFRACTION

A Thesis  
submitted to  
the University of Poona  
for the Degree of  
DOCTOR OF PHILOSOPHY



539.23:621.385.833(043)

BAD

by

S. B. Badachhane

Physical Chemistry Division

National Chemical Laboratory

POONA - 8.

February 1962



## C\_O\_N\_T\_E\_N\_T\_S

		<u>Page</u>
I.	GENERAL INTRODUCTION	1-3
II.	EXPERIMENTAL	9-13
III.	STRUCTURE AND CRYSTAL GROETH OF CUPROUS IODIDE, CUPROUS BROMIDE AND CUPROUS CHLORIDE FILMS	14-58
	A. Introduction	14
	B. Experimental	18
	C. Results	20
	a. Cuprous Iodide	
	i) On Rock-salt (100),(110) and (111) faces	30 31
	ii) On KCL (100) face	32
	iii) On Calcite (1011) face	33
	iv) On Ni ca (0001) face	35
	V) Glass	
	b. Cuprous Bromide	
	i) On Rock-salt (100), (110) and (111) faces	38 42
	ii) On Glass	....
	c. Cuprous Chloride	
	i) On Rock-salt (100) and (110) faces	44
	ii) On Glass	47 50
	D. DISCUSSION	59 - 78
IV.	STRUCTURE ANALYSIS	
	A. Principle of Structure analysis by Electron Diffraction	59
	B. A new spinol from cuprous chloride	63
	C. Investigation on the structure of evaporated tin sulphide	73

V.	STRUCTURES AND THE GROWTH OF SULPHIDE FILMS	
	OF TIN, ANTIMONY AND BISMUTH . . . .	79-99
	A. Introduction . . . .	79
	B. Experimental . . . .	82
	C. Results . . . .	83
	a. Tin sulphide on rock salt . . . .	83
	b. Bismuth sulphide . . . .	87
	i) On rock-salt . . . .	87
	ii) On mica . . . .	90
	c. Antimony sulphide on rock-salt . . . .	91
	D. DISCUSSION . . . .	97
VI.	EFFECT OF TEMPERATURE ON THE EPITAXIAL GROWTH	
	OF SILVER ON LEAD SULPHIDE SINGLE CRYSTALS	100-109
	A. Introduction . . . .	100
	B. Experimental . . . .	102
	C. Results . . . .	103
	D. DISCUSSION . . . .	107
VII.	SUMMARY AND CONCLUSIONS . . . .	110-114

ACKNOWLEDGEMENTS

REFERENCES (i-vi)



## CHAPTER I

### GENERAL INTRODUCTION

Surface properties of solids and liquids differ considerably from those of the bulk materials. This is due to the fact that arrangement of atoms at the surface region is different from those well inside the materials where atomic forces are well balanced amongst themselves. It is not, however, the case at the surface layers because of considerable unbalancing of them. This results in peculiar surface properties as shown by thermionic emission, surface tension, adsorption and catalysis etc. Surface layers are also responsible for many reactions in solid-solid phases. In many cases, irrespective of the method of preparation, these layers often show different structures than those of the bulk materials. It is, therefore, of great importance to know the structure of surface layers as many of their physico-chemical behaviour can be traced to surface structures.

Sulphides and halides often show semiconducting properties. Examples may be given of zinc sulphide, cadmium sulphide, tin sulphide, antimony and bismuth sulphide and cuprous iodide, silver iodide etc. [ Seitz 1945, Lyashenk & Snitko<sup>k</sup> 1954, Ioffe 1960, Dunlap 1957 ]. Thin films because of properties different from the bulk materials find wide scope of use in many fields, especially in electrical devices, such

as rectification, amplification, doping and in optical instruments viz. antireflecting systems, interference filters, polarizers etc. [Heavens 1955, Holland 1956, Dowden & Yoffe 1958]. They generally show a wide variety of structures from irregular amorphous aggregates to well defined single crystal flakes. Changes of structures often take place during the preparation of films by processes such as evaporation and condensation, sputtering, electrodeposition etc.

Since the first application of X-ray technique to the study of crystal structures this method has provided much information and proved to be an essential tool in the field of crystallography. Even though there are many advantages of this technique to determine the bulk structure, this method cannot be used for the study of surface layers and thin films. The discovery of electron diffraction and its applications [Thomson and Cochrane 1939, Finch & Wilman 1957, Pinsker 1953 and Raether<sup>1951</sup> 1957] to thin films and surface structure have solved the above difficulty.

Electrons are highly scattered by the nucleus or rather by the potential field of the atom. The scattering of electrons by atoms is about  $10^7$  times more than that of X-rays. As a result even a few layers of atoms in a crystal are sufficient to give a coherent and good diffraction pattern. In the case of X-rays, however, comparatively a much thicker sample about [0.1 mm.] thickness of crystalline materials is necessary for the diffraction. Electrons are highly

scattered and cannot penetrate much inside the crystals. The penetration for about 40-60 KV electrons is limited to about the order of only a few hundred  $\text{A}^\circ$  thickness for heavy atoms and few thousand  $\text{A}^\circ$  for materials having low atomic weight. In the case of reflection technique the penetration is much less and is of the order of 10 to 15  $\text{A}^\circ$ . Pashley and Newman (1955) have observed good diffraction patterns even from a layer of average 2-5  $\text{A}^\circ$  thickness of Ag and Cu layers.

Since electron diffraction technique can be used both by reflection as well as by transmission methods it can show the difference, if any, in the structure of surface layers from those layers sandwiched between the substrate and the top surface layers and thus providing a means for identifying any phase change occurring during the growth process. If the structure is temperature-sensitive this can also be noted easily during the electron diffraction studies at different temperatures. Thus electron diffraction provides an ideal tool for the study of surface structure, thin films, phase transition etc.

#### Crystal growth :

In a crystal atoms or ions are arranged regularly in a three dimensional frame work extending in space. In the ideal case, the atoms or ions occupy positions conforming to minimum potential energy state. Crystals normally grow atom by atom, layer by layer and many times before a layer



is completed another layer starts growing. In fact the growth takes place simultaneously either on the same or different layers. At the junction of two or more crystallites the atoms are not in their maximum stability condition and hence may give rise to some faults in the growth process such as dislocations, stacking faults, twinning etc.

The first quantitative theory for the study of crystal growth processes was given by Gibbs (1878) on thermodynamical grounds. Curie (1885), Wulf (1901) and others followed it. During the last many years atomic theory of the crystal growth has been developed by Volmer (1939), Kossel (1927, 1928), Stranski and his co-workers (1928, 1949), Becker and Doring (1935, 1949B), and Frenkel (1945, 1946). Burton, Cabrera and Frank (1949, 1951) have developed a theory of crystal growth taking into account the presence of imperfections and dislocations. Wells (1946) and Duckley (1952) have made reviews of the above work.

The habits of growing crystals often depend on the surrounding conditions though their structures remain unchanged. As for example sodium chloride crystals grow with a cubic habit from neutral solutions but with octahedral faces in the presence of urea and they show tree-like growth in the presence of gum arabic, retaining same crystal structure all the while.

In the present work we are mostly concerned with the deposits obtained from vapour phase deposition process.

It is now well known that the substrate has great influence on <sup>the</sup> epitaxial growth of crystals, their structures and also on their orientations. Epitaxial growth or orientated over-growth of the crystals was first observed in case of naturally occurring minerals as given by Wallerant (1902) and Mugge (1903). Observations of this led to some experiments to achieve <sup>the</sup> epitaxial growth and early experiments were also made by Frankenheim (1836) and <sup>he</sup> observed parallel orientation developed by  $\text{NaNO}_3$  crystals on calcite. The term 'epitaxy' was first introduced by Royer (1928, 1936) after making an extensive study on the growth of crystals on different substrates. He observed that the deposit atoms or ions take up orientation as to follow the substrate structure such that there is a close fit between the two dimensional net work of deposit and substrate at the interface. This was termed "Epitaxy".

He also found that in such case, there was one densely populated lattice row in the deposit parallel to the one of the substrate, provided that their relative identity spacing did not differ by more than 15%. Frank and Van der Merwe (1949) treated the substrate as two dimensional network and found a similar limit for the formation of pseudomorphic layers (Finch & Quarxrell 1933, 1934) which they considered essential for epitaxial growth. They suggested that for the epitaxial growth the misfit between atoms of the substrate and the deposit should not exceed 15%. It is, however, well

known now from many experiments that epitaxial growth can take place even when misfit is as high as 50% or more (see Pashley 1956).

#### Phase transition and Polymorphism :

Recent studies on the structure of many thin films have shown that the phenomenon of polymorphism is not only exhibited by metals but also by many compounds. Schulz (1951) showed that rubidium bromide having normal NaCl type of structure developed CsCl type of structure when deposited on silver substrate. He (1952) also showed that some halides such as CsCl, CsBr, CsI, TlCl, TlBr, TlI having CsCl type of structure developed NaCl type of structure when grown from the vapour phase on appropriate single crystal substrates. Unlike the halides comparatively less work has been carried on the polymorphism of sulphides. Goswami and Trehan (1959) observed two new cubic structures in case of copper sulphide during the study on the reaction of sulphur vapour on copper single crystals. Aggarwal (1958) observed some hexagonal phase even from the  $\beta$  form of ZnS and CdS. Piggot and Wilman (1958) observed some superstructures of some sulphides.

It is well known that  <sup>$\alpha$</sup>  <sub>$\beta$</sub>  new phase often appears due to heat treatment. The transition of one phase to another takes place at a certain temperature. In case of thin films, however, this transition temperature is much lower than that of the bulk. Examples for this may be given as for the case of CuI as observed by Hoshino and Miyake (1952) and ZnS, CdS

etc. by Aggarwal (1958). In our present study also, similar results for halides were observed.

In the recent times sulphides, selenides, tellurides and also some of the halides had gained much importance because of their semiconducting properties and also their uses in semiconducting devices. Photoconducting properties of the sulphides, selenides, phosphorescence of cadmium sulphide, zinc sulphide, thermoelectric properties of bismuth-telluride and uses of germanium as crystal rectifier etc. are well known (Ioffe 1960, Dunlap 1957). In the search for new compounds having semiconducting properties, some materials have also been studied. It is of interest to point out that thin films of these compounds may have some different structure than those of the bulk as has been pointed out in previous section and it is likely that they may as well considerably modify the so-called semiconducting properties also. With the above idea in view work has been carried out on some of the halide as well as sulphide deposits obtained from vapour phase.

Present Study :

The present work may be classified as follows :

(a) Structure and crystal growth of copper halides with special reference to the effect of temperature on various substrates, such as single crystals of rocksalt, KCl, calcite, mica and amorphous substrate like glass.

- (b) Structure and crystal growth of evaporated films of tin, antimony and bismuth sulphides.
- (c) Investigation on the relation between total blackening of the photographic plates and energy of the diffracted electron beam and its application to some structure analyses.
- (d) Epitaxial crystal growth of silver on lead sulphide single crystals at different temperatures.

\* \* \* \*

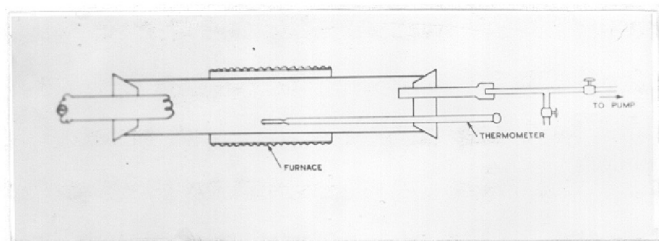


Fig. 1

CHAPTER II

EXPERIMENTAL

(a) Preparation of Specimens :

The apparatus for preparing the deposit-films is shown in fig. (1). A wide pyrex glass tube about 30 cms in length was clamped horizontally and rubber stoppers were inserted at the two ends. Two copper terminals for carrying current to heat the filament were put through one of the stopper. The tube was evacuated by a rotary oil pump through the other end. The vacuum used was of the order of  $10^{-2}$  to  $10^{-3}$  mm Hg. When high vacuum was needed, the evacuation was carried out through an oil diffusion pump along with the rotary pump leading to a pressure of about  $10^{-4}$  mm Hg. Substrates were generally placed at about 2-4 cms away from the filament. Before deposition, however, these were heated to the required temperature by a tubular furnace which could be slid over the pyrex tube. The filament was initially flashed to white hot and when <sup>cooled</sup> the materials to be evaporated were put into it. When the substrates attained the required temperature the deposition was carried out by raising the temperature of the filament. After the deposition the deposits were cooled to room-temperature in vacuo. They were then removed and examined by electron diffraction in the manner described later on.

contamination

The filaments were in the basket form and made from Kanthal or tungsten wires. The initial flashing of filament was necessary in order to avoid the surface impurities with the deposit material. The heating of the filament was controlled by a variac. When the deposits or substrates were to be heated separately, it was carried out in vacuo in the same apparatus. The temperature was measured by a suitable thermometer.

(b) Preparation of the Substrates :

The substrates used for depositing films were (100), (110) and (111) faces of rocksalt crystals, cleavage faces of KCl, mica, calcite and also amorphous glass pieces.

The cleavage faces of rocksalt or KCl were obtained by cutting the single crystals with a clean and sharp edged knife by applying a little pressure along the cube edge direction. The untouched cleaved surfaces were then used as substrates. If particles were adhering to the surface they were removed with a camel hair brush before using. Proper care was, however, taken to avoid the contamination of grease with the substrate surface.

Two other faces namely (110) and (111) of rocksalt were prepared by carefully grinding the crystals at appropriate angles with different grades of emery papers down to 0000. Afterwards the surface was etched with running distilled water



and dried immediately by pressing between filter papers. These were then examined by electron diffraction technique. The surfaces were reground, if necessary, to get the appropriate faces.

Calcite cleavage faces were obtained by cutting single crystals of these along appropriate direction with knife. Mica substrates were prepared by cleaving them immediately before the deposition.

Glass substrates were prepared by cutting the microscope slides into convenient sizes, treating them with chromic acid and finally washing with distilled water. The pieces were then dried by pressing between filter papers. Substrates thus prepared were then put into the evacuation chamber and deposition was carried out in the manner described previously.

(c) Examination of Specimens :

Deposits obtained on various substrates were studied by reflection or by transmission technique. The deposits obtained on rocksalt or KCl after being examined by reflection were also studied by transmission method. This was done by removing the films from the substrate in the following way. The deposits along with the substrate was kept in a petri-dish and distilled water was then poured very slowly so that there was not much disturbance during the rise of water level. Water slowly dissolved the substrate underneath the films, finally

leaving them floated on the water surface. The detached films were washed several times with distilled water and then taken on clean monel gauze of about 200 mesh, for studying by transmission method.

These specimens were then examined in a Finch type electron diffraction camera using cold cathode. The details of the camera have already been given in <sup>a</sup>paper by { Finch & Wilman (1937) and hence have not been described here. The electrons used during the present study were normally accelerated to 40-50 KV. The specimens were examined in more than one azimuths by rotating the specimen around an axis perpendicular to the beam direction. From the electron diffraction patterns obtained at various azimuths the nature of the deposits were identified. Colloidal graphite or graphite powder was used as the internal standard for the measurement of 'd' values of various reflections obtained.

(d) Interpretation of Electron Diffraction Patterns :

General methods of interpretation of the electron diffraction patterns have been already discussed by many workers (Finch & Wilman, 1937, Thomson & Cochrane 1939, Beeching 1936, Wilman 1948 a,b, 1949, 1952, Pinsker 1953 etc.) and hence are not given here in details.

Normally the diffraction patterns obtained can be broadly classified in the following main categories :

(i) Patterns due to single crystals (mosaic) or two-degree orientated deposit crystals mostly consisting of spots sometime with a slight spread depending on the degree of the perfection of orientation.

(ii) Ring patterns not showing any change in the intensity distribution along the rings with the change of beam direction are due to unorientated polycrystalline deposits.

(iii) Patterns consisting of arcs or with a change in intensity distribution along the rings but remaining unchanged with change of beam direction are normally due to polycrystalline deposits having a preferred orientation (one degree).

+ + + +

CHAPTER III

STRUCTURE AND CRYSTAL GROWTH OF CUPROUS IODIDE,

CUPROUS BROMIDE AND CUPROUS CHLORIDE

A. Introduction

Nyckoff and Posnak (1922) studied the structures of cuprous halides by following the general method based upon use of the theory of space group and taking diffraction data from the powder photographs. They showed that the atoms in crystal of  $\text{CuCl}$ ,  $\text{CuBr}$  and  $\text{CuI}$  have the 'zinc blende' arrangement. The cuprous halides were prepared in the ordinary fashion, the chloride and the bromide by the reduction of the corresponding cupric salt with  $\text{SO}_2$  and the iodide by the reaction between cupric salt and  $\text{KI}$ . Davey (1922) determined the absolute size of certain univalent and bivalent ions and found to be  $= 0.76 \text{ \AA}^0$  for  $\text{Cu}^+$  in ( $\text{CuCl}$  &  $\text{CuBr}$ ) and  $0.65 \text{ \AA}^0$  in ( $\text{CuI}$ ). Barth and Lunde (1925) determined lattice constants for cuprous and silver halides. Thomson (1931) found that copper (ous) compound to be orientated in a definite way on the etched surface of a  $\text{Cu}$  single crystal. Maxwell and Mosley (1939) measured the internuclear distances in the gas molecules of  $\text{Cu}_2\text{Cl}_2$ ,  $\text{Cu}_2\text{Br}_2$  and  $\text{Cu}_2\text{I}_2$  etc. by electron diffraction. Germer (1939) during an electron diffraction study of thin films observed a curious and unexplained anomaly in the intensity of a diffraction ring in patterns from films of  $\text{CuCl}$ . Shin-ichi Shimadzu (1939) investigated by rotation

photograph with FeK radiation the orientation of thick layers of various substances on different substances and found that no preferred orientation was found for CuI on Cu, CuCl, on Cu, Cu<sub>2</sub>O on Cu (I) etc. Thick layers of AgBr formed on AgCl by treatment with a KBr solution on the other hand showed completely parallel orientation of the AgBr and AgCl lattices. Wilman (1940) made electron diffraction studies of the reaction of Ag films ( $\approx 500 \text{ \AA}^0$  prepared by condensation on hot NaCl cleavage faces) with halogen vapours and found that the rapid attack by concentrated vapour yielded a randomly disposed layer of halide crystals whereas slower attack yielded halide crystals which were orientated relative to the original silver lattice.

Usmani (1941) studied the growth of chemical compounds on a copper single crystals by method of electron diffraction. He observed that thin films of CuI, CuBr, Cu<sub>2</sub>O and Cu<sub>2</sub>S electrolytically deposited on an etched surface of a copper single crystal were orientated with  $\langle 111 \rangle$  of the deposits parallel to  $\langle 110 \rangle$  of Cu and with  $\langle 112 \rangle$  of deposit parallel to  $\langle 110 \rangle$  of Cu in the case of CuI and CuBr. Miyake Hoshino and Takenaka (1952) studied the phase transition occurring in cuprous iodide by X-ray powder method and by calorimetric measurements and observed that  $\beta$ -phase was obtained <sup>even</sup> at about <sup>200°C</sup> which was much less than the bulk transition temperature 369°C (A.S.T.M. Card No. 6-0246).

Goswami (1950, 1954, 1961) studied the epitaxial

growth of cuprous halide films obtained by anodic treatment in a solutions of KBr and KI and also by the reaction of iodine and bromine vapours on the different faces (100), (110) and (111) of copper single crystals. He observed that inspite of the difference in lattices, the deposits grew epitaxially and the deposits were entirely of  $\alpha$ -form. Reactions carried out for longer times, however, led to the formation of polycrystalline coatings. Often epitaxial disorientation of substrate lattice was also observed. Hoshino (1952) has worked on the crystal structure of cuprous bromide by X-ray powder method and calorimetric measurement and obtained the lattice constants for the three modifications  $\gamma$ ,  $\beta$  and  $\alpha$  as mentioned later in this chapter (discussion).

Recently it has been shown that the phenomenon of polymorphism is exhibited not only by metals but also by many halides and sulphides. Seig (1953) showed that AgI (zinc blende) treated with iodine vapour developed a wurtzite structure and the removal of excess of iodine in vacuo caused reversion to zinc blende structure. The behaviour of AgBr thin films when exposed to light and to electron bombardment was examined and the deposition of silver was demonstrated by the appearance of Ag diffraction rings (Trillat 1951).

From above literature survey it will be seen that not much work has been carried out on the structures of thin films of cuprous halides obtained by vapour phase deposition process. In the following an account is given of the work

carried out on the evaporated thin films of cuprous halides on various substrates with special reference to the epitaxial growth, structures, orientation, phase transition and polymorphism and also the effect of temperature on these films.

539,23;621,385,833(043)

BAD

## B. Experimental

The deposits of cuprous iodide, bromide and chloride were prepared in the manner described previously (Chapter II). The substrates used were (100), (110) and (111) faces of rock-salt, (100) of KCl, (0001) of mica, (10 $\bar{1}$ 1) of calcite and on amorphous glass. The temperature of the substrate was between room temperature to about 430°C. The deposits after being cooled were examined by electron diffraction technique both by reflection and transmission. The details of technique and the removal of deposits from substrates etc. are given in the previous Chapter II.

Before evaporating the cuprous halides from filament they were initially examined by X-ray diffraction spectrograph for their bulk structures. Occasionally powder was also examined by electron diffraction method after sprinkling them on collodion film.

### Preparation of Materials :

i) CuI : Cuprous iodide used was procured from the British Drug House Ltd., London (B.D.H. Laboratory reagent).

ii) CuBr : Cuprous bromide was prepared by heating a mixture of one part of copper turnings, one part of crystalline copper sulphate and four parts of glacial acetic acid. The boiling solution was then poured into cold distilled water and the precipitate of cuprous bromide obtained thereby was washed several times with distilled water and then with alcohol. The precipitate was dried in a vacuum desiccator.



iii) CuCl : Cuprous chloride was prepared by boiling the mixture of 25 gms of cupric oxide, 250 c.c. of concentrated hydrochloric acid and 50 gms of copper turnings, in a fuming cupboard till the solution was colourless. This solution was then poured into a litre of previously boiled distilled water. The precipitate of cuprous chloride obtained was filtered off from a buchner funnel and washed rapidly with boiling water and then with alcohol and ether. Finally the precipitate was dried in a vacuum desiccator on a porous plate over sulphuric acid.

---

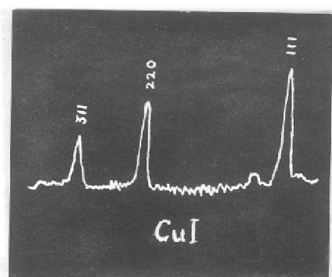


Fig. 2

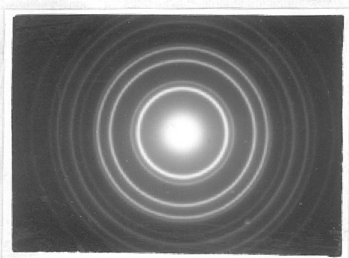


Fig. 3  
CuI on NaCl (100) face  
at room temperature

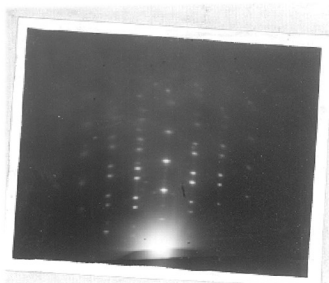


Fig. 4  
CuI on NaCl (100) face  
at 200°C.

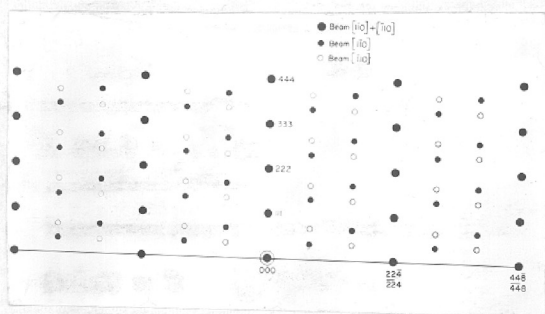


Fig. 6  
Theoretical pattern

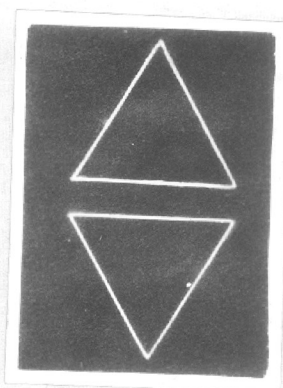


Fig. 5

Table No. I

Analysis of the pattern of fig. (3)

$I/I_0$	$dA^\circ$	hkl	$a_0$
vs	3.51	111	6.07
f	3.01	200	6.02
s	2.15	220	6.08
s	1.81	311	6.00
vf	1.73	222	5.99
m	1.51	400	6.04
ms	1.39	331	6.06
ms	1.24	422	6.07
m	1.15	511+333	5.97
f	1.03	531	6.09
f	0.945	620	5.97
f	0.91	622	6.03

Mean  $a_0 = 6.03 \text{ \AA}^\circ$

v = very, s = strong, m = medium, f = faint

### C. Results

Cuprous iodide (bulk materials when examined by X-ray spectrograph yielded curve (fig. 2). The 'd' values and the peak heights of the different reflection were found to correspond to normal  $\gamma$ -cuprous iodide alone thus showing that the material we started with consisted entirely of  $\gamma$ -CuI.

#### (a) Cuprous iodide on Rock-salt :

i) On (100) face : The deposits from cuprous iodide on rocksalt cleavage face at room temperature were polycrystalline in nature. The patterns were sharp (fig. 3) and consisted of either all odd or all even reflections (table I) of a f.c.c. structure. The lattice constant  $(6.03) \text{ \AA}^0$  as measured with graphite standard showed that the deposits were due to  $\gamma$ -CuI alone. These deposits when studied by transmission method also showed similar results.

Deposition at  $200^{\circ}\text{C}$  yielded patterns (fig. 4) consisting of rings as well as spots. These spots lie on ring position thus showing that they were due to the same crystalline materials. The rings were found to be due to polycrystalline  $\gamma$ -cuprous iodide deposits.

The presence of 111, 222 etc. reflections and their higher orders in the plane of incidence and the fact that the spot pattern changed with change of beam direction suggested the development of 2-d  $\{111\}$  orientation by the deposit crystals. In case of two-degree  $\{111\}$  orientated

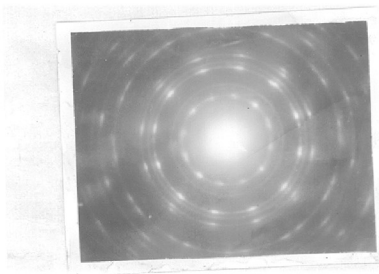


Fig. 7  
CuI on NaCl (100)  
at 250°C.

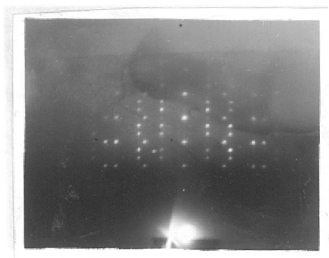


Fig. 8  
CuI on NaCl (100)  
at 300°C.

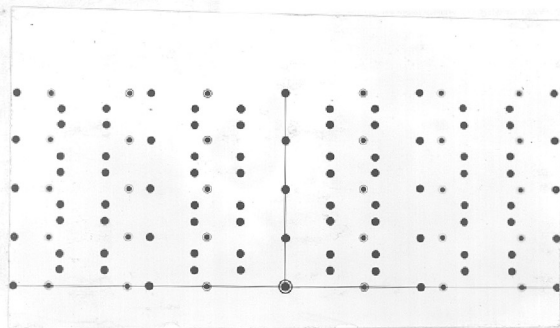


Fig. 9  
Theoretical pattern for  
2-d {111} orientation (beam along  $\langle 110 \rangle + \langle 112 \rangle$ ).

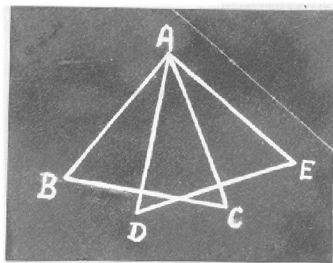


Fig. 10

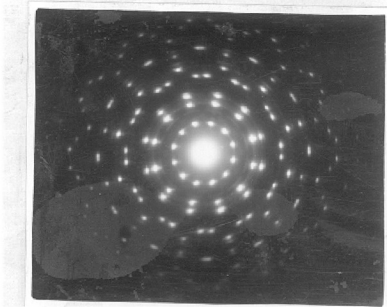


Fig. 11

Table No. II

Analysis of the pattern of fig. (7)

$I/I_0$	$d \text{ \AA}^\circ$	hkl Cubic	hkl hexagonal.
ms	3.71	-	100
ms	3.50	111	002
f	3.06	200	-
	2.88	-	-
s	2.14	220	110
f	2.03	-	103
s	1.86	311	200
f	1.77	222	004
mf	1.67	-	202
f	1.52	400	-
ms	1.39	331	211
ms	1.26	422	204

s = strong, m = medium, f = faint

deposits the pattern should repeat after  $60^\circ$  rotation of specimen which was also noticed in this case. The main two important azimuths for 2-d  $\{111\}$  orientated crystals, lying in the plane of orientation are  $\langle 110 \rangle$  and  $\langle 112 \rangle$  which are at  $30^\circ$  to each other. In the present pattern (fig. 4) the presence of the spots due to 111, 200 and 311, 222 along 111 direction and at distance equal to  $1/3$  or  $2/3$  respectively suggested that the beam direction was along 100. The theoretical pattern for 2-d  $\{111\}$  or<sup>n</sup> with beam direction as  $\langle 110 \rangle$  should be asymmetric whereas the observed pattern was symmetrical. This suggested the development of parallel and antiparallel orientation and the disposition of crystals would be as in fig. (5). Such crystals would give rise to symmetrical pattern (fig. 6) since the direction of the beam will coincide with  $[1\bar{1}0] + [\bar{1}10]$  direction similar to the observed one. From the transmission picture also similar conclusion was drawn.

In some experiments at about  $250^\circ\text{C}$ , deposits yielded patterns (fig. 7) (by transmission method) which consisted not only of rings and spots due to the f.c.c.  $\gamma$ -CuI but also extra rings not accounted by the presence of  $\gamma$ -form alone. The 'd' values (table II) suggested that these can be explained by the formation of a hexagonal structure ( $\beta$  form) with  $a_0 = 4.31 \text{ \AA}$ ,  $c_0 = 7.09 \text{ \AA}$ ,  $c/a = 1.642$ . Thus though the initial materials was of  $\gamma$ -form the deposits tended to develop a  $\beta$  form along with the  $\gamma$ -CuI.

Deposits formed on rock-salt cleavage face at  $\approx 300^{\circ}\text{C}$  when examined by reflection method yielded patterns (fig. 8) consisting mostly of spots with beam along 100 of rocksalt. This pattern changed considerably as the specimen was rotated around the axis perpendicular to the beam direction and resulted again in the same pattern (fig. 8) as above when the rotation was by  $30^{\circ}$ ,  $60^{\circ}$  or  $90^{\circ}$  etc. It was also noticed that the spots due to 111, 222 etc. were present in the plane of incidence in all these patterns. The change of the pattern while rotating the specimen and presence of 111, 222, etc. reflections in plane of incidence suggested the development of 2-d  $\{111\}$  orientation of the deposit crystals. As mentioned earlier for the 2-d  $\{111\}$  orientated crystals the pattern should repeat only when the specimen is rotated by  $60^{\circ}$ , whereas in the present case it was repeating after  $30^{\circ}$ . From the observed pattern it is seen that many of the spots can be accounted for by the 2-d  $\{111\}$  orientation of the crystal with the beam ~~along~~ along  $[\bar{1}10] + [1\bar{1}0]$  of the deposit crystals and the other by the presence of 111 orientation, but beam being along  $\langle 112 \rangle$  direction of the crystals. The rectangular type of pattern with the side in the ratio equal to  $\sqrt{3} : \sqrt{3}$  also showed the presence of the later orientation. Thus the observed patterns were due to 2-d  $\{111\}$  orientated crystals with the beam grazing along  $[\bar{1}10] + [1\bar{1}0]$  and  $\langle 112 \rangle$  directions at the same time. Superimposition of the theoretical patterns <sup>fig.</sup> (9) due to such 2-d  $\{111\}$  orientated crystals conforms to the above view. The disposition of crystals is shown in fig. (10). The two



# Theoretical patterns

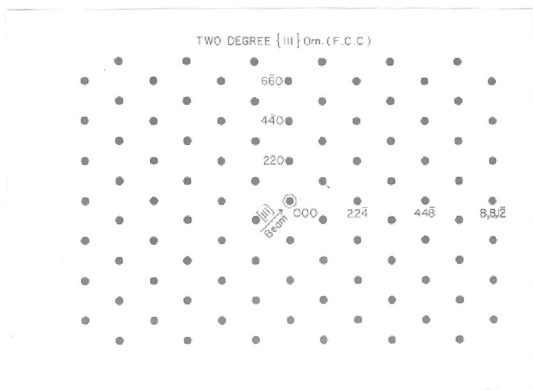


Fig. 12

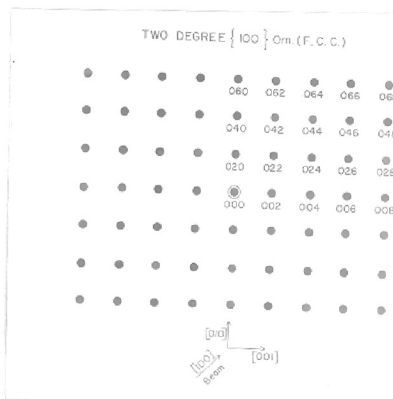


Fig. 13

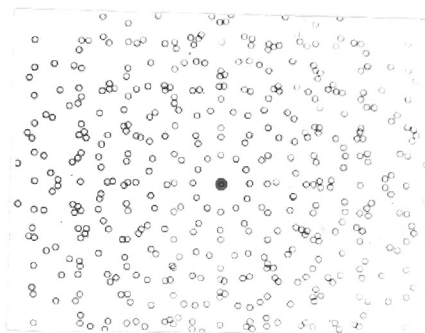


Fig. 14

2-d  $\{211\}$  orientation rotated by  $30^\circ$ .

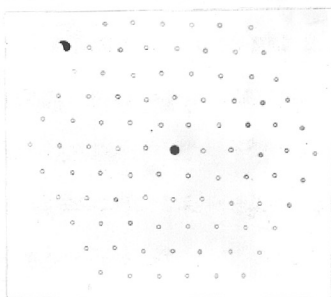


Fig. 15

2-d  $\{0001\}$  orientation

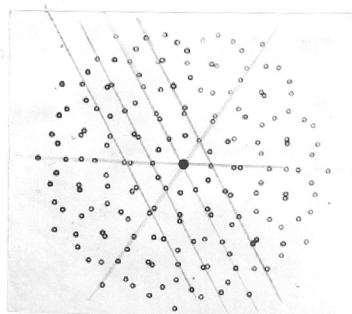


Fig. 16

2-d  $\{001\}$  or  $n$  rotated by  $30^\circ$ .

crystals ABC and ADE if they grew making an angle of  $30^\circ$  (i.e. BAD) when the beam grazes along AD it corresponds to the direction  $\langle 112 \rangle$  for ABC whereas at the same time also it corresponds to beam direction along  $\langle 110 \rangle$  for ADE. Similar is the case when the beam grazes along AC which corresponds to as if the crystal was rotated by  $30^\circ$ . Thus the electron beam along particular main azimuth  $\langle 110 \rangle$  or  $\langle 112 \rangle$  for 2-d  $\{111\}$  orientation gives rise to the pattern due to two different azimuths at the same time (Aggarwal and Goswami 1958).

The pattern (fig. 11) obtained from these deposits by transmission were very interesting. The deposits when examined by reflection method showed 2-d  $\{111\}$  orientation as described above and therefore it was expected that by transmission also these should show 2-d  $\{111\}$  orientation. The presence of the spots due to 111, 222 reflections suggested development of orientations other than  $\{111\}$  since in later case 111 reflections would have been absent. This is seen clearly from the theoretical pattern (fig. 12). If the deposits in contact with rock salt cleavage face would have developed parallel 2-d  $\{100\}$  orientation the pattern in that case would have been similar to fig. (13), whereas the observed one was quite different. However, the presence of 111, 222, etc. reflections can be easily explained on the basis of formation of 2-d  $\{211\}$  orientation. Fig. (14) shows the theoretical pattern from 2-d  $\{211\}$  orientated crystals rotated by  $30^\circ$ . The presence of 12 equidistant spots on 111, 220 and 311

reflections can be explained by the azimuthal rotation of the deposit crystals by  $30^\circ$ . The theoretical pattern (fig. 14) obtained from such deposit crystals and the observed one are quite similar.

It may be seen further that there are other spots and rings such as one just inside 111 reflection and some rings before 311 (cubic) which cannot be explained by the theoretical pattern (fig. 14). These extra spots and rings were found to be due to  $(10\bar{1}0$  and  $10\bar{1}\bar{3})$  reflections of hexagonal  $\beta$ -cuprous iodide. The presence of 12 spots (equidistant) lying on  $10\bar{1}0$  reflections and on  $11\bar{2}0$  reflections and so on can also be explained by the formation of  $\{0001\}$  orientation of  $\beta$ -CuI crystals. But here again the deposit crystals were azimuthally rotated by  $30^\circ$ . Theoretical patterns (unrotated and rotated) (Fig. 15 & 16) show the spot patterns expected from such type of crystals.

It is interesting to note that theoretical patterns from these crystals either cubic  $\{211\}$  or<sup>n</sup> or hexagonal  $\{0001\}$  or<sup>n</sup> rotated by  $30^\circ$  are similar to a great extent. In many cases the observed patterns can be explained by the presence of both the orientations.

It is interesting to enquire why crystals having two such different orientations should yield similar type of patterns. The two figs (16 & 14) show the different disposition of spots due to  $\{0001\}$  and  $\{211\}$  orientated rotated crystals. It is easy to see that even in case of  $\{211\}$

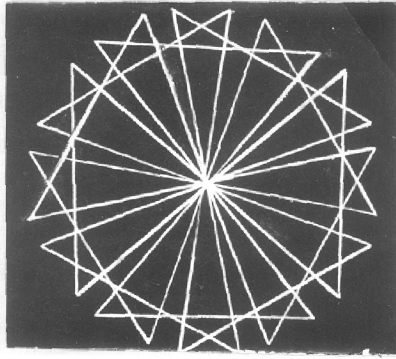


Fig. 17

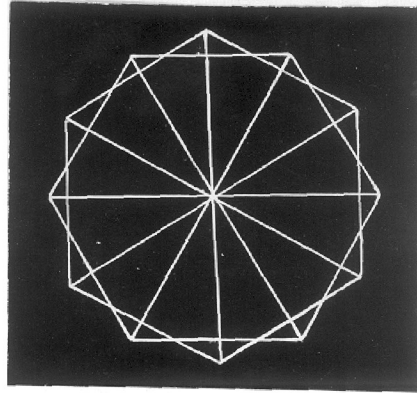


Fig. 18

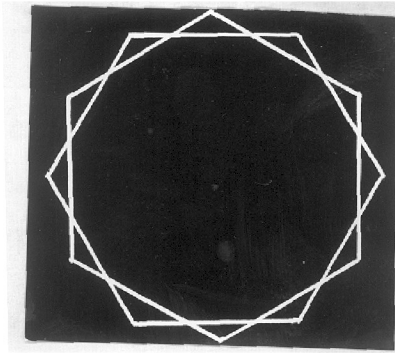


Fig. 19

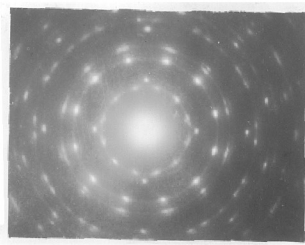


Fig. 20  
CuI on NaCl at 300°C.

orientated rotated crystals there is a basic arrangement of atoms which is very similar to that of  $\{0001\}$  orientated rotated crystals (Figures 17, 18 and 19). It is quite likely that such orientated crystals would give similar diffraction patterns. In many cases the spots arising from  $10\bar{1}0$  and  $111$  reflections due to their proximity superimposed on each other and hence it was difficult to decide the orientation uniquely unless these spots resolved distinctly. They should generally separate well at higher orders but due to fall of intensity of higher orders of reflections it was not always possible to decide the orientation uniquely.

Often deposits when examined by reflection showed charging up. At about  $300^{\circ}\text{C}$  inspite of several trials no good reflection pattern could be taken because of charging up of specimen. However, they in general show similar orientation as above by reflection. When examined by transmission they yielded good patterns (fig. 20) similar to fig.(11) showing thereby the presence of 2-d  $\{211\}$  orientation (cubic) and also  $\{0001\}$  or  $h^D$  (hex) and in both cases the crystals were rotated by  $30^{\circ}$ . From these patterns it is seen that there are four spots present outside  $111$  ring of cubic and are arranged at the corners of a square. Such spots were not observed in the previous cases. It was also noticed that the extra spots ~~are~~ such as  $200$ ,  $400$ , etc. form a lattice square net of patterns. The presence of these spots can only be explained on the basis of 2-d  $\{100\}$  orientation. The deposits, therefore in this case, develop 2-d  $\{100\}$  orientation on  $(100)$  face of rocksalt.

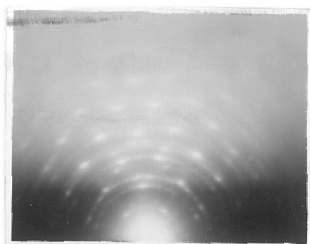


Fig. 22  
CuI on NaCl (110) at 200°C.  
Beam along  $\langle 001 \rangle$

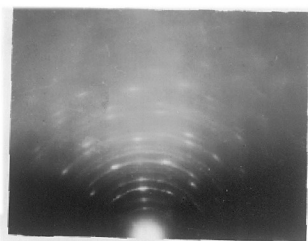


Fig. 21  
CuI on NaCl (110) at 200°C  
Beam along  $\langle 001 \rangle$

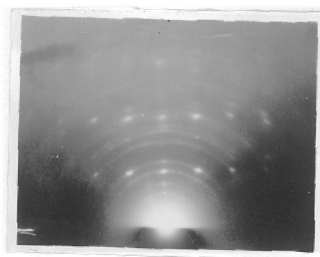


Fig. 23

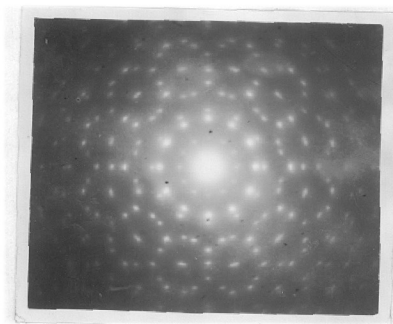


Fig. 24  
Specimen (fig. 21) by transmission.

On (110) face : The deposits formed on (110) face of rocksalt at room temperature ( $25^{\circ}\text{C}$ ) and also at about  $100^{\circ}\text{C}$  were generally polycrystalline. At higher substrate temperatures, however, the patterns became sharper and <sup>deposits</sup> had a tendency to develop 2-d orientated crystals.

Deposits formed at about  $200^{\circ}\text{C}$  yielded the patterns consisting of rings or spots or a mixture of these. On measuring the 'd' values of the different reflection it was found that they corresponded to normal  $\gamma$ -CuI. By rotating the specimen it was found that the spot pattern was changing considerably. The patterns (figs 21 and 22) were with the beam grazing along  $\langle 100 \rangle$  and  $\langle 110 \rangle$  directions of rocksalt crystal. It is seen from both the patterns that the reflections due to 110, 220, etc. are in the plane of incidence thus showing that the deposits of  $\gamma$ -CuI had developed 2-d  $\{110\}$  orientation with respect to the (110) surface of rocksalt. The patterns in two directions also correspond to beam along  $\langle 100 \rangle$  and  $\langle 110 \rangle$  directions of the deposit crystals. The pattern (fig. 23) obtained when the beam was along  $\langle 111 \rangle$  of NaCl also conformed to the above view. It was also observed that besides the spots due to 2-d  $\{110\}$  orientation there were few extra spots present in the pattern. The 'd' values of these extra spots were found to be due to hexagonal  $\beta$ -CuI. The deposits of cuprous iodide obtained in thin films thus developed hexagonal structure even at  $200^{\circ}\text{C}$  which is much less than the bulk transition temperature ( $369^{\circ}\text{C}$ ). The deposits on (110) face of rocksalt, thus, showed parallel



orientation i.e.



together with some  $\beta$ -phase at  $200^{\circ}\text{C}$ .

The above deposits when examined by transmission method yielded patterns (fig. 24) which were, however, similar to those shown in (fig. 11) obtained on the cleavage face of rocksalt at about  $300^{\circ}\text{C}$ . It was observed that though by reflection the deposits showed parallel  $\{110\}$  orientation more prominently, the same by transmission showed to have 2-d  $\{211\}$  (cubic) and also  $\{0001\}$  (hex.) orientations though rotated by  $30^{\circ}$ .

Patterns obtained by reflection from deposits at about  $300^{\circ}\text{C}$  were similar to those obtained in this case, <sup>but</sup> were, however, sharper than the former ones, thus showing better orientations. The three patterns (figs. 25, 26, 27) taken for three different azimuths  $\langle 100 \rangle$ ,  $\langle 110 \rangle$  and  $\langle 111 \rangle$  of rocksalt when compared with corresponding theoretical patterns as mentioned above conformed to 2-d  $\{110\}$  orientation of the deposit crystals alone.

These deposits yielded two types of patterns when studied by transmission method. One of which similar to that obtained in former cases was due to 2-d  $\{211\} + \{0001\}$  orientations (fig. 11). The other pattern (fig. 28) on analysis was found to be due to 2-d  $\{110\}$  orientation as

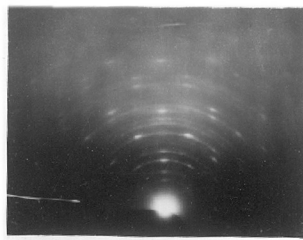


Fig. 25

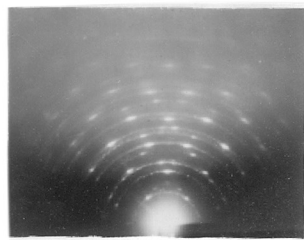


Fig. 26

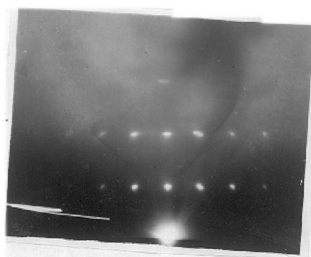


Fig. 27

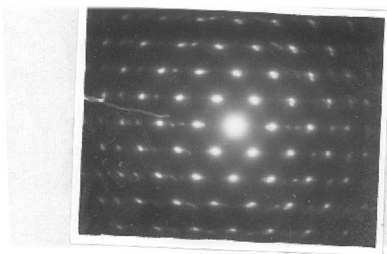


Fig. 28

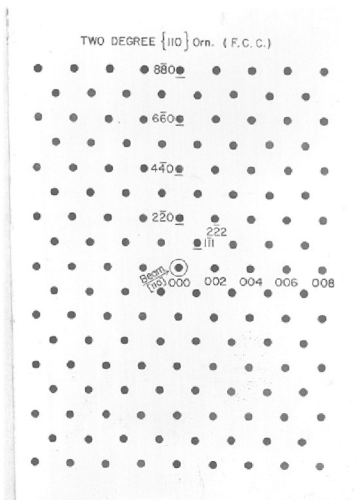


Fig. 29

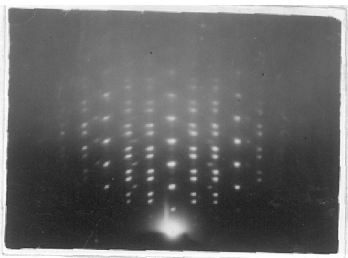


Fig. 30  
CuI on NaCl (111) at 300°C.

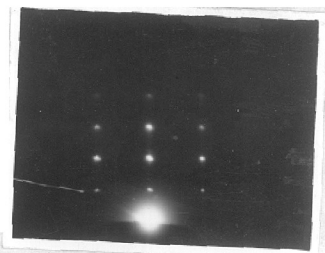


Fig. 31

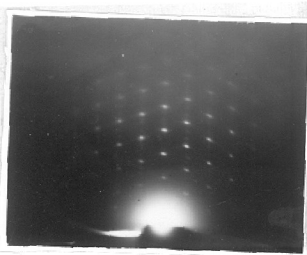


Fig. 32

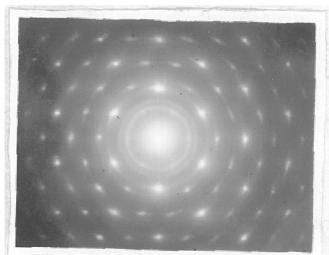


Fig. 33

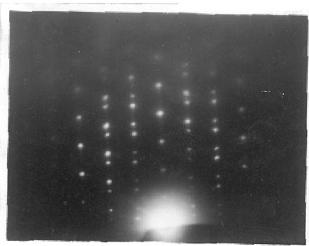


Fig. 34

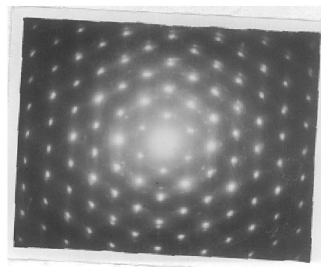


Fig. 35

compared with theoretical pattern (fig. 29). Thus at higher temperature the deposit film developed both cubic and hexagonal structures having  $\{211\} + \{0001\}$  orientations. Hence again even by transmission the 2-d  $\{110\}$  orientation was observed at higher temperatures.

On (111) face : Deposits formed on rocksalt (111) face at room temperature and about at  $100^{\circ}\text{C}$  were polycrystalline in nature similar to those obtained on (110) face. Sharper pattern due to increase in crystal size were observed with the rise of temperature.

Deposits formed at about  $200^{\circ}\text{C}$  yielded patterns as shown in figs. (30 and 31) respectively by reflection method with the electron beam grazing along  $\langle 110 \rangle$  and  $\langle 112 \rangle$  of the rocksalt crystals. The presence of 111, 222, and other higher order reflections in the plane of incidence in both the cases and also the fact that the patterns were different suggested that the deposits had developed 2-d  $\{111\}$  orientation. It is seen that in both the cases the patterns are symmetrical but in case of 2-d  $\{111\}$  parallel orientation the pattern will be symmetrical only for the beam direction  $\langle 112 \rangle$  and asymmetrical for other direction  $\langle 110 \rangle$ . Again from the pattern (fig. 31) it is seen that when beam was along  $\langle 112 \rangle$  of NaCl the sides of the rectangle formed by the diffraction spots are in the ratio  $\sqrt{5} : \sqrt{3}$  and hence clearly show that  $\langle 211 \rangle$  of NaCl was parallel to  $\langle 211 \rangle$  of CuI. The appearance of symmetrical pattern (fig. 30)

with beam along  $\langle 110 \rangle$  is, however, due to the presence of parallel and antiparallel orientations developed by the deposit film, as explained before (page 21).

Further it was also observed that though generally the deposits developed parallel and antiparallel orientations on the (111) face of rocksalt in many cases they developed only parallel orientation. The asymmetrical pattern (fig. 32) when beam was along  $\langle 110 \rangle$  clearly shows the presence of parallel orientation alone such that



Many times both the patterns due to parallel and antiparallel orientations were obtained where the pattern due to parallel orientation was more prominent.

These deposits when studied by transmission method yielded patterns similar to figs. (11 & 28) obtained in case of both (100) and (111) faces of rocksalt. This shows that in this case also the deposits when examined by transmission method showed 2-d  $\{211\}$  orientation (cubic) and also  $\{0001\}$  orientation of hexagonal but again in both cases the crystals were azimuthally rotated by  $30^\circ$ . In some patterns the deposits yielded pattern (fig. 33) where there are only six spots just inside the 111 ring instead of 12 spots as in fig. (11) and no spot on 111 ring at all. The disposition of these spots and also their higher orders on other rings suggested the development of hexagonal crystals alone but orientated in such a way that their (0001)

face // to (111) of NaCl. There was no azimuthal rotation of the crystals unlike on NaCl (100) and (110) faces.

Deposits obtained at about 300°C were also similar to those formed at about 200°C except that sometimes strong streaks were observed (fig. 34) <sup>(more strong in negative)</sup> by reflection passing through the diffraction spots indicating refraction effects due to the smooth but undulating nature of the surface layers of the deposit. The asymmetrical character of the pattern was prominent in the patterns though there were other spot, less prominent, showing thereby that the pattern was due to both parallel and antiparallel orientations.

These deposits when studied by transmission method again yielded the patterns similar to the fig. (11) obtained at 200°C, thus again showing the presence of 2-d {211} orientation (cubic) along with {0001} orientation due to hexagonal structure both rotated by 30°. As in case of the deposits formed at 200°C, and studied by transmission method these deposits when studied by transmission method these also yielded another pattern (fig. 35) due to {0001} orientation of hexagonal structure alone again showing similar results as in case of 200°C.

It is interesting to note that the deposits on (111) face of rock salt at different temperatures when studied by reflection method showed parallel orientation due to  $\gamma$ -CuI crystals whereas the same when studied by transmission method showed prominently in one case  $\beta$ -phase {0001} orientation alone

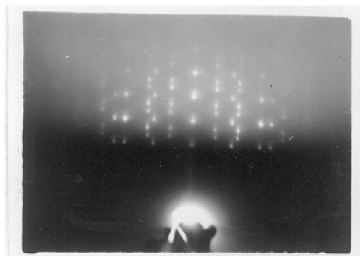


Fig-36

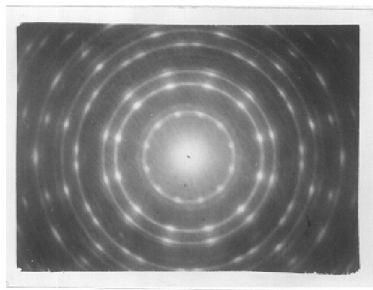


Fig-37

and in other case both 2-d  $\{211\}$  (cubic) and  $\{0001\}$  (hexagonal) orientations. The azimuthal rotation of crystals by  $30^\circ$  was predominantly noticed during the formation of cuprous iodide deposits on different faces of rocksalt at different temperatures.

ii) On KCl (100) face :

Deposits formed on KCl at room temperature and at about  $100^\circ\text{C}$  were polycrystalline in nature.

At about  $200^\circ\text{C}$  the deposits when studied by reflection method yielded pattern (fig. 36) consisting of quite sharp spots and similar to the pattern (cf. fig. 8) obtained in case of the deposits formed on cleavage face of rocksalt. It was found that the deposits in this case developed 2-d  $\{111\}$  orientation and that the deposit crystals were azimuthally rotated by  $30^\circ$ .

Examining these deposits by transmission method again yielded similar results as were obtained in case of the deposits formed on rocksalt cleavage face. The pattern (fig. 37) obtained by transmission method was quite similar to the pattern (fig. 11) and showing thereby the two orientations 2-d  $\{211\}$  cubic and  $\{0001\}$  (hex) developed by the deposits. In both the cases the deposit crystals were azimuthally rotated by  $30^\circ$ .

It was thus found that the deposits of  $\gamma\text{-CuI}$  on



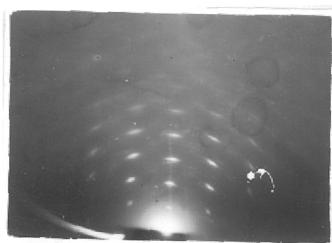


Fig. 38

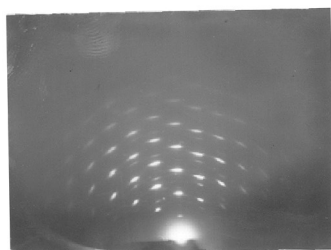


Fig. 39

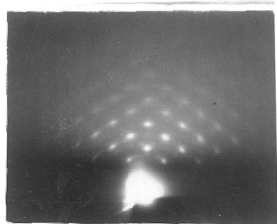


Fig. 40

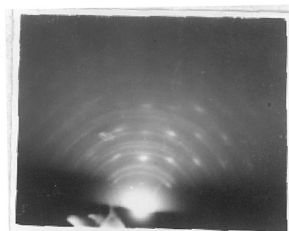


Fig. 41

KCl (100) face showed exactly similar results to that on NaCl (100) face.

iii) On Calcite ( $10\bar{1}1$ ) face :

Deposits obtained on calcite ( $10\bar{1}1$  face) at room temperature or even at about  $100^{\circ}\text{C}$  were polycrystalline in nature.

Deposits obtained at about  $200^{\circ}\text{C}$  yielded patterns (fig. 38) which consisted only of spots. It was also observed that the pattern was changing with beam direction. The pattern (fig. 38) was taken when the beam was parallel to the shorter edge of crystal and other (fig. 39) by rotating the specimen by  $30^{\circ}$ . The presence of 111, 222, etc. in the plane of incidence and other considerations as already mentioned before showed that the deposits had developed 2-d  $\{111\}$  orientation both parallel and also antiparallel type.

Though the deposits formed at about  $300^{\circ}$  were generally similar to above case showing 2-d  $\{111\}$  orientation in some of our experiments these yielded patterns as shown in (figs. 40 & 41). The patterns (fig. 40) consisted of rings as well as spots. The rings were found to correspond to normal cuprous iodide ( $\gamma$ ). It is seen that the spots due to 200, 400, etc. lying in the plane of incidence are on the corresponding rings. These spots together with the spots due to 220, 440, etc. reflections are forming a square type of arrangement. Such arrangement of spots can only be

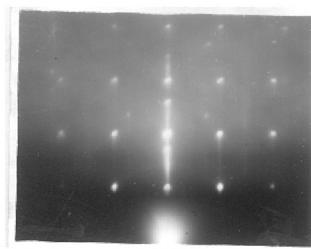


Fig. 42

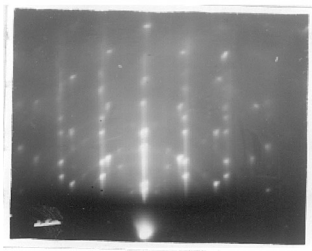


Fig. 43

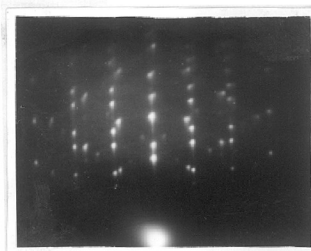


Fig. 44

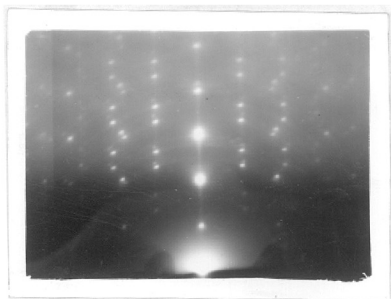


Fig. 45

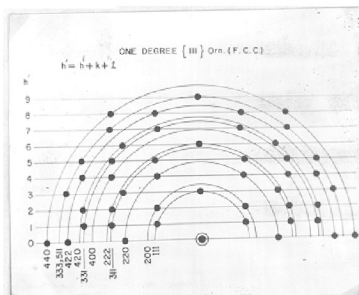


Fig. 46

explained by the formation of 2-d {100} orientation. This orientation was confirmed by observing other patterns (fig.41) by rotating the specimen by  $45^\circ$ ; the two main azimuths for 2-d {100} orientation being  $\langle 100 \rangle$  and  $\langle 110 \rangle$  are at  $45^\circ$  to each other. Thus the two patterns taken for the beam directions along  $\langle 100 \rangle$  and  $\langle 110 \rangle$  of the deposit crystals clearly showed the presence of 2-d {100} orientation developed by the deposit crystals.

It was thus concluded that cuprous iodide deposits on calcite developed both 2-d {100} and 2-d {111} orientations.

iv) On Mica (0001) face :

Cuprous iodide deposited on mica at room temperature was generally polycrystalline in nature as on other substrates discussed before.

Deposits formed on mica cleavage face at about  $200^\circ\text{C}$  yielded mostly spot patterns (fig. 42). It was observed that when the specimen was rotated by  $45^\circ$  the pattern changed considerably (fig. 43). The presence of 200, 400, etc. in the plane of incidence in both the case and also other considerations showed that the deposits had developed 2-d {100} orientation.

It is also seen from the pattern (fig. 42) that besides the spots due to 2-d {100} orientated crystals there are also other spots present in the plane of incidence. It

was found that these extra spots were due to 111 reflections and their higher orders. The deposits thus showed a trace of  $\{111\}$  orientation also. In some patterns continuous rings passing through some of the spots were also observed. Thus the deposits not only developed 2-d orientation, but some were of polycrystalline nature.

The deposits obtained at about  $300^{\circ}\text{C}$  yielded patterns consisting mostly of spots (fig. 44). The presence of 111, 200 and their higher orders in the plane of incidence showed that the deposits had developed 2-d  $\{111\} + \{100\}$  orientations as discussed in the case for  $200^{\circ}\text{C}$ . In this case the two orientations 2-d  $\{111\}$  and 2-d  $\{100\}$  are present in more or less equal amount.

Similar results i.e. the presence of 2-d  $\{111\} + \{100\}$  orientations developed simultaneously by the deposit crystals was also noticed in case of the deposits formed at about  $380^{\circ}\text{C}$ .

An interesting pattern was obtained from thick deposits from cuprous iodide at about  $400^{\circ}\text{C}$  (fig. 45). The arrangement of spots apparently suggested the formation of 2-d  $\{111\}$  orientated crystals, but detail considerations, however, show that they are due to 1-d  $\{111\}$  orientated deposit crystals. Theoretical pattern for 1-d  $\{111\}$  orientation (fig. 46) and 2-d  $\{111\}$  orientation (fig. 9) were considered in details and compared with the observed pattern. The presence of two extra spots due to 331 and 220 both in the

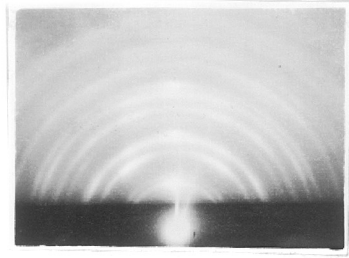


Fig. 47

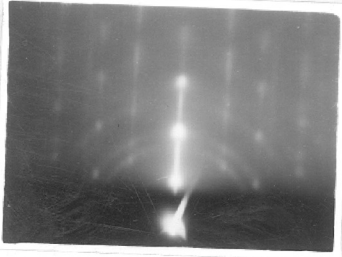


Fig. 48

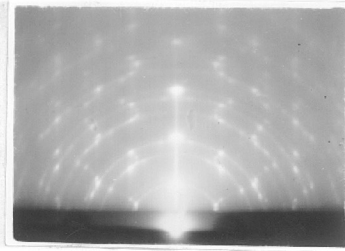


Fig. 49

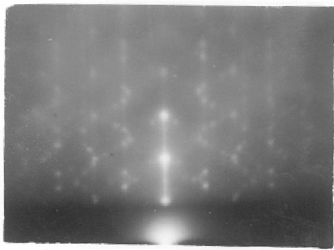


Fig. 50

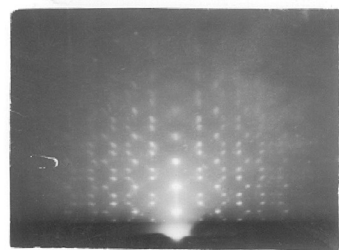


Fig. 50 a

present pattern and in the one due to 1-d {111} orientation but their absence in the pattern due to 2-d {111} orientation conclusively showed that the crystals developed 1-d {111} orientation. This has been described in details further in the case of deposits formed on glass.

Further it is seen from the observed pattern (fig.45) that higher order of 111 reflections are resolved into two spots but they are superimposed more or less, on each other at lower value ~~angle~~ of  $\sin \theta$ . Closer examination also show that there are other spots close to the diffraction spots due to 1-d {111} orientated  $\gamma$ -CuI. This suggests that CuI has developed another new phase structure which was found to be  $\alpha$ -CuI ( $a_0 = 6.15 \text{ \AA}$ ).

It is however interesting to note that the deposits though are in one-degree orientation state, showed nearly perfect orientation as seen from sharp diffraction spots.

v) On Glass :

The deposits obtained at room temperature and upto  $100^\circ\text{C}$  were polycrystalline in nature and sometimes showed a tendency to develop preferred one-degree {111} orientation especially when the deposition was carried out for a longer period of time (fig. 47).

Deposits obtained at about  $200^\circ\text{--}300^\circ\text{C}$  showed in both the cases some peculiar features. The diffraction

patterns (fig. 48 & 49) consisted mostly of spots but elongated considerably towards the shadow edge showing the smoothness of the surface layers. It is also seen from the patterns that the spots in the plane of incidence, especially the first few are much stronger than the other diffraction spots. The appearance of 111, 222 and other higher order reflections in the plane of incidence and also spot type of character suggested that the deposits had apparently developed 2-d  $\{111\}$  orientation. But then the deposits should show a change in the pattern when the specimen was rotated around an axis normal to the beam direction. In experimental results, however, no such change was observed when the specimen was rotated. This suggested the possibility that the deposits might have developed perfect one degree  $\{111\}$  orientation. Comparing the theoretical patterns due to 2-d  $\{111\}$  orientation (fig. 9) with 1-d  $\{111\}$  orientation (fig. 46) it is observed that the diffraction patterns due to both are alike in many details and comparable to the diffraction pattern obtained (fig. 48). Closer examination, however, shows that there are a few spots which should be present only in the case of one-degree  $\{111\}$  oriented crystals but absent for 2-d  $\{111\}$  orientation. The two pairs of spots such as 111 and 200, 311 and 222, etc. should appear only in 2-d  $\{111\}$  orientation. (fig. 9). A pair of spots such as 331 and 420 should appear only in the case of one-degree  $\{111\}$  orientation and should be absent in case of 2-d  $\{111\}$  orientation. Therefore the presence of the spots due to 331 and 420 reflections clearly suggest that the deposits had developed one-degree  $\{111\}$  orientation.



As mentioned above the patterns obtained at  $200^{\circ}$  and  $300^{\circ}\text{C}$  though were generally similar in nature the one obtained at about  $300^{\circ}\text{C}$  was much sharper than those at lower temperature. The streaks observed along with the spots were much more elongated in the former case than in later and thus showing that those deposit surface layers were highly smooth. Similar perfect one-degree  $\{111\}$  orientation was observed in case of  $\text{As}_4\text{O}_6$  deposits by Webb (1951).

Deposits formed at  $350^{\circ}$ -  $400^{\circ}\text{C}$  yielded patterns having peculiar features. The diffraction spots (fig. 50) were quite sharp and the disposition of the spots were such that they formed hyperbolic loci. Similar patterns having the formation of hyperbolic loci were observed by Goche and Wilnan (1959) in case of silver deposits on rocksalt (100) face when studied by transmission method. The formation of hyperbolic loci by the diffraction spots was also observed in case of the deposits prepared at  $300^{\circ}\text{C}$  but was not that prominent as in this case.

Further from the pattern one can see that the spot due to 222 is elongated and the spots in the region of 333 and 444 reflections are not single spots but they consisted of two in each case. Careful examination of the pattern shows that there are pairs of spots due to two different types of crystals in each diffraction region. The arrangement of the diffraction spots in both the cases is quite similar showing that the same orientation was developed by the

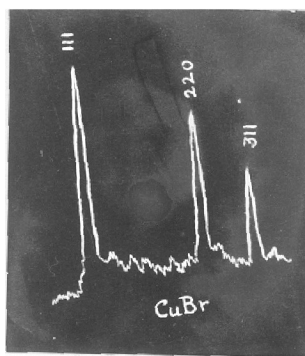


Fig. 51

Table No. III

$I/I_0$	$d \text{ \AA}^\circ$	A.S.T.M.		$a_0$	Mean $a_0$
		$d \text{ \AA}^\circ$	hkl		
v	3.32	3.28	111	5.74	
vf	2.84	2.84	200	5.68	
s	2.04	2.01	220	5.78	
s	1.73	1.71	311	5.73	
f	1.67	1.64	222	5.78	5.74 $\text{\AA}^\circ$
m	1.44	1.42	400	5.76	
mf	1.33	1.306	331	5.79	
ms	1.19	1.16	422	5.81	
f	1.01	1.006	440	5.71	

v = very, s = strong, m = medium, f = faint

two different types of deposits. That the deposits had developed one-degree  $\{111\}$  orientation was also confirmed since the pattern did not change while rotating the specimen. This was no doubt due to the formation of  $\gamma$  as well as  $\alpha$  forms of cuprous iodide deposits both one-degree  $\{111\}$  orientated. Similar result about the simultaneous presence of  $\gamma$  and  $\alpha$  forms was also observed on mica as reported earlier.

(b) Cuprous Bromide :

Cuprous bromide prepared in the laboratory was examined by X-rays. The curve obtained by X-ray spectrograph method is shown in fig.(51). It is seen that the 'd' values and the corresponding peak heights obtained due to different reflections correspond to  $\gamma$ -cuprous bromide having zinc-blende type of structure.

i) Deposition on Rock-salt :

On (100) face : Deposits obtained on rock-salt at room-temperature were polycrystalline in nature and were mostly due to  $\gamma$ -CuBr.

Deposits formed at about  $150^{\circ}\text{C}$  yielded patterns (fig. 52) consisting of rings as well as spots. The 'd' values of the different rings and spots present were found to correspond to normal  $\gamma$ -CuBr (table III). The spots due to 111, 222, etc. in the plane of incidence and other features as already mentioned in case of cuprous iodide deposits clearly



Fig. 52  
CuBr on NaCl (100) at 150°C.

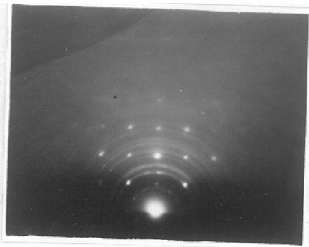


Fig. 53  
CuBr on NaCl (100) at 200°C.  
Beam along  $\langle 001 \rangle$

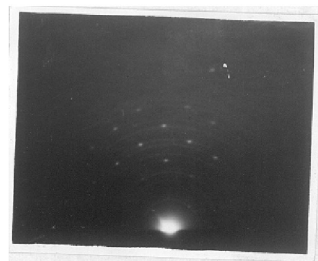


Fig. 54

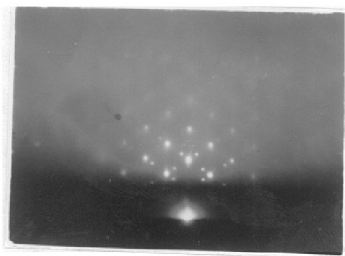


Fig. 55



Fig. 56

indicated that the deposits had developed 2-d  $\{111\}$  orientation, both parallel and anti-parallel type.

Deposits formed at about  $200^{\circ}\text{C}$  when examined by reflection method yielded patterns (figs. 53 & 54) consisting of rings as well as spots. It was also found that the pattern was changed considerably while rotating the specimen around the axis perpendicular to the beam direction. The pattern (fig. 53) was taken when the beam was grazing along  $\langle 001 \rangle$  of NaCl. The square type of arrangement of the spots with the 200, 400 reflections etc. in the plane of incidence showed the presence of 2-d  $\{100\}$  orientation. For 2-d  $\{100\}$  orientation the other important azimuth being  $\langle 011 \rangle$  ( $45^{\circ}$  to  $\langle 001 \rangle$ ) the other patterns (fig. 54) were also taken by rotating the specimen by  $45^{\circ}$ . The above two patterns conformed to the 2-d  $\{100\}$  orientation of the deposits.

Deposits obtained at about  $250^{\circ}\text{C}$  also showed the presence of 2-d  $\{100\}$  orientation. It is also noticed that there are some extra spots (fig. 55) along the direction  $\langle 111 \rangle$  at about  $1/3$  or  $2/3$  distances, thus indicating the presence of  $\{111\}$  twinned structures of the deposits. The deposits thus grew with parallel orientation such that



These deposits when studied by transmission method yielded patterns as shown in fig. (56). The arrangement of the spots is such that they form squares. The comparison

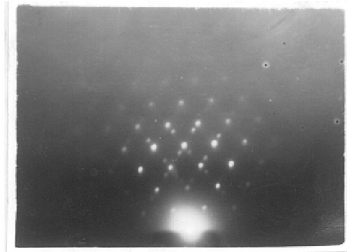


Fig. 57

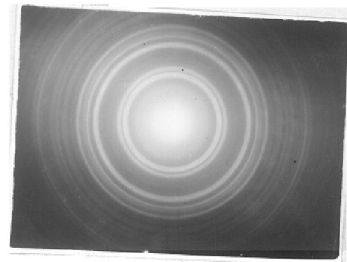


Fig. 58

of this pattern with theoretical 2-d  $\{100\}$  orientated pattern showed that the observed pattern is due to 2-d  $\{100\}$  orientate deposit crystals of cuprous bromide.

It is here interesting to point out that  $\delta$ -CuBr deposits formed at 200-300°C showed 2-d  $\{100\}$  orientation along both by reflection and by transmission methods whereas in case of  $\gamma$ -CuI the deposits showed mostly 2-d  $\{111\}$  orientation by reflection and 2-d  $\{211\} + \{0001\}$  by transmission.

On (110) face : Deposits on (110) face of rock-salt formed at room-temperature were normally polycrystalline in nature and again consisted of  $\delta$ -CuBr.

Deposits formed at about 150°C yielded the patterns as shown in fig. (57) which was taken with the beam grazing along  $\langle 100 \rangle$  of NaCl. It is seen that the pattern consisted of rings and spots due to  $\delta$ -CuBr. Pattern changed considerably when the specimen was rotated around the axis perpendicular to the beam. The spots of 220, 440 reflections etc. in the plane of incidence suggested that the deposits had developed 2-d  $\{110\}$  orientation. It is also seen from the pattern that there are many extra spots present along  $\langle 111 \rangle$  direction of the crystals which are due to the formation of twinned crystals. Similar spots due to twinning were also obtained from deposits formed at higher temperature as described further and were much more prominent. Orientation of the deposit crystals in this case was such that

$\{110\} \langle 110 \rangle$  of CuBr // (110)  $\langle 110 \rangle$  of NaCl





Fig 59  
CuBr on NaCl (111) at 200°C.

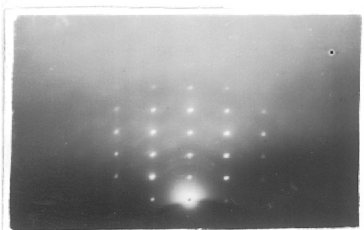


Fig. 60  
CuBr on NaCl (111) at 300°C  
beam along  $\langle 112 \rangle$

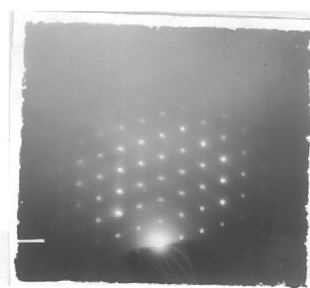


Fig. 61  
CuBr on NaCl (111) at 300°C  
beam along  $\langle 110 \rangle$ .

Deposits formed at about 200°C and 300°C were similar in nature developing 2-d  $\{110\}$  orientation as seen from the patterns taken in different azimuths and comparing them with the corresponding theoretical patterns. The twinning spots obtained in case were more sharp than in the above case.

Patterns from the deposits formed at about 350°C were not good enough to record due to charging up of the specimen. The same deposits when detached from rock-salt in water studied by transmission method yielded pattern as shown in fig. (58). The pattern consisted only of sharp rings indicating that it was due to polycrystalline deposits and the crystals developed were of large size. Measuring the 'd' values of the different rings it was seen that these were corresponding to hexagonal  $\beta$ -cuprous bromide (table IV). It is thus seen that the deposits obtained at 350°C developed  $\beta$ -phase though the initial material was  $\gamma$ -CuBr alone. Thus the deposits of  $\gamma$ -cuprous bromide also showed hexagonal structure at temperature much lower than the bulk transition temperature (391°C) similar to cuprous iodide as reported earlier.

On (111) face : Deposits formed at about 200°C yielded patterns (fig. 59) when the beam was along  $\langle 112 \rangle$  of rocksalt. The arrangement of the diffraction spots are forming rectangles with the sides in the ratio  $\sqrt{3} : \sqrt{8}$ .



Fig. 62

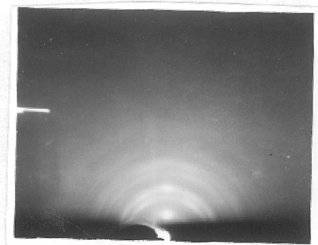


Fig. 63

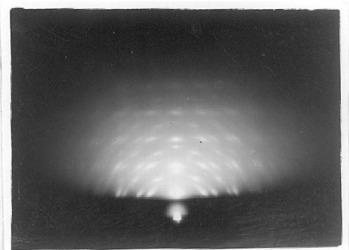


Fig. 64

This together with the presence of 111, 222, etc. in the plane of incidence showed that the deposit crystals developed 2-d {111} orientation.

Similar results i.e. formation of 2-d {111} orientated crystals were obtained from the deposits formed at about 300°C. The pattern (fig. 60) was taken for the beam along  $\langle 112 \rangle$  of rocksalt. The other pattern (fig. 61) was taken when the beam was grazing along  $\langle 110 \rangle$  direction of rocksalt. It is seen that the arrangement of the diffraction spots in this pattern is not symmetrical but asymmetric. This suggested that the deposit crystals had developed parallel 2-d {111} orientation on (111) face of rocksalt, i.e.

$$\{111\} \langle 110 \rangle \text{ of CuBr } // \text{ (111) } \langle 110 \rangle \text{ of NaCl.}$$

ii) On Glass :

Deposits formed on glass at room-temperature yielded patterns similar to fig. (62) due to  $\gamma$ -CuBr.

Deposits obtained at about 150°C yielded patterns as shown in the fig. (63). It is seen that the pattern consisted of rings as well as spots (arced) also. The pattern did not change with change of beam direction. The appearance of 111 and higher orders of these reflections in the plane of incidence suggested the formation of one degree {111} orientation. Deposits obtained at about 250°C yielded patterns (fig. 64) which consisted mostly of arced spots. The presence

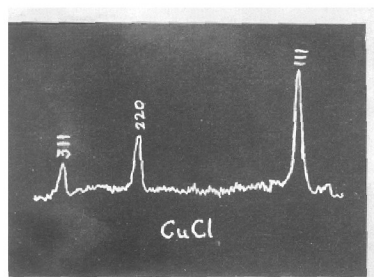


Fig. 65

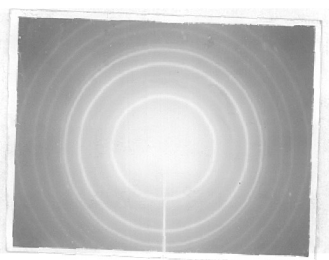


Fig. 66

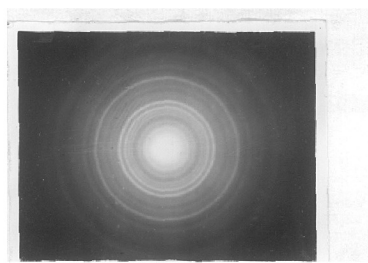


Fig. 67

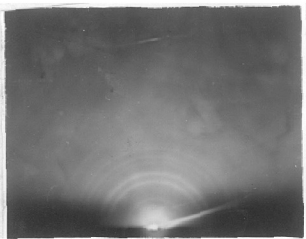


Fig. 68

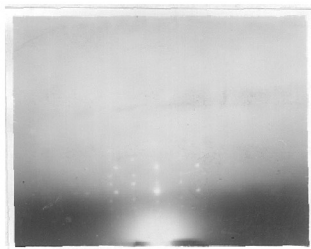


Fig. 69

of 111, 222 etc. and also 200, 400 etc. in the plane of incidence together with the fact that they remained unchanged with change of beam direction indicated that the deposits had developed one degree  $\{111\} + \{100\}$  orientations.

(c) Cuprous Chloride :

Cuprous chloride powder prepared in the laboratory was examined both by X-rays and electron diffraction method. The curve obtained by X-ray spectrograph is shown in fig. (65). The analysis of the same showed that the spacings and the peak heights of the different reflections are corresponding to normal  $\delta$ -cuprous chloride.

Cuprous chloride powders were also sprinkled on the collodion film and then taken on clean monel metal wire gauze and examined in electron diffraction by transmission method. One of the patterns obtained by this method is shown in fig. (66). On analysis of the pattern (table <sup>X</sup>VI) it was observed that the 'd' values of the different rings were quite similar to normal cuprous chloride ( $a_0 = 5.416 \text{ \AA}$ ).

In many of our experiments by this method the specimen yielded along with pattern due to  $\delta$ -cuprous chloride another pattern as shown in fig. (67). The ~~relative~~<sup>relative</sup> position of the different rings as seen from the pattern suggest the presence of another structure other than of cuprous chloride. One of such patterns which was taken along with the pattern due

Table No. V

Analysis of the pattern of fig. (66)

$I/I_0$	$d \text{ \AA}^0$	hkl	$a_0$
vs	3.14	111	5.43
vf	2.73	200	5.44
s	1.90	220	5.37
s	1.62	311	5.37
m	1.36	400	5.44
m	1.22	331	5.32
m	1.11	422	5.43
m	1.03	511+333	5.35
mf	0.96	440	5.42
f	0.90	551	5.32

$$\text{Mean } a_0 = 5.39 \text{ \AA}^0$$

v = very, s = strong, m = medium, f = faint

Table No. VI

$I/I_0$	$d\lambda^{\circ}$	hkl	$a_0$
s	5.439	200	10.88
f	4.049	220	11.30
f	3.334	311	11.10
s	2.783	400	11.10
s	2.23	422	11.17
ns	1.839	600	11.02
ns	1.720	531	11.23
m	1.629	440	10.81
mf	1.587	444	10.99
f	1.487	642	11.12
m	1.386	800	11.08

Mean  $a_0 = 10.88 \text{ \AA}^{\circ}$

s = strong, m = medium, f = faint



to normal cuprous chloride indicated that the pattern was due to a structure other than normal cubic and may be due to a cubic structure but having high lattice parameter. The different 'd' values of the rings obtained as measured with the rings due to normal cuprous chloride are given in table (VI). It is seen from the 'd' values that almost all the rings could be well accounted for a cubic structure with lattice parameter, equal to  $10.98 \text{ \AA}^{\circ}$  (table VI)

i) Deposition on Rock-salt :

On (100) face : Deposits of cuprous chloride formed at room temperature on rock-salt cleavage face when studied by reflection method yielded patterns as shown in fig. (63) which is exactly similar to the one obtained by sprinkling cuprous chloride powder on collodion film (fig. 66). The analysis of the pattern showed that evaporated film consisted entirely of  $\gamma$ -CuCl.

These deposits when studied by transmission method after detaching the film from rock-salt substrate under water yielded pattern which was exactly similar to fig. (67). Thus it was seen that though by reflection  $\gamma$ -CuCl was observed, by transmission the deposit film showed another structure having  $a_0 \approx 10.58 \text{ \AA}^{\circ}$ . This has been repeated several times. All the time the reflection pattern gave normal  $\gamma$ -CuCl whereas transmission patterns were due to another structure.

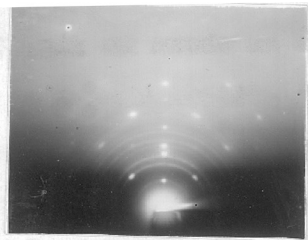


Fig. 70  
CuCl on NaCl (100) at 300°C  
Beam along  $\langle 001 \rangle$  NaCl.

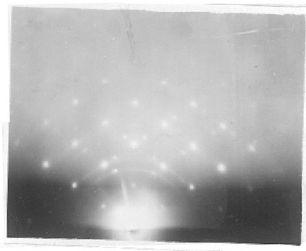


Fig. 71  
CuCl on NaCl (100) at 300°C  
beam along  $\langle 001 \rangle$  NaCl.



Fig. 72  
CuCl on NaCl (110) at 200°C  
beam along  $\langle 001 \rangle$

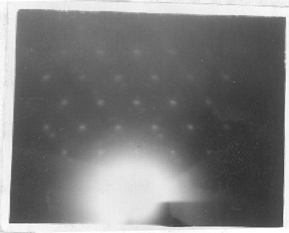


Fig. 73  
CuCl on NaCl (110) at 200°C  
beam along  $\langle 011 \rangle$



Fig. 74  
CuCl on NaCl (110) at 200°C  
beam along  $\langle 111 \rangle$

Deposits formed at about 200°C and when studied by reflection method yielded patterns as shown in fig. (69) with beam along  $\langle 001 \rangle$  of NaCl. It was noticed that the pattern was changing as the specimen was rotated and the same pattern was obtained when the specimen was rotated by 30°. Similar results were also obtained in case of cuprous iodide deposits on cleavage face of NaCl. As explained in case of cuprous iodide deposits it was observed in this case also that the deposits had developed 2-d  $\{111\}$  orientation where the deposit crystals were azimuthally rotated by 30°.

The above deposits when examined by transmission method again yielded the pattern similar to fig. (67). This again showed that though the deposits showed 2-d  $\{111\}$  orientation by reflection due to  $\delta$ -CuCl by transmission entirely another structure other than  $\delta$ -CuCl was obtained.

Deposits at about 300°C when examined by reflection method yielded pattern (fig. 70) with beam along  $\langle 001 \rangle$  of NaCl. It is seen that the pattern consisted mostly of spots and due to 2-d  $\{100\}$  orientation. The other pattern (fig. 71) taken with beam along  $\langle 011 \rangle$  of NaCl conform to the above mentioned orientation. From the pattern (fig. 71) it is also seen that along with the main spot pattern due 2-d  $\{100\}$  orientation there also spots present along  $\langle 111 \rangle$  direction and at distances  $1/3$  and  $2/3$  along this line. This indicated the presence of  $\{111\}$  twinning of the crystallites. It was thus noticed that

cuprous chloride deposits obtained at about  $300^{\circ}\text{C}$  showed a tendency to develop parallel orientation along with  $\{111\}$  twinned crystals.

The above deposit when studied by transmission again yielded the pattern exactly similar to the one as shown in fig. (67). It was also noticed that the pattern is due to polycrystalline material as was also observed in previous cases.

On (110) face : Deposition of cuprous chloride at room temperature on (110) face of rocksalt showed that the deposits were polycrystalline in nature.

Deposits formed at  $200^{\circ}\text{C}$  and  $300^{\circ}\text{C}$  were quite similar in nature and yielded patterns when examined by reflection method as shown in figs. (72, 73, 74). The change in the pattern while rotating the specimen indicated that the deposits had developed 2-d orientation. The pattern (fig. 72) taken with the beam direction parallel to  $\langle 100 \rangle$  of rocksalt cube face showed the spots due to 220, 440 in the plane of incidence. This suggested that the crystals developed 2-d  $\{110\}$  orientation. Pattern (fig. 73) was obtained with beam along  $\langle 110 \rangle$ . Comparing the theoretical patterns of 2-d  $\{110\}$  orientations for these two directions it was concluded that the deposits had developed parallel orientation i.e. 2-d  $\{110\}$  orientation on (110) face of rocksalt. From the pattern it is also seen that there are some extra spots which

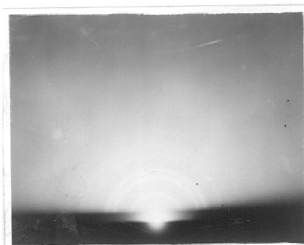


Fig. 75  
CuCl on glass at room temp.



Fig. 76  
CuCl on glass at 150° to 200°C

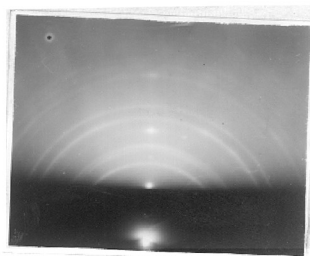


Fig. 77

were accounted by twinning on  $\{111\}$  plane. Patterns (fig.74) with beam along  $\langle 111 \rangle$  direction also conform to the above view.

When these deposits were examined by transmission method after detaching these from rocksalt (110) face yielded pattern similar to (fig. 67) consisting only of rings. It was, therefore, observed in case of (110) face of rocksalt deposits were of  $\gamma$ -form as noticed by reflection method and they yielded patterns different from those due to normal  $\gamma$ -CuCl.

ii) On Glass :

The deposits obtained at room temperature were polycrystalline in nature. The sharp rings obtained (fig.75) indicated the formation of large crystallites of  $\gamma$ -cuprous chloride (Table V).

Deposits formed at about  $150^{\circ}\text{C}$  on glass yielded pattern as shown in fig. (76). It is seen that the pattern is consisting of rings and also spots. The presence of rings and spots showed the polycrystalline deposit was accompanied by orientated one also. The spots on the rings 111, 222, 333 and so in the plane of incidence suggest the formation of  $\{111\}$  orientation. It was also noticed that rotating the specimen around an axis perpendicular to the beam there was no change in the pattern. If the deposits would have been 2-d orientated

the pattern for two azimuths  $\langle 110 \rangle$  and  $\langle 112 \rangle$  would have been different. Again comparing the theoretical 2-d  $\{111\}$  orientated pattern and 1-d  $\{111\}$  orientated with the observed one also shows it was due to 1-d  $\{111\}$  orientated crystals. As explained in case of cuprous iodide deposits, though patterns due to 1-d  $\{111\}$  and 2-d  $\{111\}$  orientated deposits are quite similar in nature, the presence of the pair of spots due to 331 and 420 clearly conform to 1-d  $\{111\}$  orientation.

Deposits obtained at  $200^{\circ}\text{C}$  again developed one degree  $\{111\}$  orientation. The pattern (fig. 76) was consisting mostly of spots. There was not much indication of the presence of rings and thus showing that the deposits showed nearly perfect one degree  $\{111\}$  orientation.

At about  $250^{\circ}\text{C}$  the deposits developed more than one orientations. The prominent orientation was 1-d  $\{111\}$  as obtained in above cases also. The extra spots <sup>(fig. 77)</sup> such as 200, 400, etc. in the plane of incidence showed that  $\{100\}$  orientation of the  $\text{CuCl}$  crystals was also present. It was also noticed that rotation of the specimen around the axis perpendicular to the beam the pattern remained unchanged. It was thus seen that the deposit developed both 1-d  $\{111\}$  and  $\{100\}$  orientations.

Action of Water : It was often noticed in the case of cuprous chloride deposits that they showed  $\gamma$ -structure by reflection method. As soon as these deposits came in contact

with water while removing from the substrate by dipping in water they showed invariably a structure different from  $\gamma$ -CuCl. It appears to be linked with the treatment of water.

To investigate the action of water on CuCl the deposits were initially examined by reflection and then dipped in water for a few seconds to a minute and again re-examined by reflection method. This showed similar results as were obtained by transmission method. These deposits were also tested by dipping in alcohol. No change in the nature of the deposits was however observed. Finally the deposits ( $\gamma$ -CuCl) after dipping in alcohol were dipped in water for about a minute and again studied by reflection method. The pattern in this case was exactly similar to fig. (67) giving  $a_0 \approx 10.33 \text{ \AA}^\circ$ .

Thus it seems that the deposits of  $\gamma$ -CuCl as soon as came in contact with water they changed to another compound. It is also known that when CuCl is dissolved in water the solution soon turns turbid and finally changes to  $\text{Cu}_2\text{O}$  after long standing. CuI and CuBr, however, do not show such change. Thus it appears that the water treated compound having ( $a_0 = 10.33 \text{ \AA}^\circ$ ) seems to be some sort of a basic hydroxide of copper.



D. DISCUSSION

Cuprous halides generally have either zinc-blende ( $\gamma$ ) or wurtzite ( $\beta$ ) type of structure though another modification ( $\alpha$ ) has some times, been reported for CuI, and CuBr. Three crystallographic modifications of CuI are (1)  $\gamma$ -CuI having a f.c.c. type of structure with  $a_0 = 6.05 \text{ \AA}^0$ , (2)  $\beta$ -CuI, hexagonal ( $a_0 = 4.31 \text{ \AA}^0$ ,  $c_0 = 7.09 \text{ \AA}^0$ ,  $c_0 / a_0 = 1.645$ ) and (3)  $\alpha$ -CuI again f.c.c. with  $a_0 = 6.15 \text{ \AA}^0$ . (A.S.T.M. card Nos. 6-0246, 6-0685, 6-0623). Cuprous bromide has similar modifications viz. (1)  $\gamma$ -CuBr f.c.c. ( $a_0 = 5.69 \text{ \AA}^0$ ), (2)  $\beta$ -CuBr hexagonal ( $a_0 = 4.06 \text{ \AA}^0$ ,  $c_0 = 6.66 \text{ \AA}^0$ ,  $c_0 / a_0 = 1.64$ ) and (3)  $\alpha$ -CuBr is body centred cubic ( $a_0 = 4.5 \text{ \AA}^0$ ) (A.S.T.M. Card Nos. 6-0292, 6-0700, 6-0310).  $\gamma$ -form of cuprous chloride with  $a_0 = 5.416 \text{ \AA}^0$  is supposed to exist at room temperature alone (A.S.T.M. Card No. 6-0344). Lorenz and Prener (1956) observed high temperature form with  $a_0 = 3.91 \text{ \AA}^0$ ,  $c_0 = 6.42 \text{ \AA}^0$ ,  $c_0 / a_0 = 1.64$  which seems to be the  $\beta$ -form. No  $\alpha$ -form is yet been reported.

From the above studies it is seen that though materials started with were of  $\gamma$ -forms of cuprous halides, the deposits obtained were either of  $\gamma$  or  $\beta$  in the case of CuI and CuBr or a mixture of them depending upon the temperature of deposition. For CuCl only  $\gamma$ -form was observed. Occasionally, however,  $\alpha$ -form of CuI was also observed along with  $\gamma$ -form. In the case of CuCl, new structures, one of spinel type and another having double the lattice parameter of that of  $\gamma$ -form were noticed. In one case, however, one b.c.c. type of compound having  $a_0 = 4.5 \text{ \AA}^0$  was observed from CuCl. This may be the  $\alpha$ -form of CuCl. It is interesting to mention that the deposits of cuprous iodide

formed on the surface layer invariably had  $\gamma$ -form as seen by reflection but those in between of the substrate and top layers consisted of a mixture of  $\gamma$  and  $\beta$  forms.

Orientations of halide crystals :

Deposits of cuprous iodide both on rock-salt and KCl cleavage faces at temperatures varying from  $150^{\circ}$  to  $300^{\circ}\text{C}$  developed mostly 2-d  $\{111\}$  orientations (cubic) as observed by reflection method and the top surface layers consisted entirely of  $\gamma$ -CuI crystals. The symmetrical nature of the pattern in the  $\langle 110 \rangle$  directions of the crystals showed that the deposit crystals had developed parallel and antiparallel  $\{111\}$  orientations with respect to the substrate such that  $\langle 110 \rangle$  of crystal //  $\langle 100 \rangle$  of rocksalt or KCl. These deposits, however, by transmission showed the presence of 2-d  $\{211\}$  (cubic) orientation of  $\gamma$ -CuI together with  $\{0001\}$  orientation developed of the  $\beta$ -form. In both the cases the crystals were azimuthally rotated by  $30^{\circ}$ . The reason for the presence of  $\gamma$ -CuI alone at the surface layers, but a mixture of  $\gamma$  and  $\beta$  forms in the underneath layers is discussed below.

The appearance of 2-d  $\{211\}$  and  $\{0001\}$  orientations by transmission method but only 2-d  $\{111\}$  orientation by reflection suggested that the former might have arisen from the double twinning phenomena. It is well known that in case of f.c.c. crystals twinning occurs on  $\{111\}$  planes. Cuprous iodide has also  $\{111\}$  twinning plane. Dana (1957)<sup>reported</sup> ~~observed~~

repeated twinning in the case of CuI. We have observed that evaporated halide (CuI) often grew with  $\{111\}$  planes parallel to the substrate planes. Twinning on  $\{111\}$  planes of the  $\{111\}$  orientated crystals would give rise to (115) plane parallel to the initial plane. This twinned crystal on retwinning on (111) would bring (13, 7, 5) exactly parallel to the initial (111) plane. This last mentioned plane (13, 7, 5), is nearly equivalent to (2 1 1) plane, though off by about  $5.5^\circ$  (Trehon and Goswami 1959). In the case of transmission patterns the detached films are often bent and hence  $\{211\}$  plane not being far off from the initial orientation is likely to give diffraction pattern, thus suggesting that the crystals had also developed nearly  $\{211\}$  orientation along with the initial  $\{111\}$ .

Similar results i.e. 2-d  $\{211\}$  and 2-d  $\{0001\}$  orientations were also obtained by transmission method both on (110) and (111) faces, though by reflection method it was noticed that the deposits on these faces developed parallel orientations. It is interesting to note here that though by reflection usually 2-d  $\{111\}$  orientation was noticed on (100) face but at higher temperature ( $\approx 340^\circ\text{C}$ ) the deposits showed a tendency to develop parallel i.e. 2-d  $\{100\}$  orientation.

On calcite CuI developed mostly 2-d  $\{111\}$  orientation at temperatures ranging between  $200^\circ$  to  $300^\circ\text{C}$ . Sometimes a mixture of both 2-d  $\{111\}$  and 2-d  $\{100\}$  orientations was also

observed. Similar mixed orientation were also observed on mica. At low temperatures on mica, however, 2-d  $\{100\}$  or<sup>n</sup> was more prominent than 2-d  $\{111\}$  whereas at higher temperatures both the orientations were equally prominent. At about 400°C, sometimes, the deposits obtained were due to both  $\gamma$ -CuI and also  $\alpha$ -CuI forms. It was also noticed that the crystals of both these structures developed perfect one degree  $\{111\}$  orientation as observed by the sharp distinct spots in the diffraction pattern.

On glass deposits developed perfect 1-d  $\{111\}$  orientation associated with hyperbolic loci. The reason for this will be discussed later on.

Cuprous bromide deposits at higher temperatures grew epitaxially showing parallel orientations of  $\delta$ -form on all the three faces (100), (110) and (111) of rock-salt sometimes with the formation of  $\{111\}$  twinned crystallites. On glass, however, these deposits developed mostly one degree  $\{111\}$  orientation sometimes with one degree  $\{100\}$  orientation.

Cuprous chloride crystals grew epitaxially on cleavage face of NaCl even at lower temperature and developed 2-d  $\{111\}$  orientation similar to CuBr and CuI but at higher temperatures they developed parallel orientations on the (100) face. Similarly a 2-d  $\{110\}$  orientation was also observed on (110) face of rocksalt. As in case of cuprous bromide extensive twinning on  $\{111\}$  planes was also noticed even by reflection method.

CuCl film showing  $\gamma$  structure, however, changed to a new form ( $a_0 = 10.88 \text{ \AA}^0$ ) when treated with water. This seems to be due to formation of a basic hydroxide not so far reported. A new form of spinel ( $a_0 = 8.265 \text{ \AA}^0$ ) has also been observed and an investigation on its structure is given in chapter IV.

Phase Transition :

As mentioned before the deposits on the surface layer were of  $\gamma$ -form whereas those in between the substrate and the surface layers often showed hexagonal structure along with  $\gamma$ -form even though the material started had a  $\gamma$ -structure. The hexagonal phase was observed at a temperature as low as  $200^\circ\text{C}$  whereas the bulk transition temperature for cuprous iodide is reported to be  $369^\circ\text{C}$  (A.S.T.M. Card No.6-0246). The probable reason for the appearance of both  $\gamma$  and  $\beta$  forms seems to be linked with the growth mechanism of crystals during the deposition process. This can be understood from the consideration of different layers of atoms in  $\{111\}$  planes of f.c.c. crystals. In this plane there are layers of atoms occupying three different positions as denoted by A, B, C in the layers.

A B C A B C A B C etc.

If the layers grow in the above sequences they will form the f.c.c. crystals with maximum close packing of atoms.

It is also possible that sequences of layers may slightly change such that atoms in any one layer viz. the third layer 'C' instead of occupying its normal position which is different from that of A or B may be just above 'A' thus still retaining the maximum packing of atoms. This will give rise to a sequence

A B A B A B . . . etc.

which is nothing but the structure for a close packed hexagonal crystals. This sort of growth of layers can be caused both by twinning process or due to a fault in the stacking arrangement of the atoms during the growth process.

It is well-known that f.c.c. crystals generally tend to develop  $\{111\}$  twinned structures causing a reversal of stacking of atoms. The sequence of layers may be illustrated as

A B C A <sup>\*</sup>B A C <sup>\*</sup>B C A B . . . etc.

where the reversal of sequence of layers take place at the position marked with asterisk due to the formation of  $\{111\}$  twinned crystallites. This reversal need not only be on the same layers as 'B' as shown above, but can be random and on any of the A, B or C layers. This growth can also be viewed from the point of faults in stacking of layers. In the ideal case the sequence of layers will be as

A B C A B C A B C . . . etc. as before.

A random reversal of layers amounts to the development of stacking fault. The formation of twinned crystallites or the appearance of a regular stacking fault in the layers will give rise to a hexagonal structure with  $c/a = 1.623$  retaining the same packing of atoms similar to that of f.c.c. type structure. Irregular stacking faults will, however, give rise to an additional effect in the diffraction pattern such as streaks passing through the normal diffraction spots. This has been observed often in the case of many transmission patterns of cuprous iodide and many sulphide crystals (Chapter V).

Thus the appearance of hexagonal structure can be attributed to twinning or stacking fault. It may, however, be mentioned here that  $\{0001\}$  orientation of hexagonal crystals is equivalent to  $\{111\}$  orientation of the cubic form. Hence it may be considered that the layers underneath top surface had mostly 2-d  $\{211\}$  along with  $\{111\}$  orientation the later being equivalent to  $\{0001\}$  of hexagonal. It has already been shown that  $\{211\}$  orientation could have come from initial  $\{111\}$  orientation by double twinning phenomena.

The reason for the appearance of  $\gamma$ -form on the surface layers but both  $\gamma$  and  $\beta$  in between layers seems to be the following.

During the initial stage of the growth cuprous iodide deposits grew epitaxially on rocksalt, with  $\{111\}$  orientation. As the deposition proceeded further because of

the double twinned phenomena the crystals developed  $\{211\}$  orientations along with  $\{0001\}$  of hex. It seems that this process continued and ultimately the top surface had also possibly similar orientations. The substrate along with the deposits was generally cooled slowly in the furnace when the deposition was over. It is likely that during this process the top surface layers were annealed thus removing their twinned structures or stacking faults without affecting the underneath layers which still retained the growth faults. Such a removal of twinned structure or stacking fault as shown by <sup>Goche &</sup> Wilman (1939) in case of silver deposits on rock salt will favour the formation of the f.c.c. structure. It is quite possible that annealing for a longer time would have completely removed all the faults including those underneath the surface layers, as mentioned above especially if the deposit film was detached from the substrate surface.

Hyperbolic loci :

Interesting diffraction patterns were obtained from cuprous iodide deposits formed on glass. These patterns, as described before, consisted of sharp distinct spots apparently due to nearly perfect one degree  $\{111\}$  orientation developed by the deposit crystals. The spots were arranged in such a way that they formed a hyperbolic loci. Similar patterns have been observed by rotation of single crystal flakes of  $\text{MoS}_2$  (Finch & Wilman 1937) or mica (Finch & Wilman 1936). Hyperbolic loci have been explained from the point of view



of bending of the flakes along certain crystallographic directions. In the present case, however, hyperbolic loci was observed even in case of reflection patterns. <sup>Goche</sup> & Wilman (1939) observed similar hyperbolic loci in transmission patterns of silver deposits on rocksalt and suggested that they arose from bending of the film caused by strain after removal from the substrates. A similar explanation may also hold good here. Though bending or buckling of the films cannot be adduced in the present case to their removal from substrates, it is quite likely that deposits would be under strained condition because of inhomogeneous cooling through the different layers and this may result in buckling or rotation of the deposit crystals.

\* \* \* \*

CHAPTER IV

STRUCTURE ANALYSIS

A. Principle of Structure Analysis by Electron Diffraction :

During the electron diffraction studies on evaporated films of cuprous chloride and tin sulphide some new structures were observed. It was thought necessary to carry out the intensity measurements of the different reflections in order to investigate into their structures in more details. The location of atoms in thin films can be achieved by electron diffraction technique but not by X-ray method. Recently electron diffraction methods have been used for a number of structure analyses both for organic and inorganic materials (Z.C.Pinsker 1953, B.K.Vainshtein 1956, J.H.Cowley 1954, Cowley & Rees 1958, Cowley, Rees and Spink 1951, Cowley and Goswami 1961).

The diffracted beam is suitably collected and recorded. The intensities of the different reflections were then compared with those from trial structures similar to X-ray method. Though the general principle is similar to that of X-rays the structure analysis by electron diffraction is beset with many difficulties such as unreliability in the electron scattering factors for different atoms, ions etc. (ii) appearance of dynamical effect along with kinematical scattering for thicker films, shape factors, orientations etc. With proper care most of the above difficulties can be surmounted.

The intensity of scattered electrons can be measured either (a) in a Faraday cylinder by measuring the current with an electrometer which is time consuming or (b) by the photographic method. In the later case the intensity of the beam is determined as a function of the blackening of the photographic plates.

The relation between the density of blackening of plates with Electron Energy :

The relationship between the intensity of diffracted beam on a given area of a photographic plate is known as the 'Law of photographic blackening for electrons'.

The magnitude of photographic blackening of plates is given by the relation

$$D = \log \frac{I_0}{I} \quad (1)$$

$I_0$  is the incident light upon the plates and  $I$  is the light passing through that area of the plate.

The law relating to the photographic blackening of the plates by electron beam is given by the relation

$$D = D ( It^P ) \quad (2)$$

where  $D$  is the total blackening,  $I$ , the incident radiation of electrons,  $t$ , the exposure time and  $P$ , a constant.

Generally for fast electrons and X-rays

$$D = D(I t) \quad \text{or} \quad D = D(S) \quad (3)$$

where  $S = I t$

Thus it is seen that  $D$  depends both on  $I$  and  $t$ . The relation in equation (3) is known as "Linearity law" for photographic blackening.

Further the relation between  $D$  and  $S$  is not constant since it depends to a great extent on the nature of photographic emulsions, conditions of developing, fixing etc.  $D$  also depends though to a smaller extent on the voltage of the electron beam. Different types of photographic plates have different characteristics with respect to their sensitivity to electron beam. Hence the density range for linearity law varies with different types of plates when exposed to electron beam. The characteristics can also vary to some extent with electron volts. Bushkin and Keyner (1948) have shown that for the electrons accelerated by  $\approx 20$  KV or less the curves obtained ( $D$  vs  $\log S$ ) became useless for intensity measurements. Charlesby (1940), Bognolov and Sevast'yanova (see Pinsker 1953) have found that the relation between the photographic density of the plates and the total electron energy impinging on the plates can be represented by

$$D \propto S \quad \text{or} \quad D \propto \log S \quad (4)$$

For some plates, however, the range of linearity law or logarithmic law can be very narrow.

For our investigation we have used Ilford special rapid plates and studied its characteristics with respect to electron beam.

Multiexposure method :

The method used in electron diffraction to measure the intensity of different reflections is slightly different from that of X-rays. In the later case multi-film technique is used i.e. packets of different films are used and X-rays are allowed to pass through them. Intensity of beam falls exponentially in the successive films. In case of electron diffraction multi-film method cannot be used since electrons cannot pass through these films at all. Multi-exposure method is therefore used for the electron diffraction case. In this method a number of exposures are given to the photographic plates with increasing time keeping the incident electron energy constant. Thus the blackening of the successive plates will be proportional to 't' or "log t" depending on the plate characteristics. Emission of electrons from cathode was kept constant during the recording of the patterns. Exposed plates were then developed and fixed under standard conditions and at constant temperature (20°C) and finally dried at room-temperature. Each series of plates was normally developed and fixed under the same conditions and at the same time.

The density of the exposed plates was measured with a non-recording type microphotometer made by Hilger (H.451 type). The density of blackening of the plates at different positions

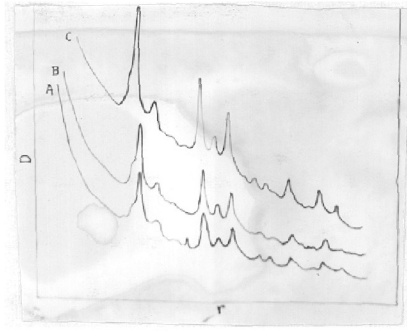


Fig. 78

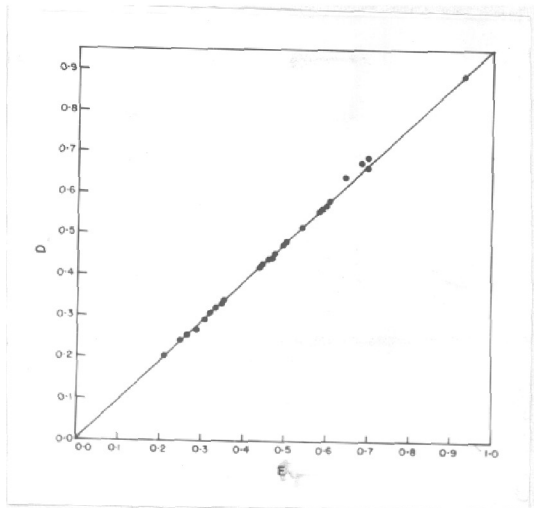


Fig. 79

Table No. VII

<del>(<math>\frac{D_1}{D_2}</math>)</del>	$D_1$	$D_2$	$R = D_1/D_2$	Mean R i.e. $R_m$
8.4	0.830	0.886	0.936	
9.8	0.553	0.582	0.950	
11.2	0.451	0.479	0.941	
12.5	0.405	0.437	0.926	
13.0	0.416	0.444	0.936	
13.6	0.620	0.662	0.936	0.950
14.3	0.440	0.474	0.928	
15.9	0.330	0.334	0.980	
18.9	0.330	0.332	0.993	
20.6	0.299	0.319	0.937	
24.6	0.255	0.268	0.951	

was calculated from the deflection of galvanometer. Normally the background density falls monotonically with the radial distance ('r' or  $\sin \theta/\lambda$ ) from the central beam position.

Characteristics of the plates with regard to electron beams :

Before carrying out the structure analysis one should know whether the linearity law or logarithmic law holds good within the working range of intensity of diffracted beam. This is done by plotting 'density' against 'r' or ( $\sin \theta/\lambda$ ) for successive plates. Fig. (78) shows such a plot for three plates.

Since our aim was to find out the density region within which the linearity relationship holds good the ratio 'R' of the density of total blackening of two plates exposed by multi-exposure method at the different distances was calculated. This may be written as

$$R = \frac{D_1}{D_2} \quad (5)$$

where  $D_1$  and  $D_2$  are the total blackening of the two plates at the corresponding distance 'r' or ( $\sin \theta/\lambda$ ) from the central spot. The ratio 'R' was calculated for different positions of graphs (maxima or minima) at different density regions and tabulated in table (No.VII). Their mean value ( $R_m$ ) was then used in determining  $R_1$  factors where  $R_1$  is given as

$$R_1 = D_1/R_m \text{ or } D_2/R_m \quad (6)$$



These  $R_1$  values were then plotted against the corresponding  $D$  values ( $D_1$  or  $D_2$ ) and the graph thus obtained is shown fig. (79).

From the graph it is seen that linearity relation for Ilford special rapid plates holds good for the density region of 0.2 and 0.9. It is also seen further that variation at position beyond the range of 0.2 to 0.9 is not much different from the linearity relationship. For accuracy we have mostly used the density range of 0.3 to 0.8 for intensity measurements in the investigation of the structures, as described in part (B) and (C) of this chapter.

For carrying out the intensity measurements one has to measure the actual contribution due to the different hkl reflections. This was done by the method of Karle and Karle (1950). In this method the background intensity which was mostly caused by the inelastic scattering of electrons by the crystals is deducted from the total intensity by drawing a smooth continuous curve (see fig. 82). Then the area under each peak gives the contribution from the different reflections.

---

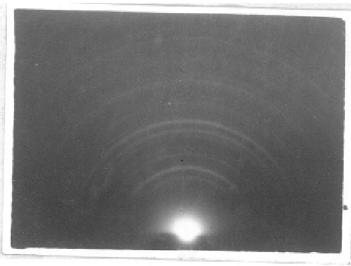


Fig. 80  
CuCl on NaCl(100) at 230°C

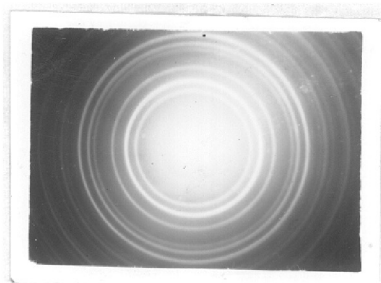


Fig. 81  
Specimen (Fig. 80) by transmission.

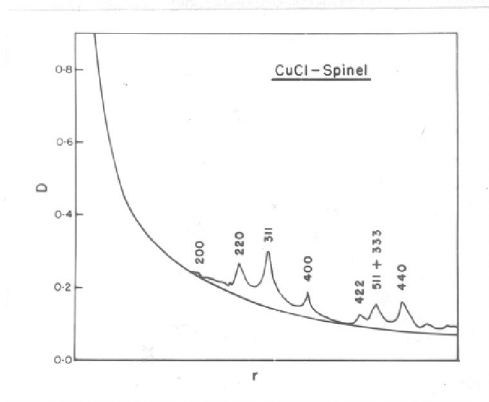


Fig. 82

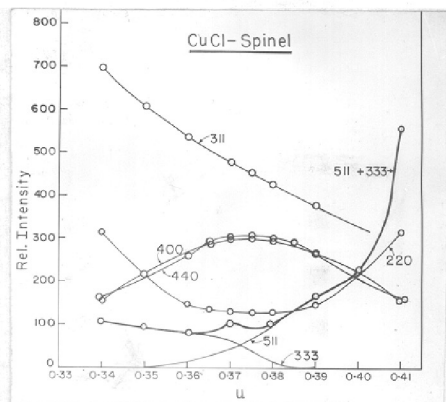


Fig. 83

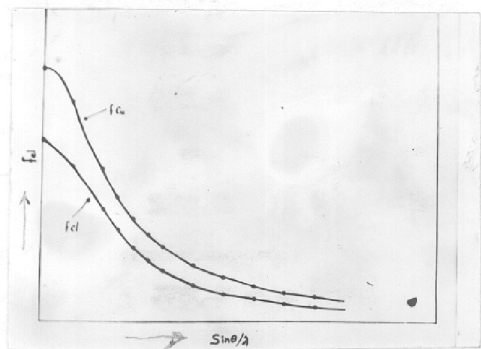


Fig. 84

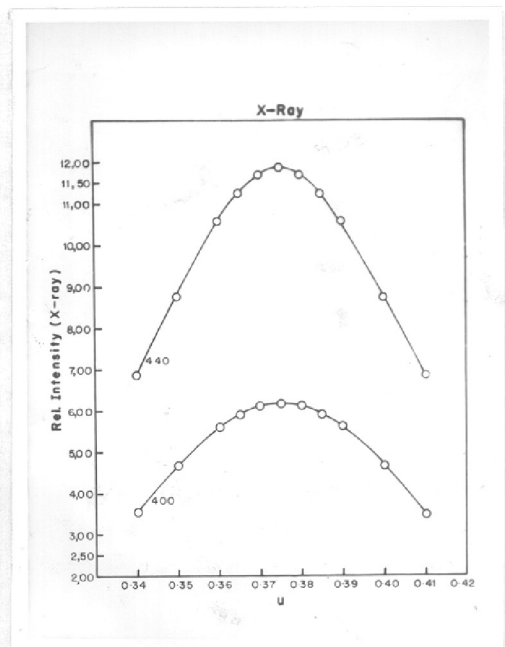


Fig. 85.

Table No. VIII

CuCl - SPINEL

Analysis of the pattern of fig. (81)

Intensity	d Å <sup>o</sup>	hkl	a <sub>o</sub>
	4.73	111	8.182
s	2.916	220	8.246
vvs	2.483	311	8.224
s	2.074	400	8.296
m	1.689	422	8.274
s	1.595	511,333	8.287
vs	1.464	440	8.151
vf	1.416	531	8.378
mf	1.315	620	8.316
m	1.264	533	8.288
f	1.198	440	8.299
vf	1.152	711	8.226
f	1.109	731,553	8.224
ms	1.081	-	-
f	1.039	800	8.312

Mean a<sub>o</sub> = 8.265 Å<sup>o</sup>

v : very, s = strong, m = medium, f = faint

B. A New Spinel from Cuprous Chloride :

Spinel usually have  $AB_2X_4$  type of composition where A and B are di- or tri-valent metal atoms and X the anions normally oxygen or sulphur. Spinel having anions other than the above divalent oxygen or sulphur have not so far been reported.

During electron diffraction studies of deposits obtained from  $\gamma$ -CuCl as mentioned previously [Chapter III(c)] we occasionally observed a new type of structure, the intensity of hkl reflections of which was quite different from those of normal  $\gamma$ -CuCl. Such deposits were obtained by evaporating  $\gamma$ -CuCl on glass or on rocksalt at about  $230^\circ\text{C}$ . Fig. (80) shows the different rings obtained from the compound. The pattern did not change even by treatment of water.

Fig. (81) shows the transmission pattern obtained from the deposits on rocksalt. It is seen that both the patterns (figs. 80 & 81) are quite similar in nature. The 'd' values of different hkl reflections were measured using  $11\bar{2}0$  ring of graphite ( $1.230 \text{ \AA}^0$ ) as standard and tabulated in (Table VIII). The lattice constant  $a_0$  was found to be  $= 8.265 \text{ \AA}^0$ . It is also seen from the pattern that the reflections present were either all odd or all even and that 311 reflection was the strongest. The other important reflections in order of decreasing intensity distribution were 440, 400, 511, 333 and 111 and also that 200 was practically absent. The large value of the lattice constant ( $a_0 = 8.265 \text{ \AA}^0$ ) along with the fact that 311 reflection was strongest suggested

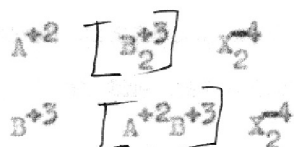
the possibility that the deposits had developed a spinel type of structure where 311, 440 and 400 are characteristic reflections in decreasing order of intensity. It is also known that spinels normally have high lattice constant of the order of  $7.9 \text{ \AA}^0$  or more.

Before the structural analysis of the above compound was carried out, the relationship between total blackening of the photographic plates and the energy of the electron beam was investigated for the Ilford special rapid plates, which were used in our work. All calculations were carried out for the reflections having intensity region between 0.5-0.8. The line profile due to the different reflections was obtained from the microphotometer readings and integrated intensities were evaluated by the method of Karle and Karle (1950). The microphotometer readings of the ring patterns due to unorientated polycrystalline deposits of spinel structure yielded the curve shown in fig. (82). In this curve density of blackening of the plate was plotted against 'r', (or  $\sin \theta/\lambda$ ). The crystal size was determined from the measurement of half width of the different peaks. The average crystal size was found to be of the order of  $42 \text{ \AA}^0$ . The integrated intensities of the different reflections were calculated by measuring the area under the corresponding peaks after deducting the background effect due to inelastic and also elastic scattering of electrons by the atoms of the crystal. These were then normalized by converting the value of 311 reflection to  $\frac{\text{hundred}}{\lambda}$  and the other values proportionately. The theoretical intensities

were also calculated assuming a trial structure and compared with observed intensities.

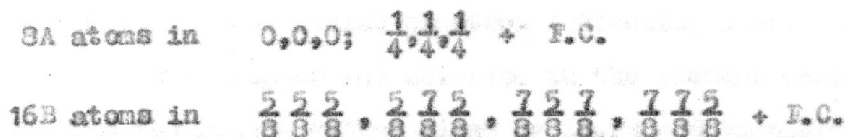
Structurally spinels belong to the space group  $O_h^7$  -  $Id3m$  having 56 atoms in the unit cell where the anions form the lattice frame work in which metal ions occupy the tetrahedral and octahedral holes created by the anions. There are 8 molecules in an unit cell in which A atoms occupy 8 of the 64 possible tetrahedral sites and B atoms, 16 of the 32 possible octahedral positions (Wyckoff 1948).

Spinel can be of the two types normal and inverse and can be written as :



In the inverse spinel 8 of the B atoms occupy the tetrahedral sites and  $8A^{+2}$  ions and  $8B^{+3}$  ions occupy the octahedral sites. Structurally there will not be any difference in the intensity of reflection arising out of normal or inverse spinel if there is only one type of metal ions present.

The coordinates of the positions of 56 atoms in case of the ideal spinel are as follows :



$$\begin{aligned}
 32X \text{ atoms in } & u u u ; u \bar{u} \bar{u} ; \frac{1}{4} -u, \frac{1}{4} -u, \frac{1}{4} -u ; \frac{1}{4} -u, \\
 & \frac{1}{4} +u, \frac{1}{4} +u ; \bar{u} u \bar{u} ; \bar{u} \bar{u} u ; \frac{1}{4} +u, \frac{1}{4} -u, \\
 & \frac{1}{4} +u ; \frac{1}{4} +u, \frac{1}{4} +u, \frac{1}{4} -u + \text{F.C.}
 \end{aligned}$$

The value of 'u' for ideal case is 0.375 (= 3/8), but it may vary slightly depending on the nature of the spinel. It is seen that 'u' determines the position of anions. However, for all real spinels the value of 'u' is slightly different from the ideal one (u = 3/8) as given above.

Assuming that the spinelization has taken place from cuprous chloride deposits, the electron diffraction intensity distribution from different reflections can be calculated theoretically from the relation

$$I \propto F^2 d^2 p$$

where I = the integrated intensity from different hkl reflections;

$$F = \sum f_{el} \cos 2\pi (hx + ky + lz) + \sum f_{el} \sin 2\pi (hx + ky + lz);$$

d = the corresponding lattice spacing of the reflection;

p = multiplicity factor i.e. the number of planes taking part during scattering.

The value of  $f_{el}$  the atomic electron scattering factors for different atoms (copper and chlorine in the present case) was taken from the recent values given by Ibers and Vainshtein (1960), (fig. 84).

The general formulae for the above space group ( $O_{h}^7$  -  $Rd3M$ ) were taken from International tables for X-rays and it was found that it can be reduced into simpler formulae for each reflection which were used in the present case and are given below :

---

hkl (cubic)

---

111	$4\sqrt{2} f_A - 8f_B + 16\sqrt{2} f_X (\cos^3 2\pi u + \sin^3 2\pi u)$
220	$8f_A + 32f_X \cdot \cos^2 4\pi u$
311	$4\sqrt{2} f_A + 8f_B + 16\sqrt{2} f_X (\cos^2 2\pi u \cos 6\pi u - \sin^2 2\pi u \sin 6\pi u)$
222	$16f_B + 32f_X (\sin^3 4\pi u)$
400	$8f_A - 16f_B + 32f_X (\cos 8\pi u)$
331	$4\sqrt{2} f_A - 8f_B + 16\sqrt{2} f_X (\cos^2 6\pi u \cos^2 2\pi u + \sin^2 6\pi u \sin 2\pi u)$
422	$8f_A + 32f_X (\cos 8\pi u \cos^2 4\pi u)$
511	$4\sqrt{2} f_A + 8f_B + 16\sqrt{2} f_X (\cos 10\pi u \cos^2 2\pi u + \sin 10\pi u \sin^2 2\pi u)$
333	$4\sqrt{2} f_A + 8f_B + 16\sqrt{2} f_X (\cos^3 6\pi u - \sin^3 6\pi u)$
440	$8f_A + 16f_B + 32f_X (\cos^2 8\pi u)$

and so on

---

At first calculations were made for each hkl with  $u = 3/8$  ( $= 0.375$ ) and then value of 'u' was slowly varied by



Table IX (a)  
 Calculated <sup>Absolute</sup> ~~Relative~~ Intensity (I)

u →	0.34	0.35	0.36	0.37	0.375	0.38	0.39	0.40	0.41
hkl ↓	I								
220	314	218	144	131	129	131	144	218	314
311	702	609	539	483	457	431	382	363	265
400	156	221	271	298	302	298	271	221	156
511	-	4	16	44	69	98	166	220	565
333	106	90	64	57	25	13	3	-	-
440	156	213	269	303	308	303	269	213	156

Table No. IX (b)

<u>hkl</u>	<u>i<sub>obs.</sub></u>	<u><math>\frac{i_{cal}}{u=375}</math></u>
111	10	7
220	58	23
311	100	100
400	26	66
422	18	7
511+333	35	20
440	52	67

$\pm 0.04$  on either side and the corresponding calculations were made for all the reflection for different values of  $u$ . Table (IX) shows the different values of  $I_k$  for different hkl reflections with change of  $u$  <sup>and table IX b</sup> ~~along with~~ the observed values. The calculated values of  $I_k$  <sup>when normalised</sup> do not fit well with observed ones (of table IX). There are some discrepancies in the intensity of some hkl reflections and especially in case of 440, 400 and 220 reflections.

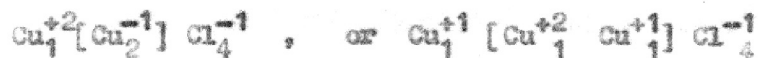
Graphs plotted for the relative intensity of different hkl reflections against the values of  $u$  are shown in fig. (83). These have some special features. It is seen that 311 reflection is strongest for all reasonable values of  $u$  and that it gradually decreases with increase in  $u$ . Both 440 and 400 reflections gradually rise in values and then fall symmetrically around the ideal value of  $u$ . They have more or less same values for a particular value of  $u$ . The 220 reflection gradually decreases in the beginning and again rises symmetrically contrary to 400 and 440 where it is in the reverse way. Contributions of 511 + 333 are such that 333 contributes most at low values of  $u$  where as 511 at higher values of  $u$ . The combined effect of both is such that at higher values of  $u$  at 0.4 the contribution becomes very high even much more than 311. A striking discrepancy is observed in the case of 440 and 400 reflections. In no case however  $I_{400}$  becomes much less than  $I_{440}$  but the observed intensity of 400 reflection is much less than that of 440.

This difference can only be removed when  $f_{el}$  for 400 has less value than given by Ibers and Vainshtein. Using the X-ray atomic factors for  $I_{400}$  and  $I_{440}$  (~~3:1~~) the ratio of  $I_{440} / I_{400}$  becomes comparable with the observed one. The variation of the intensity of  $I_{440}$  and  $I_{400}$  with change of 'u' in case of X-rays is shown in fig. (85).

It is further seen from graph (fig. 83) and the corresponding table (IX) that for the position of  $u = 0.35$  the results agree reasonably well with the observed one. At this position the intensities of  $I_{220}$ ,  $I_{440}$  and  $I_{511 + 533}$  are quite comparable with the observed ones. But then  $I_{511} / I_{440}$  becomes 3:1 whereas the observed ratio is 2:1. This discrepancy may not be too much considering many factors contributing to it. These are (1) the uncertainty in the position of metal atom different from the ideal position at centre of the tetrahedral and octahedral holes because of their small sizes (0.7 to 0.9 Å<sup>0</sup>) compared to anion (1.81 Å<sup>0</sup>). This may be more aggravated in thin films where they may not be in their most stable state; (2) inaccuracy in atomic scattering factor  $f_{el}$ . Ibers (1960) has shown that the values of  $f_{el}$  are not much accurate at smaller values of  $\sin \theta / \lambda$ . (3) the possible non-stoichiometric composition in the above spinel type of compounds. Wyc<sup>k</sup>off (1948) have suggested that discrepancy in the intensities of different reflections is well-known in case of many spinels due to hapazard arrangement of metallic atoms.

Thus the best fit in the intensity of hkl reflections theoretically compared with the observed ones seems to be near at position with  $u \simeq 0.35$ . Since the experiment could not often be repeated a thorough study on the structure could not be carried out.

The observed integrated intensities of the different reflections also indicated the compound to be of the type  $R_3 X_4$  i.e.  $Cu_3Cl_4$  in the present case. From structural consideration its composition would be



which also satisfy the neutrality of charge in the molecule.

It will be interesting to know how the new spinel could be formed from cuprous chloride. Since cuprous chloride has low melting point, it is likely that it might decompose in the filament itself during evaporation in the following way.



In fact it was found that the filament was coated with red coloured deposit during evaporating process. This supports the above view of formation of a new spinel.

The above mentioned mechanism of the spinel formation seems to be more probable than the alternate one as



since cupric chloride is soluble in water its presence in cuprous chloride does not seem to be likely. Further there was no trace of cupric chloride in the original sample of cuprous chloride.

From the cell constant it is possible, however, to estimate the ionic radius of the chlorine atom. Since the cell constant of a spinel is not affected by the metal atoms but only by the effective radii of anions the ionic character of chloride was roughly estimated from the measured lattice constant. From the calculated radius  $1.46 \text{ \AA} \left( \frac{8.265}{4\sqrt{2}} \right)$  compared to fully ionic radius  $1.81 \text{ \AA}$  it seems that the ionic character of chloride is decreased considerably. This decrease in the ionic character shows the tendency towards the tetrahedral or neutral atomic state.

---

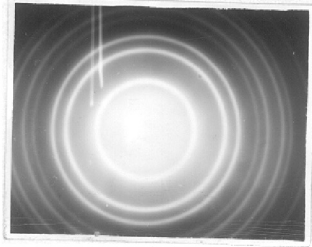


Fig. 86

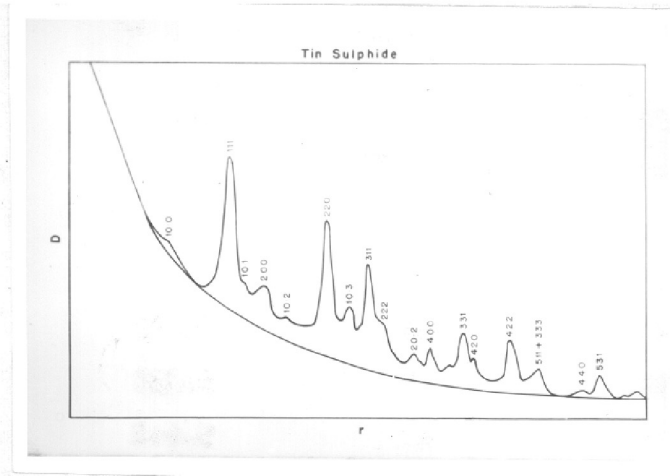


Fig. 87

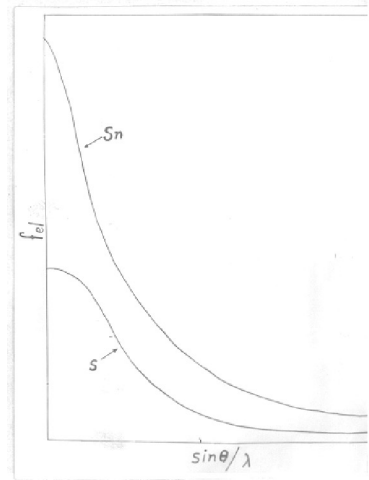


Fig. 88

Table No. X

Tin Sulphide (Cubic)

Analysis of the pattern of fig. (86)

Intensity	$dA^{\circ}$	hkl	$a_0$
VVS	3.134	111	5.422
f	2.829	Due to normal SnS	-
Spot	2.758	200	5.516
VS	1.922	220	5.435
S	1.644	311	5.453
f	1.584	222	5.487
m	1.360	400	5.440
ms	1.251	331	5.453
ms	1.111	422	5.442
m	1.048	333 + 511	5.445

Mean  $a_0 = 5.454$

---

V : very,    S = strong,    m = medium,    f = faint



C. Investigation on the Structure of evaporated tin sulphide

During the evaporation of tin sulphide prepared in the laboratory various structures such as h.c.p., along with its cubic form, normal orthorhombic as mentioned further (Chapter V) a f.c.c. type of structure was also observed. In the following investigation has been made on the last mentioned compound.

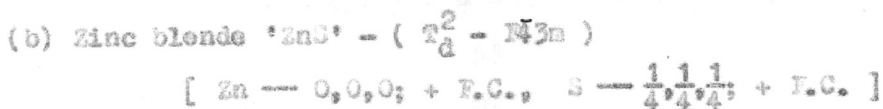
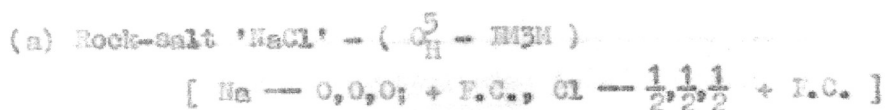
The tin sulphide prepared in the laboratory (cf. Chapter V) was evaporated from a filament on rocksalt substrate, at room or higher temperatures. These deposits were then heated further to about  $425^{\circ}\text{C}$  in vacuo either in contact with the substrate or after its removal from the substrate. After heating the specimen for the required period of time (one hour generally) these were examined in electron diffraction camera by transmission methods.

The pattern obtained from such specimens is shown in fig. (86). Table (X) shows the 'd' values of the different reflections having the lattice constant =  $5.445 \text{ \AA}$ . It is also seen that the 'hkl' reflections present had either all even or all odd values. No mixed indices were present at all. Since there was no change in the intensity of the rings while tilting the specimen around an axis normal to the beam direction, it was concluded that the pattern was due unorientated polycrystalline deposits alone.

It is seen from the pattern (fig. 86) that the

relative intensities of 111, 220 and 311 reflections were in decreasing order and 200 was practically absent. Neither the intensities nor the 'd' values, however, correspond to any of the known sulphide compounds of tin namely stannous sulphide and stannic sulphide.

To evaluate the general structure of the deposits, the integrated intensities of the different hkl reflections were measured with non-recording type microphotometer and then compared with the following possible structures such as



From the microphotometer readings the curve for 'r' or  $\sin \theta/\lambda$  against density was plotted. (fig. 87). The background intensity was deducted by drawing a smooth curve as described previously. A few of the many curves drawn, however, showed extra maxima other than those due to cubic structure. From the curves (fig. 87) it will be seen that the positions of the extra maxima correspond to a h.c.p. type of structure ( $a_0 = 3.34 \text{ \AA}$ ,  $a_0 = 5.36 \text{ \AA}$ ,  $c_0/a_0 = 1.603$ ). From these curve integrated intensities were also measured. In cases where hexagonal phase was present the contribution from h.c.p.

Table No. XI

Crystal Size

hkl	Crystal size in $\text{\AA}^{\circ}$ (approx.)	Mean
111	33	
220	34	
311	37	
400	37	36 $\text{\AA}^{\circ}$
331	36	
422	35	

type of structure was deducted from the total contribution in order to get the value of cubic phase alone. The crystal size was also measured from the half width intensity maxima. These results are shown in table (XI). It is seen that the average crystal size was of the order of  $36 \text{ \AA}$ .

To compare the observed integrated intensities of the different reflections theoretical intensities were also calculated from the relation.

$$I \propto F^2 d^2 p$$

where  $I$ ,  $F$ ,  $d$  and  $p$  have their usual meanings as given earlier.

For different structures e.g. NaCl, ZnS and CaF<sub>2</sub> types.

Atomic scattering factors for electrons for different values of  $\sin \theta/\lambda$  for the atoms 'Sn' and 'S' were taken from the recent values of Ibers and Vainshtein (1960) and are shown graphically in fig. (88). No temperature effect was taken into consideration in the present case.

The relative values of 'I' for the three different type of structures e.g. 'NaCl', 'ZnS' and 'CaF<sub>2</sub>' type were then compared with the observed values. The results obtained for these three types of structures and also the observed values are shown in table (XII) after normalizing the calculated and observed values of 220 reflection to 100.

Table No. XII

hkl	Relative Intensities			Observed
	ZnS type	NaCl type	CaF <sub>2</sub> type	
111	222	42.5	118	215
200	21	182	10	-
220	100	100	100	100
311	58	14	3	62
222	4	28	1	-
400	11	11	11	15
331	18	4	9	26
420	5	27	-	4
422	18	18	-	19

It is seen from table (XII) that the sulphide of tin having 'NaCl' type of structure would have 200 reflections strongest whereas it is practically absent in the pattern. Another obvious discrepancy in this case is that of the intensity of 111 reflections which should be less than 200 for 'NaCl' type of sulphide whereas it is more in the observed case. For 'CaF<sub>2</sub>' type of structure also the agreement is not good enough with the observed one since 111 and 220 reflections are nearly equal in the former case whereas it is in the ratio of 2:1 (approx) in the later. Other anomalies can also be noticed for the other reflections of 'NaCl' type and 'CaF<sub>2</sub>' type of structures compared with the observed one.

Another probable cubic structure which is sometimes observed in sulphides or oxides having all odd or all even reflections present is of spinel type. Since all spinels have normally high lattice parameter (  $8 \text{ \AA}^0$  ) and 311 reflections are the strongest and 111 comparatively weak, contrary to our observation, spinel structure is thus ruled out. It, therefore, appears that the sulphide of tin had its atomic coordinates at positions.



similar to that of zinc blende.

Consideration of atomic radii of in cubic close

packing system determines the structure of many compounds. Thus  $r_c / r_a$  for ZnS, NaCl and CsCl structures are respectively between 0.22 to 0.41, 0.41 to 0.71 and 0.71 to 1.0. The ratio  $r_{Sn} / r_S = (0.386)$  also conforms to the above mentioned structure. It may be argued that, both lead and tin belonging to the same group should have similar PbS structures (NaCl) type but its, lower  $r_c / r_a$  value, compared for PbS (0.456) favours ZnS type of structure.

CHAPTER V

STRUCTURES AND THE GROWTH OF SULPHIDE FILMS OF TIN,

BISMUTH AND ANTIMONY

A. Introduction

Tin is known to form two well defined sulphides namely stannous sulphide ( $\text{SnS}$ ) (A.S.T.M. Card No.1-0984) and stannic sulphide ( $\text{SnS}_2$ ) (A.S.T.M. Card No.1-1010). Another sulphide of tin, however, less well established is tin sesoqui-sulphide,  $\text{Sn}_2\text{S}_3$  (Neller 1930). Hofmann (1935) suggested that stannous sulphide has a deformed structure similar to galena. Wells (1958) has suggested that the structure of stannous sulphide consisted of very buckled hexagonal nets in which alternate atoms are tin and sulphur.

Among the known sulphides of antimony only the structure of stibnite,  $\text{Sb}_2\text{S}_3$ , is well established one. It is orthorhombic with  $a_0 = 11.229 \text{ \AA}$ ,  $b_0 = 11.310 \text{ \AA}$ ,  $c_0 = 3.839 \text{ \AA}$  (A.S.T.M. Card No.6-0474). Bridgmann (1916, 1955) presented data for the polymorphic transitions of antimony sulphide. According to Harold and others (1939) red  $\text{Sb}_2\text{S}_3$  showed no evidence of crystalline nature but the black variety prepared by heating the red form at about  $115^\circ\text{C}$  gave a pattern identical with that of stibnite thus indicating that there could be little if any amorphous material present. Tatarinova (1957) showed by the method of integral analysis that in stibnite each antimony atom is surrounded by 5.7 atoms



of sulphur and each sulphur atom is surrounded by 3.8 atoms of antimony indicating that atoms in amorphous  $Sb_2S_3$  tend towards a dense packing.

Bismuth sulphide,  $Bi_2S_3$ , is the only well known sulphide of bismuth. It is analogous to antimony sulphide being orthorhombic in structure ( $a_0 = 11.15 \text{ \AA}$ ,  $b_0 = 11.30 \text{ \AA}$ ,  $c_0 = 3.981 \text{ \AA}$ ) (A.S.T.M. card No.6-0333). Another sulphide of bismuth,  $BiS$ , has occasionally been reported (Mellor 1933) but its structure, has not been established.

Clark and Anderson (1943) reported that stannous sulphide is an electrical semiconductor at all temperatures. According to them even at  $750^\circ\text{C}$  the ionic component is less than 1% of the total and also even fused 'SnS' is a probable semiconductor. Anderson and others (1945) have presented an evidence to conform the suggestion that the high temperature conduction of SnS represents the intrinsic electronic conductivity of the crystal lattice. Yurkov (1953) has studied the rectifying properties of the stannous sulphide crystals. Grimm and Masel'dov (1956) have given data on the conductivity of sulphides and selenides of tin for mass and thin layers.

Tika Asai (1940, 1941) has studied the relation between the structure and photoconductivity of the layer of bismuth sulphide. They observed that the layers of  $Bi_2S_3$  crystals with excess of bismuth prepared by evaporating Bi and S separately in vacuo have the largest photo-conducting

effect. They also studied the effect of change of temperature and the degree of vacuum on structures and properties of the films. The uses of such layers of the films have also been mentioned. Yurkov (1952) has measured the electrical conductivity and thermoelectric power for  $Sb_2S_3$  from R.T. to  $620^{\circ}C$ . Lyashenko and Snitko (1954) studied the effect of adsorption of some organic compounds for the semiconductors like  $Cu_2S$ ,  $Sb_2S_3$ ,  $Bi_2S_3$ ,  $SnS$ , etc.

From the above survey of literature it will be seen that the sulphides of tin, antimony and bismuth have got semi-conducting properties. These are also being used in some solid state devices. Apart from their uses in vacuum tube amplifier, crystal rectifier etc. not much is known about their structure, orientation etc. It is known that many properties especially the electrical and photo-conducting depend much on the crystal structure, and orientation. A change of structure may also take place in thin films made by evaporation process. It was, therefore, thought necessary to study the structure of thin films of these sulphides and results are described in the following sections.

### B. Experimental

#### Preparation of Stannous Sulphide :

Stannous chloride (pure cryst) obtained from Riedel-de-Hoen, A.G.; was dissolved in 1:1 hydrochloric acid (AnalaR) by warming for sometime in presence of granular tin metal to prevent the oxidation.  $H_2S$  gas (washed with distilled water) was passed for several hours (about 8 hours) in the clear solution. The precipitate thus obtained was washed with distilled water till it was free from chloride. The precipitate was then washed with ethyl alcohol and finally dried in vacuum desiccator<sup>c</sup>.

Bismuth sulphide, bismuthinite, was obtained from M/s B.D.H. (London) and antimony sulphide from (S.Merck, Darmstadt).

The above sulphides were evaporated from Kanthal filament in vacuo in the manner as described earlier (Chapter II). The patterns taken were mostly by transmission type since the reflection patterns were not good enough in most cases for recording due to too much charging up of the specimen.

---

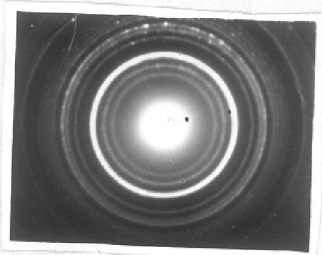


Fig. 89  
SnS on collodion film

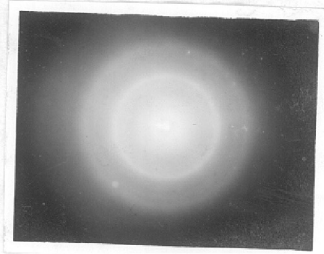


Fig. 90  
SnS on NaCl(100) at room temp.

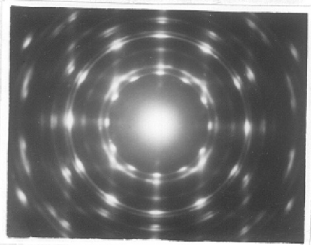


Fig. 91  
SnS on NaCl(100) at 200°C

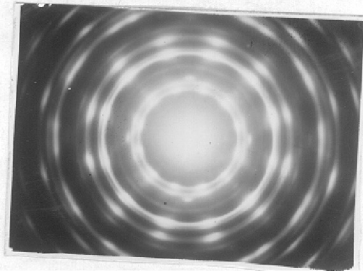


Fig. 92  
SnS on NaCl(100) at 300°C

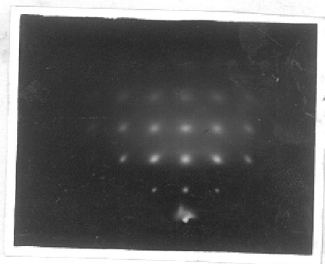


Fig. 93  
SnS on NaCl(100) at 400°C  
beam along  $\langle 001 \rangle$  of crystals

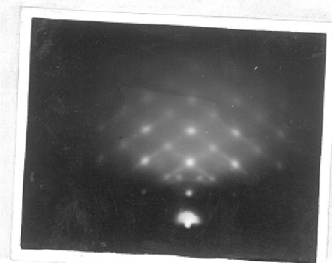


Fig. 94  
SnS on NaCl(100) at 400°C  
beam along  $\langle 011 \rangle$ .

### C. Results

X-ray studies of the stannous sulphide powder did not yield any suitable maxima probably due to fine grain nature of the compounds.

Sprinkling of the stannous sulphide powder on collodion film and then examining by diffraction condition in an electron microscope, however, yielded patterns as shown in fig. (89). On analysis of the pattern it was found the 'd' values and the intensity distribution of the different reflections corresponded to normal stannous sulphide (Table XIII) having a orthorhombic structure (A.S.T.B. Card No.1-0984).

#### Deposition on Rock-salt :

At 25<sup>o</sup>-100<sup>o</sup>C : Deposits obtained at room temperature yielded halos (diffuse) type of patterns. One or two specimens out of the several, however, showed that the deposit crystals had very fine grain structure as could be seen from diffuse rings (fig. 90). Similar results were also obtained from the deposits formed at about 100<sup>o</sup>C.

At about 200<sup>o</sup>C : Deposits formed at this temperature yielded patterns (fig. 91) consisting of spots as well as rings. On analysis the same showed that the 'd' values (Table XIV) of the different reflections did not correspond to normal 'SnS'. Normally these deposits developed a 2-d orientation, sometimes along with polycrystalline deposits. Though the 'd' values

Table No. XIII

Analysis of the pattern of fig. (89)

$I/I_0$	$d \text{ \AA}^{\circ}$	$d_{(X\text{-ray})}$	hkl
ms	4.06	4.04	110
ms	3.47	3.42	120
vs	2.84	2.83	040
m	2.32	2.30	041
ms	2.12	2.12	210
ms	2.03	2.02	220
mf	1.85	1.87	211
mf	1.80	1.73	112
f	1.73	1.72	240
mf	1.63	1.62	042
m	1.46	1.45	202

v = very, s = strong, m = medium, f = faint

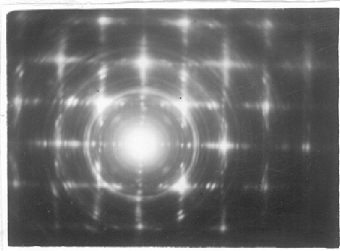


Fig. 95

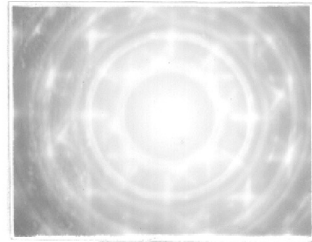


Fig. 96

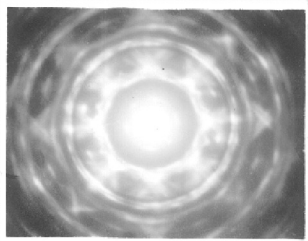


Fig. 97

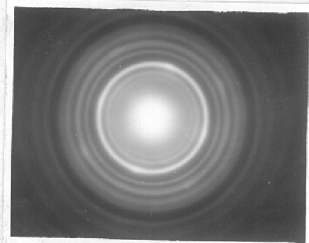


Fig. 98a

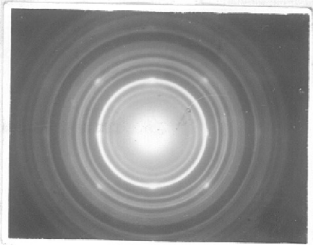


Fig. 98b

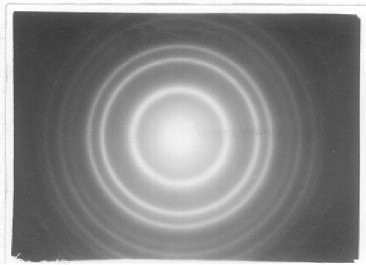


Fig. 99a

Table No. XIV

Analysis of the pattern of fig. (91)

$I/I_0$	$d \text{ \AA}^0$	hkl	$c_0 (\text{\AA}^0)$
vf	4.46	-	-
f	4.06	-	-
s	3.128	10.0	5.10
m	2.89	00.2	5.01
s	2.77	10.1	5.12
m	2.17	10.2	5.16
f	2.03	00.3	5.28
vs	1.816	11.0	5.13
m	1.736	11.1	5.27
f	1.59	2.00	5.19
mf	1.539	11.2	5.18
f	1.184	21.0	5.14

$$\text{Mean } c_0 = 5.14 \text{ \AA}^0, \quad a_0 = 3.13 \text{ \AA}^0$$

$$c_0 / a_0 = 1.64$$

v = very, s = strong, m = medium, f = faint



of the different hkl reflections could not be explained on the basis of orthorhombic structure all the reflections could be accounted for with a new h.c.p. structure (Table XIV) having  $a_0 = 3.14 \text{ \AA}$ ,  $c_0 = 5.17 \text{ \AA}$ ,  $c_0 / a_0 = 1.64 \text{ \AA}$ . Some of the deposits, however, developed 2-d  $11\bar{2}0$  orientations. Along with the h.c.p. phase, sometimes, there also appeared rings or spots due to cubic ( $a_0 = 5.14 \text{ \AA}$ ) form which was more prominent in the cases of deposits formed at about  $300^\circ\text{C}$ .

At  $250^\circ\text{--}300^\circ\text{C}$  : These deposits were similar to those obtained at about  $200^\circ\text{C}$ . The sharp diffraction spots and rings (fig. 92) indicated that the crystals dimensions were larger in size and also that they developed better orientation. From the patterns, it could be seen that the deposits had developed, along with the h.c.p. structure as in the former case, a cubic phase. This cubic structure seems to be associated with the above h.c.p. structure. The four spots just outside the  $10\bar{1}1$  reflection and forming a square network of pattern showed the formation of a cubic structure. The lattice constant ( $a_0$ ) calculated from the 200 reflections was found to be  $= 5.17 \text{ \AA}$ . The pattern from cubic structure in this case was more pronounced than those obtained at about  $200^\circ\text{C}$ .

At about  $400^\circ\text{C}$  : The deposits of stannous sulphide gave better patterns only by transmission method as mentioned earlier. At this temperature, however, one of the specimens

yielded reasonable patterns by reflection. The patterns (fig. 95) by reflection were taken for the beam direction along 001 of NaCl and the others (fig. 94) along  $\langle 011 \rangle$  of NaCl. It is seen that the diffraction spots had formed a square type of net-work thus suggesting the formation of 2-d 100 orientation. This was also confirmed from the pattern (fig. 94) taken with beam along  $\langle 110 \rangle$  direction. The lattice constant was measured in the usual way was found to be  $a_0 = 5.48 \text{ \AA}$ .

These deposits when studied by transmission method yielded patterns (fig. 95) which are very complex. It is seen that they consisted of very sharp spots arranged on a square type of net work. There are also many extra reflections along the line joining the spots rows. Closer examination shows that these extra reflections arise due to the intersection of the straight lines have zones and the rings due to polycrystalline deposits. Though the pattern consisted mostly of spots there are many continuous rings passing through them. It appears that the square type of pattern is due to a cubic structure having  $a_0 = 5.48 \text{ \AA}$ . Some times slightly different but complicated patterns (fig. 96) were also obtained. A close examination of the pattern showed that the diffraction spots are arranged on two square type of net works which are rotated arbitrarily by  $32^\circ$ .

The pattern due to more than two such type of crystals is shown in fig. (97). This result about the growth

of crystals making arbitrary angles between their surface planes is similar to our results on antimony sulphide deposits as described later on in this chapter.

To study the effect of temperature on the deposit films these were initially formed at room temperature then heated to different higher temperatures either along with the substrate (rocksalt) or after its removal from the substrate. When the deposits were heated upto  $100^{\circ}\text{C}$  along with the substrate not much change in the pattern was observed after the heat treatment of the deposits. Heating at about  $250^{\circ}\text{C}$  also did not cause any change in the characteristics of the patterns.

The patterns (fig. 98a) were obtained from the deposit, heated to at about  $400^{\circ}\text{C}$  for one hour (approx.). The presence of sharp rings showed that the pattern was from unorientated polycrystalline material. On analysis it was found that the 'd' values of the 'hkl' reflections corresponded to those of normal orthorhombic stannous sulphide. The strongest ring in the pattern (fig. 98a) corresponded to the 'hkl' reflection having  $d_{hkl} = 2.83 \text{ \AA}$  of orthorhombic SnS. By eye-estimation the general distribution of the intensities of the different reflections corresponds to those of SnS.

In many of our experiments, the deposits yielded patterns (fig. 98b) consisting both of rings as well as spots. It is seen that the rings are exactly similar to those obtained in the above case (fig. 98a). The arrangement of the spots

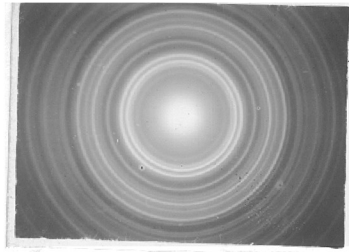


Fig. 99b

Table No. XV

Analysis of the pattern of fig. (99)

$I/I_0$	$d \text{ \AA}^0$	hkl	$c_0 (\text{\AA}^0)$
f	3.944	-	-
mf	3.32	SnS	5.41
vs	3.12	10.0	5.39
ms	2.989	(111) cubic	5.34
vs	2.806	SnS	-
f	2.659	(200) cubic	5.32
ms	2.004	00.3	5.33
mf	1.978	-	-
vs	1.908	11.0	5.39
m	1.765	10.3	5.36
s	1.625	(311) cubic	5.38
m	1.562	00.4	5.39
mf	1.447	20.2	5.31

$$\text{Mean } c_0 = 5.36 \text{ \AA}^0, a_0 = 3.34 \text{ \AA}^0$$

$$c_0 / a_0 = 1.603$$

is such that they form a square type of net work. The 'd' values of these spots when measured with the known 'd' values of the rings due to 'SnS' gave the lattice constant for the spot pattern  $a_0 = 5.48 \text{ \AA}$ . This lattice constant is nearly equal to the one obtained with the deposits heated to  $425^\circ\text{C}$ .

An interesting pattern was, obtained when the deposits initially formed at room temperature were heated to about  $425^\circ\text{C}$  for a few hours. These deposits yielded patterns (fig. 99a) of f.c.c. structure similar to zinc blende type of structure. A detail structural analysis of this is described previously in chapter IV (C).

When the above deposits having zinc blende type of structure when heated at about the same temperature but for a longer period they yielded patterns as shown in (fig.99b). On analysis of the pattern it was found that almost of all the reflections could be accounted for with a h.c.p. type of structure with  $a_0 = 3.34 \text{ \AA}$ ,  $c_0 = 5.36 \text{ \AA}$ ,  $c_0 / a_0 = 1.603$ . Further from the 'd' values (table KV) it was also found that many reflections corresponded to the normal stannous sulphide and the remaining were due to the f.c.c. structure.

#### Bismuth Sulphide :

The specimen prepared by rubbing the powder with collodion and when studied by transmission method yielded patterns (fig. 100) which consisted of rings alone, due to polycrystalline film. Measurement of the 'd' values of the

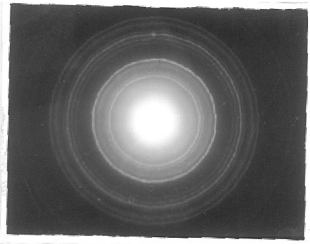


Fig. 100  
Bi<sub>2</sub>S<sub>3</sub> on collodion film.

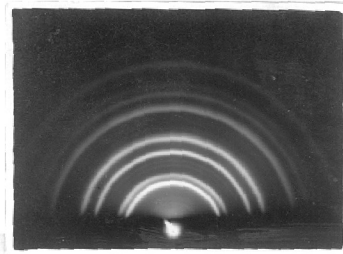


Fig. 101  
Bi<sub>2</sub>S<sub>3</sub> on NaCl(100) at 200°C



Fig. 102  
Bi<sub>2</sub>S<sub>3</sub> on NaCl(100) at 300°C

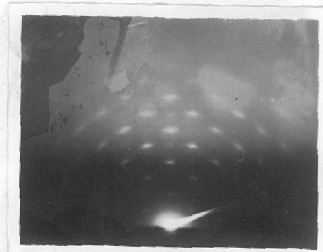


Fig. 103  
Bi<sub>2</sub>S<sub>3</sub> on NaCl(100) at 300°C

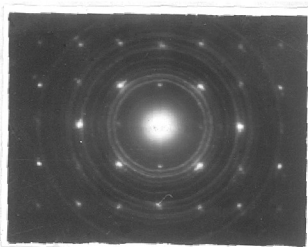


Fig. 104.

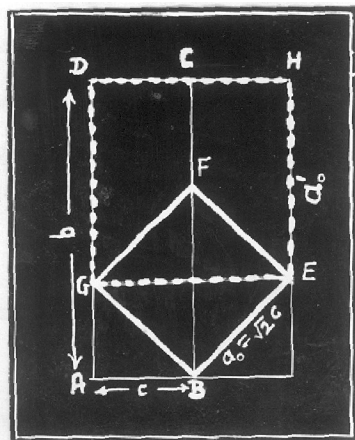


Fig. 105

Table No. XVI

Analysis of the pattern of fig.(101)

$I/I_0$	$d \text{ \AA}^0$	hkl	$a_0$
f	-	-	-
f	-	-	-
vs	3.29	111	5.69
s	2.81	200	5.62
f	2.36	-	-
f	2.18	-	-
s	1.98	220	5.60
s	1.77	311	5.67
m	1.62	222	5.60
ms	1.30	331	5.67
m	1.16	422	5.68
m	1.08	511+333	5.61
ms	0.988	440	5.71
			<u>Mean <math>a_0 = 5.647 \text{ \AA}^0</math></u>

v = very, s = strong, m = medium, f = faint



different reflections present showed that they corresponded to orthorhombic bismuth sulphide ( $\text{Bi}_2\text{S}_3$ ). The intensities of some of the reflections are slightly different from those given by X-ray which might be due to the fact that while rubbing slight orientation of the crystals might have taken place. From 'd' values it seems that the bulk material was mostly bismuthinite ( $\text{Bi}_2\text{S}_3$ ).

Deposition on NaCl :

At  $25^\circ\text{C}$  -  $100^\circ\text{C}$  : Deposits obtained at room temperature were polycrystalline in nature. The sharp rings obtained showed that the crystals formed were considerably large. The measurement of 'd' values of the different reflections showed that the deposits were due to normal orthorhombic bismuth sulphide. Deposits obtained at about  $100^\circ\text{C}$  showed similar results.

At  $200^\circ\text{C}$  : Deposits formed at about  $200^\circ\text{C}$ , however, showed diffractions which could not be accounted for by the normal  $\text{Bi}_2\text{S}_3$  (fig. 101). On measurement of the different 'd' values from the reflections present, it was found that most of the rings could be accounted for by a cubic structure with  $a_0 = 5.65 \text{ \AA}$  (Table XVI). There are a few faint rings present which seem to be due to normal bismuthinite. Similar results were also obtained on mica and discussed in more details later on.

At  $300^{\circ}$ - $350^{\circ}$ C : Deposits obtained at about  $300^{\circ}$ - $350^{\circ}$ C showed that the deposits were similar in nature in both the cases as observed from the patterns. The patterns (fig. 102) were taken when the beam was grazing along cube face i.e.  $\langle 001 \rangle$  of rocksalt. It is seen that the diffraction spots form a square net work of pattern which changed considerably when the specimen was rotated. Fig. (103) shows the pattern with beam along cube face diagonal of the rocksalt crystal i.e.  $\langle 011 \rangle$ . The presence of 200, 400, etc. reflections in the plane of incidence showed that the deposits had developed 2-d  $\{100\}$  orientation. The lattice parameter as measured with graphite as standard gave the value  $a_0 = 5.65 \text{ \AA}$  which is similar to the previous result in case of the deposit formed at  $200^{\circ}$ C and also to the deposits on mica as discussed further.

To study the effect of temperature on the deposit film the deposits obtained at room temperature were heated along with rocksalt to different temperatures such as  $200^{\circ}$ C,  $300^{\circ}$ C,  $400^{\circ}$ C etc. The one which was heated to about  $200^{\circ}$ C yielded patterns (104) consisting of rings as well as spots. On the measurement of 'd' values of the rings it was found that they corresponded to the normal bismuth sulphide. From the pattern one can see that the spots are arranged on square type net work indicating thereby the development of a cubic structure by the deposits along with the normal bismuth sulphide. The lattice constant measured from the spot pattern gave the value  $a_0 = 8.13 \text{ \AA}$ .

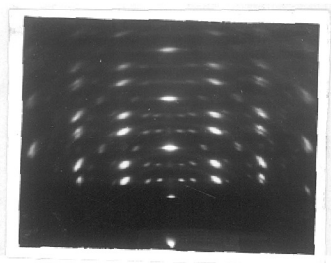


Fig. 106  
 $\text{Bi}_2\text{S}_3$  on mica at  $200^\circ\text{C}$   
beam along  $\langle 110 \rangle$

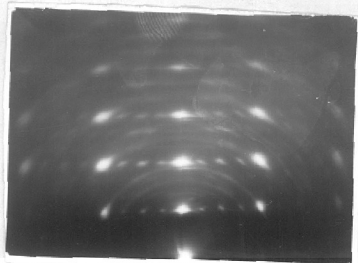


Fig. 107  
 $\text{Bi}_2\text{S}_3$  on mica at  $\approx 200^\circ\text{C}$   
beam along  $\langle 112 \rangle$

It is worth noting here that this lattice constant is  $\sqrt{2}$  times the lattice constant obtained for a cubic structure as mentioned previously. In the former case the lattice constant is  $5.65 \text{ \AA}$  which is nearly  $\sqrt{2}$  times the  $c_0$  axis of  $\text{Bi}_2\text{S}_3$  i.e.  $(3.98 \times 1.42)$  whereas the present one is  $8.13$  is again nearly  $\sqrt{2}$  times the former lattice constant  $(5.65 \times \sqrt{2})$ . The probable way of formation of these cubic structures seems to be the following.

In the fig. (105) AB represents the c-axis and AD the b-axis of orthorhombic crystal. It is seen from the lattice constants of ' $\text{Bi}_2\text{S}_3$ ' that c-axis is nearly equal to  $1/3$  of b-axis. During crystal growth process a slight displacement of atoms may result in a cubic structure with  $a_0$  equal to  $\sqrt{2}$  times c-axis. In the fig. (105) ABCD is the original crystal (orthorhombic) and the new crystal is GBEF ( $a_0 = \sqrt{2}c_0$ ). This process may continue further and might give rise to another crystal, again cubic with  $a'_0 = \sqrt{2} a_0$ . The crystal, DEEH is the another cubic crystal with  $a'_0 = \sqrt{2} a_0$  (fig. 105). Thus the new structures are related to the basic bismuth sulphide structure.

#### Deposition on Mica :

Deposits obtained at room temperature were mostly polycrystalline in nature. Interesting patterns (fig. 106) which appears to be from cubic crystals with beam along  $\langle 110 \rangle$  direction were obtained from the deposits formed at about  $200^\circ\text{C}$ .

It is seen that the pattern consisted mostly of spots indicating the deposits grew epitaxially on the substrate. This was also confirmed from the fact that patterns changed considerably as the specimen was rotated around the axis perpendicular to the beam direction. The other pattern, with beam along  $\langle 112 \rangle$  of the deposit crystal was obtained by rotating the specimen by  $30^\circ$  to the previous position (fig. 107). The appearance of the spots due to 111, 222 reflections and their higher orders are in the plane and disposition of main reflections suggest that the deposits had developed 2-d  $\{111\}$  orientation. The lattice parameter of this cubic structure as measured with graphite standard was found to be  $\approx 5.65 \text{ \AA}$ . It will be seen that there are a number of additional spots comparatively weaker present in the patterns besides the main spot pattern due to  $\{111\}$  orientation. The main spot rows along the horizontal direction (fig. 107) are divided into four equal parts by the faint spots thus giving rise to a superstructure. The lattice parameter of this superstructure was found to be  $\approx 22.61 \text{ \AA}$ , four times the lattice parameter of cubic structure of bismuth sulphide as mentioned above ( $a_0 = 5.65 \text{ \AA}$ ). The way of the formation of the cubic structure seems to be as described earlier in case of the deposits formed on rock-salt.

Antimony Sulphide :

Deposition on NaCl : Deposits formed at room temperature when examined by reflection method did not yield

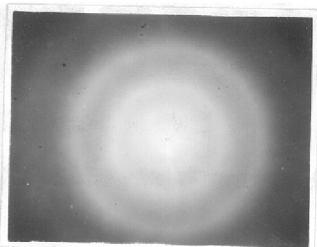


Fig. 108  
 $Sb_2S_3$  on NaCl (100) at room temp.

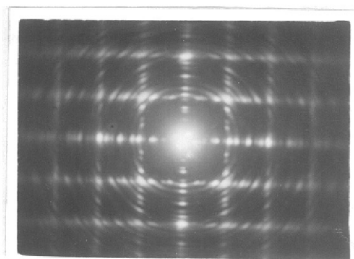


Fig. 109  
 $Sb_2S_3$  on NaCl (100) at 200°C

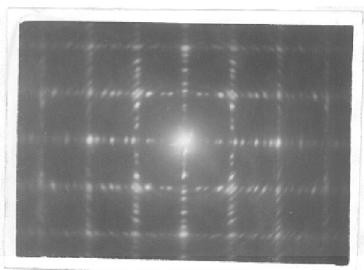


Fig. 110  
 $Sb_2S_3$  on NaCl (100) at 300°C

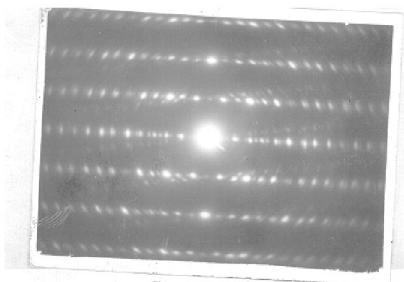


Fig. 111  
 $Sb_2S_3$  on NaCl (100) at 350°C

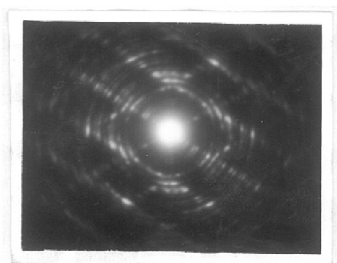


Fig. 112  
 $Sb_2S_3$  on NaCl (100) at 350°C



Fig. 113  
 $Sb_2S_3$  on NaCl (100) at 350°C

any pattern but by transmission they yielded patterns (fig. 108) consisting of diffuse rings. Though one or two rings are sharp, on the whole the diffuseness of the rings shows that the deposits were amorphous in nature or had a very fine grain structure. Deposits formed at about  $100^{\circ}\text{C}$  showed slightly better patterns.

The deposits obtained between  $200^{\circ}\text{C}$  and  $300^{\circ}\text{C}$  were similar in nature (fig. 109 & 110) but those formed at  $300^{\circ}\text{C}$  yielded sharper patterns. It is seen that the diffraction spots are arranged on two sets of parallel lines which are perpendicular to each other. They formed a square type of net work. The presence of many spots suggested that the deposits had possibly developed, many orientations at the same time. The appearance of many spots, along the rows joining to main reflections, seems to be due to the intersection of straight line Laue zones with the rings due to polycrystalline deposits. In fact many rings could be seen in negative passing through these spots.

Deposits formed at about  $350^{\circ}\text{C}$  yielded patterns (fig. 111) consisting of spots arranged on nearly parallel straight line Laue zones. The arrangement of the spots is similar to the patterns obtained for layer line type of structures. It was found that the distance between the two parallel rows of spots was equal to  $3.84 \text{ \AA}$  which is equal to c-axis, of antimony sulphide crystals. It was thus seen that the deposits had grown such that their one axis a or b

was parallel to the beam direction and hence perpendicular to the substrate surface plane. Further it was seen that reflections due to 020, 012, etc. and their respective higher orders were present, in the pattern. This suggested that the deposit crystals had developed various two degree orientations such as 020, 012 etc. Similar results were also obtained by Elleman (1948) in case of  $\text{PbCl}_2$  deposits formed on rock salt single crystals at about  $200^\circ\text{C}$ .

It is also seen that there are many faint spots present in the pattern (fig. 111). These spots are also arranged on nearly parallel straight lines but slightly tilted from the original spot rows. It seems that these spots might be due to other crystals similar to the former ones but grown such a way that it was rotated by a certain arbitrary angle with respect to the main crystals. The angle in this case was found to be  $\approx 8^\circ$ . It was found that this angle, varied in each case when experiments were repeated and the variation was from  $8^\circ$  to  $62^\circ$ . Some of the patterns obtained from the deposit crystals grown in this way are shown in figs. (112 and 113).

Deposits formed at about  $350^\circ\text{C}$  yielded complicated patterns (fig. 114). It consists of spots, strong arcs elongated on both sides of the spot along the ring and also rings. The measurement of the 'd' values of the arcs or the corresponding rings showed that these can be accounted for with the formation of a face centered cubic structure with  $a_0 = 5.73 \text{ \AA}$ .



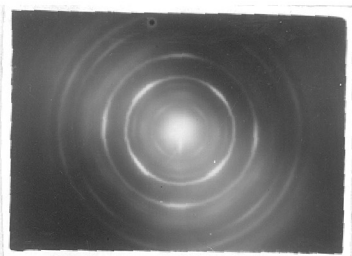


Fig. 114  
 $Sb_2S_3$  on NaCl (100) at  $350^\circ C$

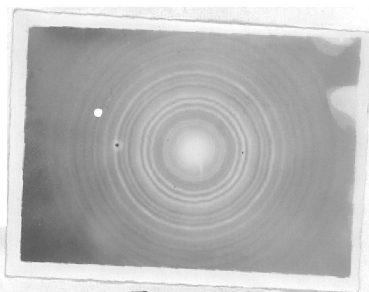


Fig. 115

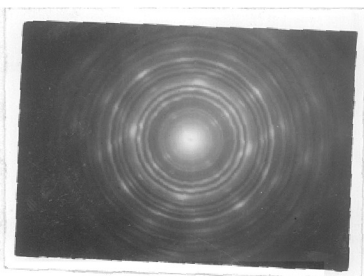


Fig. 116

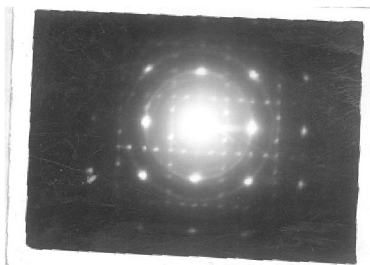


Fig. 117

Similar results were obtained in the case of the deposits initially formed at room temperature and then heated to higher temperatures and is described later on in this chapter. There are many extra spots present in the pattern which could not be accounted for the above face centered cubic structure. The 'd' values of these were found to be similar to those of normal orthorhombic antimony sulphide.

To study the effect of temperature on the deposit films the deposits were initially obtained at room temperature were heated further to different higher temperatures along with the substrate (rock-salt in the present case). When the deposits were heated to about  $200^{\circ}\text{C}$  they yielded patterns (fig. 115 & 116). It is seen that the pattern (fig.115) consisted only of rings showing the polycrystalline nature of the deposits. On analysis of the same it was found that the 'd' values of different reflections present corresponded to the orthorhombic antimony sulphide. ~~XXXXXXXXXX~~ From the other pattern (fig.116) it is seen that it consisted rings similar to those in the above case and also spots on the rings. The arrangement of the spots is such that they form a square type net work. This arrangement of the spot is similar to the pattern (fig.110) obtained in case of the deposits formed at about  $200^{\circ}\text{C}$ . As mentioned before the spot pattern appears to be due to the presence of many orientations developed by the deposit crystals. The presence of many extra spots can be attributed to the bending of the films along definite crystallographic directions while removing them from the substrate. Similar results were also

obtained in case of silver sulphide deposits (Elleman 1947) and lead chloride (Elleman and Wilman 1949). The presence of the sharp rings (fig. 115) indicated the formation of comparatively bigger crystals.

Deposits heated to about  $250^{\circ}$  and  $300^{\circ}\text{C}$  yielded patterns similar to those in figures (115 & 116). Thus as mentioned before the deposits developed many orientations and the deposit crystals grew arbitrarily making arbitrary angles between them. The results in these cases were similar to those in case of the deposits formed at the corresponding substrate temperature.

Deposits when heated to about  $350^{\circ}$  to  $400^{\circ}\text{C}$  yielded patterns (fig. 117) which consisted only of spots. It is seen that some spots are strong and broad whereas the other spots are comparatively weak and sharp. Both the spots are forming square type of net-work. The strong spots are arranged at the corners of one type of square whereas the weak spots are not only at the corners of the other squares but also along the sides of the squares. The length of the sides of the squares in both the cases is the same. It was found that the main pattern was due to a cubic structure having  $a_0 = 5.78 \text{ \AA}$ . The other pattern in which the spots are making four equal parts along the side of the cube showed the presence of a superstructure developed by the deposits giving the lattice parameter ( $a_0 = 23.02 \text{ \AA}$ ) four times the above one ( $a_0 = 5.78 \text{ \AA}$ ). The formation of the superstructure seems to be linked with the

phase and anti-phase type arrangement of the atoms. Recently it has been shown that if the atoms do not occupy their respective positions but interchange among themselves they give rise to the formation of a super-structure (see Pashley and Prosland, 1959 and Glossop and Pashley 1959). In this case the atoms interchange their positions and form a system called antiphase. The arrangement of such phase and anti-phase repeats regularly and may give rise to the formation of a bigger unit cell i.e. the formation of a superstructure.

D. DISCUSSION

During the experiments on tin sulphide deposits a number of structures were observed depending upon the temperature and other conditions of the deposit formation.

Deposits obtained at room temperature to  $100^{\circ}\text{C}$  were either amorphous in nature or the deposit crystals had very fine grain structure. The deposits formed at about  $250^{\circ}\text{C}$  developed a new h.c.p. structure ( $a_0 = 3.17 \text{ \AA}$ ,  $c_0 = 5.14 \text{ \AA}$ ,  $c_0 / a_0 = 1.64$ ) with the corresponding cubic structure with  $a_0 = 5.1 \text{ \AA}$  which was also not previously reported. At higher temperatures the deposits yielded complicated patterns arising from many orientations developed by the deposit crystals.

The deposits formed at about  $400^{\circ}\text{C}$  were due to well orientated orthorhombic crystals of stannous sulphide. The orientations developed by the crystals were  $\{010\}$ ,  $\{021\}$  and  $\{110\}$  etc.

The most interesting results were obtained when deposits prepared at room temperature were heated to  $425^{\circ}\text{C}$ . These crystals developed a new face centred cubic structure, zinc blende type, having  $a_0 = 5.445 \text{ \AA}$ . No compound of tin with sulphur is known so far having zinc blende type of structure. These deposits on further heating showed the correspondingly related h.c.p. structure with  $a_0 = 3.37 \text{ \AA}$ ,  $c_0 = 5.35 \text{ \AA}$ ,  $c_0 / a_0 = 1.603$ .

Deposits of bismuth sulphide at room temperature to about 100°C were polycrystalline in nature and had orthorhombic structure with same lattice parameter as for bismuthinite.

Deposits at 200°C when formed on rock salt, mica and also on glass developed a cubic structure with  $a_0 = 5.65 \text{ \AA}$ . It is worth noting that this lattice constant is nearly  $\sqrt{2}$  times the value of c-axis of the orthorhombic bismuth sulphide ( $\text{Bi}_2\text{S}_3$ ). This suggested the possible formation of the crystals having cubic structure.

Often along with the main cubic structure a superstructure was also obtained at about 200° and 300°C. The lattice constant of the super structure was found to be 22.61 Å. It is again interesting to note that this lattice parameter is nearly twice that of b-axis of  $\text{Bi}_2\text{S}_3$ . It might be due to the formation of antiphase structure. Recently it has shown that superstructures are many times developed due to phase and antiphase type arrangement of atoms. In this case though the composite atoms in the compound remain the same their positions are interchanged. This change is such that it repeats periodically and different from the normal one. Superstructures are formed due to such type of arrangement of the atoms has been observed by many workers (Pashley and Presland 1959 and Glossop and Pashler 1959).

Deposits of antimony sulphide crystals at higher temperatures developed two degree orientations. It was

normally observed that these deposits often yielded layer line type of patterns. These crystals often grew arbitrarily making arbitrary angles between them. These angles between the two crystals varied from  $8^{\circ}$  to  $62^{\circ}$  in the present study. Many times the angle was  $90^{\circ}$  also in which the pattern was consisting square type arrangement of diffraction spots.

It was noticed that normally at higher temperatures the deposit crystals were growing with their 'a' or 'b' axis parallel to the beam direction or perpendicular to the substrate surface.

These deposits often showed along with orthorhombic structure another structure being cubic with  $a_0 = 5.78 \text{ \AA}$ . Many times three dimensional patterns were also obtained. Superstructure with  $a_0 = 23.01 \text{ \AA}$  (nearly 4 times the lattice parameter of cubic structure) was also observed. This superstructure again seems to be resulting from phase and antiphase considerations.

+ + + +

## CHAPTER VI

### EFFECT OF TEMPERATURE ON THE EPITAXIAL GROWTH OF SILVER ON LEAD SULPHIDE SINGLE CRYSTALS

#### A. Introduction

In the recent years considerable work has been carried out on the epitaxial growth of crystals. It is now well known that the growth of crystals in their initial stage depends mostly on the atomic arrangements of the substrate crystals. The deposition of metals on metals and non-metals have been studied by many workers by electron diffraction, electron microscopy, optical microscopy etc.

Lassen and Bruck (1935) showed that only above a certain critical temperature of the substrate the deposits tend to develop 2-d orientations but at lower temperatures they are mostly randomly disposed. If the temperature is very low the deposits can be amorphous. Rudiger (1937) extended the work further and showed that the critical temperature is different for each metal on different substrates.

Epitaxial growth has also been studied by other workers (see Finch and Wilman 1937, Pashley 1956). Goswami (1954, 1956) observed the appearance of new orientation such as  $\{211\}$  along with  $\{100\}$  on rock-salt and suggested that it was due to multiple twinning phenomenon. Pashley (1956) made an extensive review on the growth of deposits on metals as well as on non-metals. Epitaxial growth in electro deposition or by



chemical reaction has also been studied by many workers. Unlike Lassen and Brucks observation of critical temperature metallic deposits by electrodeposition or by chemical growth are invariably two degree orientated on single crystal substrat (Finch, Wilman and Yang 1947, Goswami 1950, 1957, 1958). No change of 2-d orientation with temperature was observed at all either in case of vapour phase deposits or electro-deposits. Since epitaxial growth is determined mostly by the atomic arrangement of the substrate crystals on the surface the effect of temperature is not normally expected. However, in some of our experiments with CuI, CuBr and CuCl (as mentioned before in chapter III) we have observed change of orientations from 2-d {111} to 2-d {100} with temperature. In the following an investigation has been made on the orientation of silver on lead sulphide single crystals with change of temperature either by depositing at higher temperature or by depositing at room temperature and then heating at higher temperatures.

---

B. Experimental

Silver metal was evaporated from tungsten filament which was initially flashed in vacuo for sometime to remove the surface impurities. Silver was then deposited in the usual way in vacuo, after making a proper bead on the filament. Deposits were obtained on freshly cleaved single crystals of lead sulphide, (100) face, which were previously heated to the desired temperatures or kept at room temperature. The deposit film thus formed at room or higher temperature was then heated in vacuo along with the substrate to the required temperature. Deposits after cooling to room-temperature were examined in electron diffraction camera by reflection method.

---

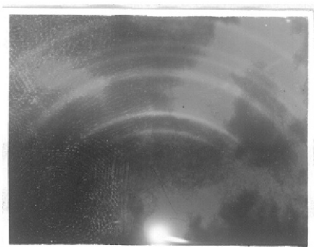


Fig. 118  
Ag on PbS(100) at room temp.

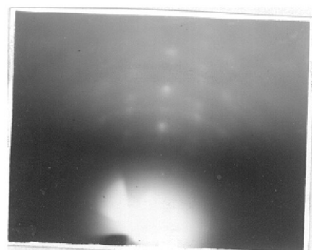


Fig. 119  
Ag on PbS(100) at 100°C.

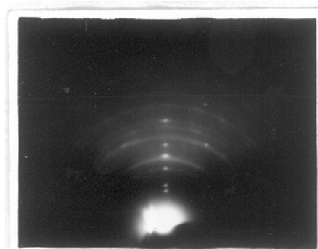


Fig. 120  
Ag on PbS(100) at 250°C.

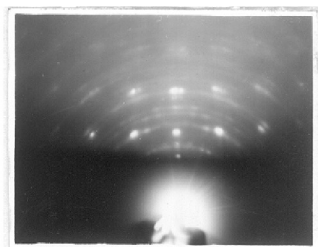


Fig. 121  
Ag on PbS(100) at 400°C.

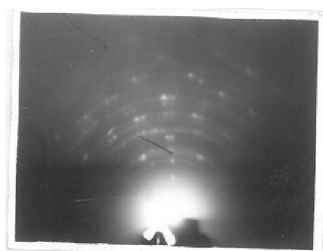


Fig. 122

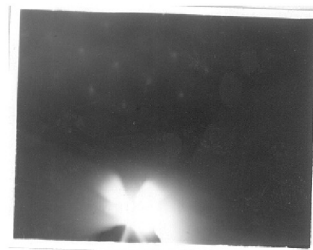


Fig. 123

### C. Results

#### Deposition on PbS (100) face :

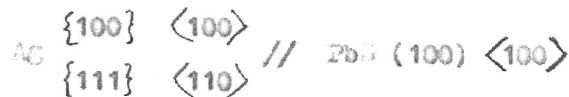
At room temperature (25°C) : Deposits obtained at room temperature were mostly polycrystalline in nature (fig. 118) but sometimes, they developed 2-d  $\{111\}$  orientation.

At about 100°C : The deposits formed at this temperature yielded patterns (fig. 119) consisting of rings as well as spots. It was found on measurement that both the spots and rings were due to silver. No reaction between Ag and PbS has taken place at the inter-face of the substrates and the deposits. The pattern (fig. 119) was taken with the beam grazing along  $\langle 110 \rangle$  of silver crystals. The presence of the spots due to 111, 222, etc. in the plane of incidence and also the fact that the pattern changed considerably while rotating the specimen suggested that the deposit crystal had developed 2-d  $\{111\}$  orientation. The theoretical pattern for 2-d  $\{111\}$  orientation with beam along  $\langle 110 \rangle$  is asymmetrical whereas the observed pattern is a symmetrical one which shows the formation of parallel and antiparallel deposit crystals.

At about 250°-300°C : At this temperature range the deposits yielded patterns (fig. 120) consisting of rings as well as spots. Again as in previous case the deposit crystals developed 2-d  $\{111\}$  orientation. It was also seen that there are extra spots present in the pattern which cannot be accounted by 2-d  $\{111\}$  orientation alone. The spots due

to 200, 400, etc. reflections in the plane of incidence indicated the presence of 2-d {100} orientation also.

At about 400°C : Silver deposited at about 400°C showed that the deposit crystals developed 2-d {100} orientation more prominently than that at about of 250°-300°C. The patterns obtained from these deposits were similar to (fig.121). On analysis of the spot pattern it was concluded that the deposits had developed mostly 2-d {100} orientation. In the pattern there were a few extra spots which were due to 2-d {111} orientated crystals. Thus in this case also the deposit crystals developed two orientations



The crystals having the 2-d 100 orientation being more prominent.

Experiments were also carried out by heating the deposits formed at room temperature or at other temperature then heating to a higher temperature to see if there was any change in the orientation of the deposits.

The deposits formed on the cleavage face of galena single crystal at room temperature were 2-d {111} orientated along with polycrystalline ones. They were then heated further in vacuo at about 450°C for about an hour and were cooled to room-temperature and examined by electron diffraction.

Fig. (122) shows pattern obtained from such deposits. It is seen that the spots due to 200, 400 etc. reflections were in the plane of incidence. This, however, suggested that the crystals after heating developed 2-d  $\{100\}$  orientation even though initially they had 2-d  $\{111\}$ .

The pattern corresponds to the

$$\text{Ag } \{100\} \langle 110 \rangle // \text{Fbs } (100) \langle 110 \rangle$$

A change in the orientation of the deposit was thus caused by heating at higher temperature.

The deposits initially formed at 250°C showing two-degree  $\{111\} + \{100\}$  orientations (fig. 120) were again heated at the same temperature for about an hour. No change of orientation was however observed by this treatment. These deposits were further heated to about 400°C for an hour and studied in the electron diffraction camera. Patterns (fig.123) taken with the direction along  $\langle 011 \rangle$  of Fbs clearly show that the deposit crystals now developed two degree  $\{100\}$  orientation alone. This showed that the deposits having either 2-d  $\{111\}$  or a mixture of 2-d  $\{111\} + \{100\}$  on heating to 400°C changed completely to 2-d  $\{100\}$  orientation.

It was thus observed that the initial deposits formed at lower substrate temperature when heated further at higher temperatures along with the substrating showed a change in the orientation of the deposit crystals. The changes of orientations being from  $\{111\}$  at lower temperatures to

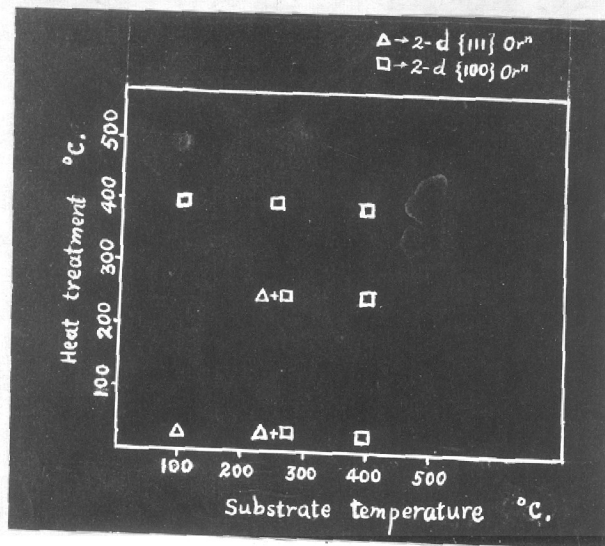


Fig. 124

$\{111\}$  +  $\{100\}$  both equally prominent at medium temperatures and finally to  $\{100\}$  at higher temperatures. Such a change of orientation is not only observed by heat treatment of deposits at different temperatures but also by depositing at different substrate temperatures (fig. 124).



D. Discussion

It is known that the arrangement of the atoms in the substrate crystal is the primary factor for the epitaxial growth of deposits and hence it is expected that deposits of any material on a substrate normally should show the same orientation. But it has been observed in the present study that deposits changed orientation from 2-d  $\{111\}$  at lower substrate temperature to 2-d  $\{111\} + \{100\}$  orientations at intermediate temperature and finally to 2-d  $\{100\}$  orientation alone at higher substrate temperatures (fig. 124). This effect of temperature is interesting. If the orientation of deposit crystals is determined by the arrangement of the substrate atoms alone then normally there should not have been any change in the orientation due to a temperature rise.

Thirsk (1950) also reported different orientations of silver deposit on mica with temperatures. Similar change of orientation has also been observed by us in the case of  $\text{CuCl}$ ,  $\text{CuBr}$ . Both of them showed 2-d  $\{111\}$  orientation at lower temperatures but 2-d  $\{100\}$  orientation at higher temperatures. The above may be explained in the following way.

Atoms in vapour state when start depositing on the substrate they condense and then move over the surface depending on their mobility and settling down at suitable positions conforming to the minimum potential energy configuration. If the substrate temperature is high the deposit

had a better chance to take up the ideal position of minimum potential energy state due to their mobility. At lower temperatures they would not have time to take up the ideal position and hence stay on the sites which are in the immediate neighbourhood of the deposition position. This state will be aggravated if the rate of deposition is very high. Such deposition condition is likely to lead to create stress in deposits. The orientation thus assumed by deposits is likely to conform to a metastable arrangement of atoms. At lower temperatures the appearance of 2-d  $\{111\}$  orientation seems to reflect such condition. At higher substrate temperatures deposits have enough mobility and hence seek the best position of minimum potential energy condition. Higher temperature also has the effect of removing the stress of the deposit by annealing. The appearance of 2-d  $\{100\}$  orientation seems to conform to the ideal condition of deposition. The above condition can also be induced by heating the specimen. Thus the appearance of 2-d  $\{111\}$  orientation at lower temperatures and its change to 2-d  $\{100\}$  orientation at higher temperatures can be explained.

It will be interesting, however, to compare the results observed with  $\text{CuCl}$ ,  $\text{CuBr}$  and  $\text{CuI}$ , when deposited on cleavage faces of  $\text{NaCl}$  and  $\text{KCl}$  (cf. Chapter III). Normally these deposits developed 2-d  $\{111\}$  orientation at lower substrate temperatures. At a high temperature  $\text{CuCl}$  and  $\text{CuBr}$  developed 2-d  $\{100\}$  orientation i.e. parallel orientation but  $\text{CuI}$  did not. The later has changed to parallel orientation

at a still higher temperature. These phenomena can be explained in similar way as discussed for silver on PbS (100) face. The substances with lower melting point have greater mobility at a particular temperature than those with having higher melting point. It is likely, that it would be more favourable for CuCl and CuBr having lower melting points ( $504^{\circ}\text{C}$  and  $422^{\circ}\text{C}$ ) to take up parallel orientation than for CuI (m.p.  $605^{\circ}\text{C}$ ).

+ + + +

SUMMARY AND CONCLUSIONS

The present electron diffraction study has thrown some new light on nature of the evaporated films of cuprous halides, sulphides of tin, antimony and bismuth, phase transition of crystals, crystal growth process and also effect of temperature on the change of orientations.

The results on evaporated films of cuprous iodide, bromide, and chloride showed that these grew epitaxially on single crystal substrates such as NaCl, KCl, CaCe<sub>2</sub> or mica at higher temperatures but they had tendency to be randomly disposed at or near about the room temperature. Normally at higher temperatures in the region of 200°C and above depending on the melting point of the crystals, the deposits had tendency to develop parallel orientations. On the three faces of rock-salt the azimuthal orientations were as follows :

Cuprous halides	{100}	<001>	//	(100)	<001>	NaCl
	{110}	<001>	//	(110)	<001>	NaCl
	{111}	<110>	//	(111)	<110>	NaCl
		<112>				

In addition to the above parallel orientations often 2-d {211} and {0001} orientations respectively of cubic and hexagonal crystals of halides were also observed. The presence of both of these orientations has been adduced to the formation of twinned crystallites or to the stacking fault, developed during the growth of the deposits. Either of them

would give rise to the hexagonal phase ( $\beta$ -form) in the subsequent deposit layers.  $\{211\}$  orientation is, however, the result of multiple twinning.

Cuprous iodide deposits developed perfect one-degree  $\{111\}$  orientation on glass and mica substrates at about  $300^{\circ}\text{C}$  and  $400^{\circ}\text{C}$ . The surface was atomically smooth though undulating. The appearance of the hyperbolic loci in the diffraction patterns of cuprous iodide by reflection suggest that surface layers were buckled to some extent.

$\gamma$ -CuI showed transition to  $\beta$ -CuI and also sometimes to  $\alpha$ -CuI even at much low temperature  $200^{\circ}\text{C}$  for  $\beta$ -CuI and  $400^{\circ}\text{C}$  for  $\alpha$ -CuI much less than the bulk transition temperatures (for  $\beta$ -CuI  $369^{\circ}\text{C}$ , for  $\alpha$ -CuI  $440^{\circ}\text{C}$ ). It has been observed that from  $\gamma$ -CuI not only  $\beta$ -phase is obtained but often at higher temperatures  $\alpha$ -phase of CuI is also observed.

Extensive twinning on  $\{111\}$  planes was observed in case of cuprous iodide, cuprous bromide and cuprous chloride also.

Cuprous chloride deposits on treatment in water changed to a new compound whereas both cuprous iodide and cuprous bromide retained their initial structures. The new compound from cuprous chloride, seems to have a f.c.c. structure with  $a_0 \approx 10.88 \text{ \AA}$ , nearly double that of  $\gamma$ -CuCl ( $a_0 = 5.416 \text{ \AA}$ ).

A new spinel type of compound was also observed during the evaporation of CuCl. An investigation into its

structure by measuring the intensities of different reflections with microphotometer method showed that it had a spinel ( $R_3X_4$ ) type of structure with  $a_0 = 8.265 \text{ \AA}$ . Discrepancy between observed and the theoretical intensities of reflections has been pointed out. Agreement was, however, better if X-ray scattering factors for some of hkl reflections were used.

The mechanism of the formation of such compound seems to be in the following way :



Deposits of tin sulphide (ous) showed a number of structures. At about  $250^\circ\text{C}$  they developed a h.c.p. structure ( $a_0 = 3.13 \text{ \AA}$ ,  $c_0 = 5.17 \text{ \AA}$ ,  $c_0 / a_0 = 1.64$ ), along with a corresponding cubic type of structure ( $a_0 = 5.15 \text{ \AA}$ ) whereas at about  $400^\circ\text{C}$  they showed the normal orthorhombic stannous sulphide form. A new f.c.c. type of sulphide of tin ( $a_0 = 5.44 \text{ \AA}$ ) was obtained at about  $425^\circ\text{C}$ .

Detail intensity measurements for the cubic sulphide of tin ( $a_0 = 5.445 \text{ \AA}$ ) was carried out and compared with other several cubic structures and found to agree very closely with the zinc blende type of structures with coordinates of tin and sulphur as



This new cubic form was also observed along with its corresponding h.c.p. structure ( $a_0 = 3.37 \text{ \AA}$ ,  $c_0 = 5.37 \text{ \AA}$ ,

$c_0 / a_0 = 1.603$ ) which was normally observed at about  $430^\circ\text{C}$  or above.

Both bismuth sulphide and antimony sulphide ( $\text{Bi}_2\text{S}_3$  and  $\text{Sb}_2\text{S}_3$ ) in addition to the normal orthorhombic structure gave rise to a number of other structures having the same basic cell structure. For  $\text{Bi}_2\text{S}_3$  we have observed the following cubic structures having the lattice constants as

- (i)  $a_0 = 5.65 \text{ \AA}$
- (ii)  $a_0 = 8.07 \text{ \AA}$
- and (iii)  $a_0 = 22.61 \text{ \AA}$

It is worth noting that the value  $a_0 = 5.65 \text{ \AA}$  in case of the compound (i) is about  $\sqrt{2}$  times the value of c-axis of the orthorhombic bismuth sulphide, whereas the lattice constant  $a_0 = 8.07 \text{ \AA}$  in case of the other compound (ii) is also nearly  $\sqrt{2}$  times that of the former one having  $a_0 = 5.65 \text{ \AA}$ . The compound (iii) seems to have a superstructure having  $a_0$  value four times that of (i) having cubic structure.

Antimony sulphide showed a similar cubic structure with  $a_0 = 5.75 \text{ \AA}$  and the corresponding superstructure with  $a_0 = 23.01 \text{ \AA}$  being four times of the former one.

Antimony sulphide crystals during their growth were azimuthally rotated amongst themselves. Normally these crystals gave patterns similar to layer line type patterns.

Their c-axis was normal to the substrate plane. These crystals often show many azimuthal orientations which are uncommon and some grew like molecular compounds.

A preliminary study on silver deposits formed on lead sulphide single crystals showed that the nature of the epitaxial orientation was dependent on the substrate temperature. This was not expected, however, in the case of epitaxially grown crystals. The changes of orientation from 2-d  $\{111\}$  to 2-d  $\{111\} + \{100\}$  and finally to 2-d  $\{100\}$  were observed with rise of temperature. Similar changes in orientation were also observed as the initial deposits at room temperature were heated to higher temperatures along with the substrates. Thus the 2-d orientation developed at lower temperature changed to a new orientation at higher temperature which does not entirely fit in with the general concept of epitaxial growth. Though the general arrangement of substrate is the main factor to determine the deposit orientation (epitaxial) at least in certain cases, temperature has a definite effect.

+ + + +



### ACKNOWLEDGMENTS

The author is much indebted to Dr. A. Goswami for supervision, many helpful discussions, interest and encouragement received from him during the present study.

The author is thankful to the Director, National Chemical Laboratory, Poona, for permission to submit this work in the form of a thesis. The author is also grateful to the Council of Scientific and Industrial Research, New Delhi, for the award of Junior Research Fellowship which enabled him to devote his whole time to carry out the present work.

+O+O+O+O+

REFERENCES

1. A.S.T.M. Card Nos 6-0246, 6-0685, 6-0623.
2. A.S.T.M. Card Nos 6-0292, 6-0700, 6-0310.
3. A.S.T.M. Card No. 6-0344.
4. A.S.T.M. Card Nos 1-0984, 1-1010.
5. A.S.T.M. Card No. 6-0333.
6. A.S.T.M. Card No. 6-0474.
7. Aggarwal, P.S. (1958) Ph.D. Thesis, Poona University.
7. Aggarwal, P.S. & Goswami, A. (1958) Z. Naturforschg. 13a, 885.
8. Anderson, J.S. & Horton, H.C. (1945) Nature, 155, 112.
9. Barth, T. & Lunde, G. (1925) Norsk.geol.tidssk, 8, 281.
10. Becker, R. & Doring, W. (1935) Ann. Phy. 24, 719.
- 10a. Becker, R. & Doring, W. (1949) Disc. Faraday Soc. No 5 (Crystal growth), 55
11. Beeching, R. (1936) "Electron Diffraction" (Mathuen, London).
12. Bowden, T.P. & Yoffe, A.D. (1958) Fast reactions in Solids.  
Dutterworth Scientific Publications (Lond.).
13. Bridgman, P.W. (1916) Proc. Am. Acad. Art. Sci. 52, 91-137.
14. Bridgman, P.W. (1955) Proc. Am. Acad. Art. Sci. 10, 710.
15. Buckley, H.E. (1952) Proc. Phy. Soc. B 65, 678.
16. Burton, W.K. & Cabrera, N. (1949) Disc. Faraday Soc.  
No. 5 (Crystal Growth).
16. Burton, W.K., Cabrera, N., & Frank, E.C. (1951), Trans. Roy. Soc. (London) A243, 299
17. Charlesby, A. (1939) Ph.D. Thesis, London University.
18. Charlesby, A. (1940) Proc. Phys. Soc. 52, 657.
19. Clark, H.C. & Anderson, J.S. (1943) Nature, 152, 75-6.
20. Cowley, J.H., Rees, A.L.G. & Spink, J.A. (1951)  
Proc. Phys Soc. A 64, 609.
21. Cowley, J.H. (1954) J. Electrochem. Soc. 101, 277.

22. Cowley, J.M. & Rees, A.L.G. (1958) *The Physical Society*,  
21, 165. Reprinted from the Reports on Progress  
in Physics.
23. Cowley, J.M. & Goswami, A. (1961) *Acta cryst.* 14, 1071.
24. Curie, P. (1885), *Bull. Soc. franc. Miner.*, 8, 145.
25. Dana, J.D. & Dana, E.S. (1951) *System of Mineralogy*, Vol. II  
New York. John Wiley & Sons, Inc. Chapman & Hall Ltd.  
London.
26. Davy, W.P. (1922), *Phys. Rev.* 19, 248-51.
27. Dunlap, W.C. (1957) *An Introduction to Semiconductors*.  
New York, John Wiley & Sons, Inc.  
London, Chapman & Hall Ltd.
28. Elleman, A.J. (1948) Ph.D. Thesis, London University.
29. Elleman, A.J. & Wilman, H. (1949), *Proc. Phys. Soc. A* 62, 344.
30. Finch, G.I. & Quarrell, A.G. (1935) *Proc. Roy. Soc. A* 141, 398.
31. Finch, G.I. & Quarrell, A.G. (1934) *Proc. Phys. Soc.* 46, 148.
32. Finch, G.I. & Wilman, H. (1936) *Trans. Farad. Soc.* 32, 1539.
33. Finch, G.I. & Wilman, H. (1937) *Erget. Exact. Nature.* 16, 353.
34. Finch, G.I., Wilman, H. & Yang, L. (1947) *Disc. Faraday Soc.*  
1, 144.
35. Frank, F.C. & van der Merwe, J.H. (1949) *Proc. Roy. Soc.*  
198, 205.
36. Frankenheim, M.L. (1836), *Ann. Phys.* 37, 516.
37. Frenkel, J. (1945) *J. Phys. Moscow*, 9, 392.
38. Frenkel, J. (1946) *Kinetic theory of liquids*, Clarendon Press,  
Oxford.

39. Gerner, L.H. (1939) *Phys. Rev.* 56, 58.
40. Gibbs, W. (1927) "Collected Papers", 5, 320 (Longman).
41. Goche, O. & Wilman, H. (1939) *Proc. Phys. Soc.* 51, 625.
42. Goswami, A. (1950) Ph.D. Thesis, London University.
43. Goswami, A. (1954) *J. Sci. & Ind. Res.* 13B, 677.
44. Goswami, A. (1956) *Proc. Phy. Soc.* 69B, 583.
45. Goswami, A. (1956) *J. Sci. & Ind. Res.* 15B, 322.
46. Goswami, A. (1957) *J. Sci. & Ind. Res.* 16B, 186.
47. Goswami, A. (1958) *Trans. Farad. Soc.* 54, 821.
48. Goswami, A. (1961) *J. Electro-chem. Soc.*, Communicated.
49. Hannay, H.B. (1959) *Semiconductors*, Reinhold Publishing Corporation, New York.
50. Harold, P., Klug, & Heisig, G.B. (1939),  
*J. Am. Chem. Soc.* 61, 1920-1.
51. Heavens, O.S. (1955) 'Optical Properties of thin solid films'  
Butterworth Scientific Publications (London).
52. Hofmann, W. (1935) *Z. Krist.* 92, 161-73.
53. Holland, L. (1953) *J. Opt. Soc. Am.* 43, 376.
54. Holland, L. (1956) *Vacuum Deposition of Thin Films*,  
Chapman and Hall Ltd., London.
55. Hoshino, S. (1952) *J. Phys. Soc. Jap.* 7, 560.
56. Ibers, J.A. (1957) *Acta. Cryst. Camb.* 10, 858.
57. Ibers, J.A. & Vainshtein, B.K. (1960)  
*Soviet Phy. Cryst.* 4, 601.
58. Ioffe, A.F. (1960), "Physics of Semiconductors"  
Infosearch Limited, London.

59. Karle, J. & Karle, I.I. (1950) *J. Chem. Phys.* 18, 957.
60. Kossel, W. (1927) *Nachr. Ges. Wiss. Göttingen*, 135.
61. Kossel, W. (1928) *Quantentheorie und chemie*, p.46, Lipsig.
- 62a. Lassen, H. & Bruck, L. (1935) *An. Phys. Lpz.* 22, 65.  
 62b. Lorenz & Prener (1956)
63. Lyashenko, V.I. & Snitko, O.V. (1954) *Trudy. Inst. Fiz.*  
*Akad. ukr. S.S.R.* 5, 65-76.
64. Maxwell, L.R. & Mosley, V.H. (1939) *Phys. Rev.* 55, 238.
65. Mellor, J.W. (1930) *A Comprehensive treatise on inorganic and theoretical chemistry*, Vol.7, Longman, Green & Co. London, New York, Toronto.
66. Mellor, J.W. (1933) *Ibid*, Vol.9.
67. Miyake, S. Hoshino, S. & Takenaka (1952)  
*J. Phys. Soc. Jap.* 7, 19.  
 67a. Mugge, O. (1903) *Jahrbuch Mineralogie, Beil. Bd.* 16 335
68. Pashley, D.W. (1951) *Proc. Phys. Soc. A* 64, 1113.
- 67b. Newman, R.C. & Pashley, D.W. (1955), *Phil. Mag.* 46, 927.
69. Pashley, D.W. (1952) *Proc. Phys. Soc. A* 210, 354.
70. Pashley, D.W. (1956) *From the Philosophical Magazine Supplement*, Vol.5, No.18, p.173.
71. Pashley, D.W. & Glossop, A.B. (1958) *Proc. Roy. Soc. A* 250, 132-146.
72. Pashley, D.W. & Presland, A.B.B. (1959) *J. Inst. Metals*, 87, 419.
73. Piggott, M.R. & Wilmen, H. (1958) *Acta Cryst.* 11, 93-7.
74. Finsker, Z.G. (1953) *"Electron Diffraction"*, London, Butterworth.
75. Finsker, Z.G. (1959) *Advances in electronics and electron Physics*, Reprinted from, Academic Press, Inc. New York.

76. Raether, H. (1951) *Ergeb. exakt. Naturw.* 24, 54.
77. Raether, H. (1957) *Handbuch der Physik* (Ed. S. Flügge),  
Vol. 32, 443. Berlin, Göttingen, Heidelberg :  
Springer Verlag.
78. Royer, L. (1928) *Bull. Soc. Franc. Min.* 51, 7.
79. Royer, L. (1936) *Compt. rend.* 202, 1687.
80. Rudiger, O. (1937) *Ann. d. Phys.* 30, 505.
81. Schenck, R. (1951) *Z. Elektro-chem.* 55, 1-7.
82. Seig, L. (1953) *Naturwissenschaften* 40, 439.
83. Seitz, F. (1950), *Phys. Rev.* 71, 723.
84. Shin-Ichi Shimadzu (1939) *Mem. Coll. Sci. Kyoto*, A22, 27-34.
85. Stranski, I.N. (1928) *Z. Phys. Chem.* 136, 259.
86. Stranski, I.N. (1949) *Disc. Faraday Soc.* No.5 (crystal  
growth), p.13.
87. Sushkin, N.G. & Kovner, I.A. (1948) *Doklady Akad. Nauk  
SSSR*, 62.
88. Tatarinova, L.I. (1957) *Kristallografiya*, 2, 260-7.
89. Thirsk, (1950) *Proc. Phys. Soc.* B 63, 833.
90. Tika Asai (1940) *Bull. Inst. Phys. Chem. Research (Tokyo)*  
19, 1403-18.
91. Tika Asai (1941) *Ibid*, 20, 1-19.
92. Thomson, G.P. (1931) *Proc. Roy. Soc.* A 133, p.1.
93. Thomson, G.P. & Cochrane, W. (1939) *Theory and Practice  
of Electron Diffraction*, Macmillan, London.
94. Trehan, Y.N. & Goswami, A. (1956) *Indian Institute of Metals.*  
10th Annual Meeting.

95. Trehan, Y.N. & Goswami, A. (1959) *Trans. Farad Soc.* 155, 2162.
- 95a. Trehan, Y.N. & Goswami, A. (1959) *Proc. Nat. Inst. Sci. Ind.* 25, 210.
96. Trillat, J.J. (1951) *Acad. Sci. (Paris)*, 233, 1188-9.
97. Usmani, I.H. (1941) *Phil. Mag.* 32, 89.
98. Vainshtein, B.K. (1956) *Structural Electron Diffraction*  
(Moscow Academy of Sciences, U.S.S.R.).
99. Volmer, M. (1939) *Kinetic der phasenbildung*, Steinkopff,  
Dresden and Leipzig.
100. Wallerant, F. (1902) *Bull. Soc. franc. Mineral.* 25, 180.
101. Webb, D.P.D. (1951) Ph.D. Thesis, London University.
102. Wells, A.F. (1945) *Structural Inorganic Chemistry*.
103. Wells, A.F. (1948) *Chem. Soc. (Lond.) Ann. Rep.* 43, 62.
104. Wells, A.F. (1958) *The Structure of Crystals*, Published by  
Academic Press, Inc., New York.
105. Wilman, H. (1940) *Proc. Phys. Soc. (Lond.)* 52, 323.
106. Wilman, H. (1948a) *Proc. Phys. Soc. (Lond.)* 60, 341.
107. Wilman, H. (1949) *Research* 2, 352.
108. Wilman, H. (1952) *Acta Cryst.* 5, 782.
109. Wilman, H. (1955) *Proc. Phys. Soc. (Lond.)*, 68B, 474.
110. Wilman, H. (1958) *J. Chem. Phys.* 53, 607-19.
111. Wulf, G. (1901) *Z. Kristallogr.* 34, 449.
112. Wyckoff, R.W.G. (1921), *Am. J. Sci.* 2, 244.
113. Wyckoff, R.W.G. & Posnjak, S. (1922) *J. Am. Chem. Soc.* 44, 30-6.
114. Wyckoff, R.W.G. (1948) "Crystal Structures" Interscience Pubins.
115. Yurkov, V.A. (1952) *Zhur. Eksptl. i, Teoret. Fiz.* 22, 223-9.
116. Yurkov, V.A. (1953) *Zhur. Tekh. Fiz.* 23, 1464-6.